COASTAL EUTROPHICATION AND HYPOXIA UNDER FOCUS: REDOX DEPENDENT BENTHIC NUTRIENT FLUXES ACROSS SEA BOUNDARIES IN THE NORTHEASTERN MEDITERRANEAN AND MARMARA SEA

A THESIS SUBMITTED TO
THE INSTITUTE OF MARINE SCIENCES
OF
MIDDLE EAST TECHNICAL UNIVERSITY

BY

İSMAİL AKÇAY

IN PARTIAL FULFILLMENT OF THE REQUIREMENTS
FOR
THE DEGREE OF DOCTOR OF PHILOSOPHY
IN
OCEANOGRAPHY

FEBRUARY 2022

Approval of the thesis:

COASTAL EUTROPHICATION AND HYPOXIA UNDER FOCUS: REDOX DEPENDENT BENTHIC NUTRIENT FLUXES ACROSS SEA BOUNDARIES IN THE NORTHEASTERN MEDITERRANEAN AND MARMARA SEA

submitted by **İSMAİL AKÇAY** in partial fulfillment of the requirements for the degree of **Doctor of Philosophy in Oceanography, Middle East Technical University** by,

Prof. Dr. Barış Salihoğlu
Director of Institute, **Institute of Marine Sciences** _____

Assoc. Prof. Dr. Bettina Andrea Fach Salihoğlu
Head of the Department, **Oceanography** _____

Assoc. Prof. Dr. Mustafa Yücel
Supervisor, **Marine Geology and Geophysics, METU** _____

Examining Committee Members:

Prof. Dr. Nuray Çağlar
Institute of Marine Sciences and Management, Istanbul University _____

Assoc. Prof. Dr. Mustafa Yücel
Supervisor, Marine Geology and Geophysics, METU _____

Assist. Prof. Dr. Koray Özhan
Oceanography, METU _____

Assist. Prof. Dr. Devrim Tezcan
Marine Geology and Geophysics, METU _____

Assist. Prof. Dr. Nazlı Olğun Kıyak
Eurasia Institute of Earth Sciences, Istanbul Technical University _____

Date: 08.02.2022

I hereby declare that all information in this document has been obtained and presented in accordance with academic rules and ethical conduct. I also declare that, as required by these rules and conduct, I have fully cited and referenced all material and results that are not original to this work.

Name Last name: İsmail Akçay

Signature :

ABSTRACT

COASTAL EUTROPHICATION AND HYPOXIA UNDER FOCUS: REDOX DEPENDENT BENTHIC NUTRIENT FLUXES ACROSS SEA BOUNDARIES IN THE NORTHEASTERN MEDITERRANEAN AND MARMARA SEA

Akçay, İsmail
Doctor of Philosophy, Oceanography
Supervisor: Assoc. Prof. Dr. Mustafa Yücel

February 2022, 154 pages

Seafloor biogeochemistry can dramatically shift in response to deoxygenation and eutrophication-driven organic carbon production. In such conditions, biogeochemical cycling of key nutrients can be highly coupled to oxygen concentrations and metal redox cycles, often leading to the increase in dissolved nutrients and metals concentrations in the deep water column. In this thesis, such biogeochemical feedbacks have been studied for the first time for the Turkish Seas. Porewater and solid-state biogeochemistry were determined in the Northeastern (NE) Mediterranean and Marmara Sea, displaying distinct biogeochemical properties, between March 2018 and July 2019. Sediment porewater diffusive nutrient fluxes were calculated from the obtained core samples in these distinct marine environments. The study results indicated that contribution of porewater diffusive nutrient fluxes to the total nutrient fluxes from sea boundaries surrounding the NE Mediterranean Sea was calculated as 5.8% for phosphate, 12% for nitrate, 19% for ammonium and 22% for reactive silicate, respectively. Porewater nitrate, sulfate and hydrogen sulfide profiles obtained in the Marmara Sea showed that organic matter degradation processes in the upper 20-30 cmbs

have occurred by oxic respiration, denitrification and sulfate reduction whilst organic matter decomposition was limited by oxic respiration in the upper sedimentary column in the southern Marmara Sea. The distribution of porewater sulfate, hydrogen sulfide, and major elements throughout the sediment cores obtained specifically from the İzmit Bay, suggested principal biogeochemical and early diagenetic processes such as anaerobic oxidation of methane (AOM), carbonate precipitation, iron reduction, iron sulfide precipitation and low-temperature silicate diagenesis. Furthermore, the biogeochemical cycling of sedimentary phosphorus (P) was studied in the NE Mediterranean, Marmara and Black Seas and the pool of "potentially mobile P" was determined for the studied sites. The study results showed that porewater and sediment biogeochemistry displayed remarkable spatial variability in the studied sites with the maximum concentrations of porewater phosphate, ammonium, reactive silicate, surface sediment organic carbon, nitrogen, phosphorus and total phosphorus measured in the hypoxic Marmara Sea and suboxic/anoxic Black Sea. The decline in the total phosphorus concentrations of all sediment core samples indicated P-mobilization to the overlying water. The pool of "potentially mobile P" varied between 0.023 and 0.148 mol/m^2 in the studied sites with the minimum values recorded in the marine environments with highly oxygenated deep waters. The correlation between calculated diffusive nutrient fluxes and the deep waters dissolved oxygen concentrations indicated the redox-dependency on the benthic nutrient dynamics in the NE Mediterranean and Marmara Sea as the lower deep water dissolved oxygen concentration resulted in higher porewater diffusive phosphate, ammonium and reactive Si fluxes. For the ecosystem health of NE Mediterranean and recently deoxygenating Marmara Sea, studying redox dependent benthic nutrient dynamics and organic matter geochemistry are of critical importance to attain Good Environmental Status (GES) for these distinct marine basins.

Keywords: Benthic nutrient fluxes, Sediment, Biogeochemistry, Northeastern Mediterranean Sea, Marmara Sea.

ÖZ

KIYISAL ÖTROFİKASYON VE HİPOKSİ MERCEK ALTINDA: KUZEYDOĞU AKDENİZ VE MARMARA DENİZİ'NDE REDOKSA BAĞLI BENTİK BESİN TUZU AKILARI

Akçay, İsmail
Doktora, Oşinografi
Tez Yöneticisi: Doç. Dr. Mustafa Yücel

Şubat 2022, 154 sayfa

Deniz sedimanı biyojeokimyasal özellikleri oksijensizleşme ve ötrofikasyon sonucu oluşan aşırı organik karbon üretimi ile yakından ilişkilidir. Ötrofik koşulların geliştiği denizel ortamlarda besin tuzları biyojeokimyası oksijen değerleri ve metal rekods döngülerine bağlıdır ve genellikle dip sularda oksijen seviyesi düştükçe sedimandan dip sulara besin tuzu ve metal girişi olmaktadır. Bu tez çalışması ile Türkiye denizlerinde ilk defa biyojeokimyasal süreçler ve geri bildirim mekanizmaları ortaya konmuştur. Farklı biyojeokimyasal özelliklere sahip Kuzeydoğu Akdeniz ve Marmara Denizi'nde gözenek suyu ve sediman biyojeokimyası Mart 2018 ve Temmuz 2019 dönemi arasında incelenmiştir. Elde edilen sediman karot örneklerinde gözenek suyu besin tuzu akıları hesaplanmıştır. Elde edilen sonuçlara, göre verimsiz ve oksik özellikle Kuzeydoğu Akdeniz'de sediman gözenek suyu besin tuzu akılarının toplam besin tuzu akılarına önemli ölçüde katkı sağladığı belirlenmiştir; toplam besin tuzu akılarının fosfat akıları %5.8, nitrat akıları %12, amonyak akıları %19 ve reaktif silikat akıları %22'sini oluşturmuştur. Marmara Denizi'nde elde edilen sonuçlara göre, nitrat, sülfat ve hidrojen sülfür profilleri organik madde degradasyonun sediman tabakasının ilk 20-30 cm'de oksik respirasyon, denitrifikasyon ve sülfat indirgenmesi ile oluştuğunu

göstermiştir. Güney Marmara Denizi'nde ise sediman üst tabakada sadece oksik respirasyonla sınırlı kaldığı görülmüştür. Ayrıca, özellikle İzmit Körfezi'nde, sediman gözenek suyu sülfat, hidrojen sülfür ve majör elementlerin derinlik profilleri, oksijensiz metan oksidasyonu (AOM), karbonat presipitasyonu, demir-oksit indirgenmesi, demir-sülfür presipitasyonu ve düşük sıcaklıkta gerçekleşen silikat diyajenezi gibi birçok biyojeokimyasal ve erken diyajenetik süreçlerin gerçekleştiğini göstermiştir. Bu çalışmada ayrıca sedimanda fosfor biyojeokimyası Kuzeydoğu Akdeniz, Marmara ve Karadeniz'de çalışılmış ve sedimandan mobilize olan fosfor miktarları belirlenmiştir. Gözenek suyu besin tuzu değerleri ve sediman biyojeokimyasal özellikleri Kuzeydoğu Akdeniz, Marmara Denizi ve Karadeniz'de dikkate değer alansal değişim göstermiştir. En yüksek gözenek suyu fosfat, amonyak ve reaktif silikat, sediman organik karbon, organik azot, organik fosfor ve toplam fosfor değerleri suboksik özellikte Marmara Denizi'nde ve Karadeniz'in suboksik ve anoksik özellik gösteren alanlarında ölçülmüştür. Sediman karot örneklerinde elde edilen toplam fosfor profilleri derinlikle azalan bir eğilim göstermiştir ve bu durum sedimandan dip sulara fosfor mobilizasyonunun olduğunu göstermiştir. Sedimandan dip sulara mobilize olan fosfor değerleri 0.023 ve 0.148 mol/m^2 arasında değişim göstermiştir ve en düşük değerler dip suları oksik özellik gösteren alanlarda hesaplanmıştır. Kuzeydoğu Akdeniz'de ve Marmara Denizi'nde besin tuzu akıları ve dip su çözünmüş oksijen değerlerinin korelasyonuna bakıldığında bentik besin tuzu dinamiklerinin redoks durumuna bağlı olduğu görülmüştür. Dip su çözünmüş oksijen değerleri azaldıkça sedimandan dip sulara yüksek miktarlarda fosfat, amonyak ve reaktif silikat girdisi olmaktadır. Kuzeydoğu Akdeniz ve oksijensizleşmenin görüldüğü Marmara Denizi'nin ekosistem sağlığının korunması ve İyi Çevresel Durum (İÇD) özelliklerine ulaşması açısından bentik besin tuzu akıları ve organik madde jeokimyasal özelliklerinin belirlenmesi kritik öneme sahiptir.

Anahtar Kelimeler: Bentik besin tuzu akıları, Sediman, Biyojeokimya, Kuzeydoğu Akdeniz, Marmara Denizi.

To my parents

To my sister

To Şeyma Nur Çetin

ACKNOWLEDGMENTS

I would like to express my deepest gratitude to my supervisor Assoc. Prof. Dr. Mustafa Yücel for his guidance, advice, criticism, encouragements and insight throughout the research.

I would like to thank Prof. Dr. Süleyman Tuğrul for his comments leading to considerable improvement in this study.

I would like to thank Assist. Prof. Dr. Devrim Tezcan for his valuable comments and suggestions.

I would like to thank Assist. Prof. Dr. Koray Özhan for his criticism to improve this study in scientific aspects.

I would like to thank my thesis invited examining committee members Prof. Dr. Nuray Çağlar and Assist. Prof. Dr. Nazlı Olğun Kıyak.

I am grateful to Dr. Hasan Örek, scientific cruise participants, crew of R/V Bilim-2 and METU-IMS technical personnel for their kind assistance.

I would like to thank my friends Ali Erdem Demir, Önder Yıldırım, İlhan Bağ, Mehmet Can Var, Eren Yıldırım, Alper Utku Çetinel, Mustafa Doğru, Selim Karaca, Mehmet Ali Demir, Oğuz Kaya, Pınar Kalegeri, Merve Açıkyol, Sıla Akıncı, Mehmet Durmaz, Mehmet Burak Yalçın, Şehmus Başduvar, Emel Kocaman, Gizem Akkuş, Serhat Sevgen, Gamze Tanık, Esra Ermiş, Mertcan Esti, Nimet Alımlı, Ehsan Sadighrad, Ceren Başduvar and Merve Yıldırım for mental support and special friendship.

I would like to thank Şeyma Nur Çetin for her unconditional and endless support.

Finally, I am very grateful to my family for encouraging me within this study.

This study has been supported by DEKOSIM (Centre for Marine Ecosystem and Climate Research, Project Code BAP-08-11-DPT.2012K120880) Project, the Scientific and Technological Research Council of Turkey (TUBİTAK-2247, 119C027) Project and TUBA-GEBIP Program of the Turkish Academy of Sciences. Riverine and wastewater samples were obtained by the projects (107G066, 111G152) supported by TUBITAK.

TABLE OF CONTENTS

LIST OF TABLES

LIST OF FIGURES

CHAPTER 1

GENERAL INTRODUCTION AND THESIS OUTLINE

1.1 General Background

The latter half of the 20th century witnessed dead zones spreading in many coastal areas mainly due to excessive anthropogenic nutrient (N, P) inputs that dramatically increased primary productivity and led to development of eutrophication and depletion of deep water oxygen in the coastal zones (Diaz and Rosenberg, 2008). Recent studies showed that the N and P releases from the estuarine and coastal marine sediments are considered to be important sources for phytoplankton production as the sediments supply an average of 15-32% of N and 17-100% of P for phytoplankton demand and in some regions, the N and P releases from sediments can be larger than terrestrial nutrient inputs (Boynton et al., 2018). In a study recently performed in the Baltic Sea, for example, annual release of P ranged between 100-1330 tonnes yr^{-1} from the sediment which is in the same order of magnitude as the regional P input from the terrestrial inputs (Malmaeus et al., 2012). Biogeochemical cycling of key nutrients (N, P) is highly coupled to oxygen concentrations and metal (Fe, Mn) cycles (Williams, 1987; Jørgensen, 1996). The increase in dissolved inorganic phosphorous and iron concentrations in the oxygen minimum zones is highly related to anoxic conditions in the marine environment as the role of sediments in the low-oxygen areas is important for dissolved iron and inorganic-P sources to the bottom water (Noffke et al., 2012; Mu et al., 2017; Schroller-Lomnitz et al., 2019; Ballagh et al., 2020; Spiegel et al., 2021; Moncelon et al., 2021).

The Mediterranean Sea is an oligotrophic sea due to limited nutrient inputs from internal and external sources (UNEP, 1989; Yılmaz and Tugrul, 1998; Kress and Herut, 2001; Krom et al., 2004; Tugrul et al., 2016; 2018). Surface dissolved

inorganic nutrient concentrations in offshore waters of the Northeastern (NE) Mediterranean Sea (Figure 1.1) are measured as low as for inorganic phosphate and nitrate during the spring-autumn period (Yılmaz and Tugrul, 1998) and increased slightly in winter due to vertical mixing (Yılmaz and Tugrul, 1998; Dogan-Saglamtimur and Tugrul, 2004, Tugrul et al., 2016 and references therein). Furthermore, atmospheric nutrient inputs, both dry and wet deposition, have remarkable contribution to sustain primary productivity in the Northeastern Mediterranean (Kocak et al., 2010; Kocak, 2015). For example, contribution of atmospheric P fluxes to the algal production was calculated as high as 0.9% in offshore waters of the Cilician Basin of the Northeastern Mediterranean whereas atmospheric N fluxes would sustain 8.4% of primary production in offshore waters and the contribution of atmospheric nutrient fluxes would become drastically high during the stratified summer-autumn period (Kocak, 2015). Though low nutrient concentrations in offshore waters of the NE Mediterranean (Figure 1.1) are recorded in the upper layer, its coastal ecosystem is highly fueled by terrestrial nutrient and organic matter inputs from the major rivers and wastewater discharges leading to development of coastal eutrophication in the inner bay waters (Dogan-Saglamtimur and Tugrul 2004; Tugrul et al., 2009; 2011; 2016; 2018). The sedimentation rates in the oligotrophic Eastern Mediterranean Sea ranges from 0.003 to 0.014 cm y^{-1} (Van Santvoort et al., 2002; Katz et al., 2020) much lower than recorded in the Marmara Sea (0.008 to 0.19 cm y^{-1}) (Ergin and Yörük, 1990; Ergin et al., 1994; Çağatay et al., 2004). The primary production in the surface waters of the oligotrophic Eastern Mediterranean is also as low as 12-88 g C m^{-2} y^{-1} (Van Santvoort et al., 2002) compared to measurements reported in the Marmara Sea (Ergin et al., 1994; Yılmaz, 2002). However, increased inputs of nutrients from terrestrial sources (rivers, wastewaters) to the NE Mediterranean coastal areas have enhanced primary production and biodegradable particulate organic matter production (Coban-Yıldız et al., 2000; Yılmaz, 2002; Dogan-Saglamtimur and Tugrul, 2004), leading to eutrophication in the inner bays (Tugrul et al., 2011, 2016, 2018, Kaptan, 2013).

The Marmara Sea (Figure 1.1) is a typical example of a two-layer enclosed sea connecting the Black Sea to the Mediterranean via the two shallow and narrow straits, called Bosporus and Dardanelles. This connected oceanographic system is also called the Turkish Straits System (TSS) (Ünlüata et al. 1990; Beşiktepe et al. 1994; Ediger et al., 2016 and references therein). Marmara Sea ecosystem has distinct biogeochemical properties due to water exchanges between the Black Sea and the Mediterranean Sea through the TSS (Polat, and Tugrul, 1995; Tugrul and Polat, 1995, Tugrul et al., 2002; Yalçın et al., 2017). It has also been affected by anthropogenic pressures by direct discharges mainly from the İstanbul city (Tuğrul and Morkoç, 1989; Tugrul and Polat, 1995; Ediger et al., 2016; Yalçın et al., 2017; Tan and Aslan, 2020). The development of eutrophication in the Northwestern Black Sea (Konovalov and Murray, 2001; Mee, 1992; Tugrul et al., 2014) also adversely affected Marmara Sea ecosystem (Polat and Tugrul, 1995; Ediger et al., 2016; Yalçın et al., 2017). Recent studies in the Marmara Sea indicated dissolved oxygen deficiency in the deep waters due to increasing organic matter inputs in the upper layer (Ediger et al., 2016; Yalçın et al., 2017) and limited ventilation of deep waters by strong density gradient between water masses (Beşiktepe et al. 1994; Tugrul and Polat, 1995; Tugrul et al., 2002; Ediger et al., 2016). Though biochemistry of water column and biogeochemistry of surface sediments in the Northeastern (NE) Mediterranean and Marmara Sea have been studied extensively, relatively few studies were performed to understand the sediment porewater and solid-phase biogeochemistry in these regions having distinct trophic conditions and deep water redox state.

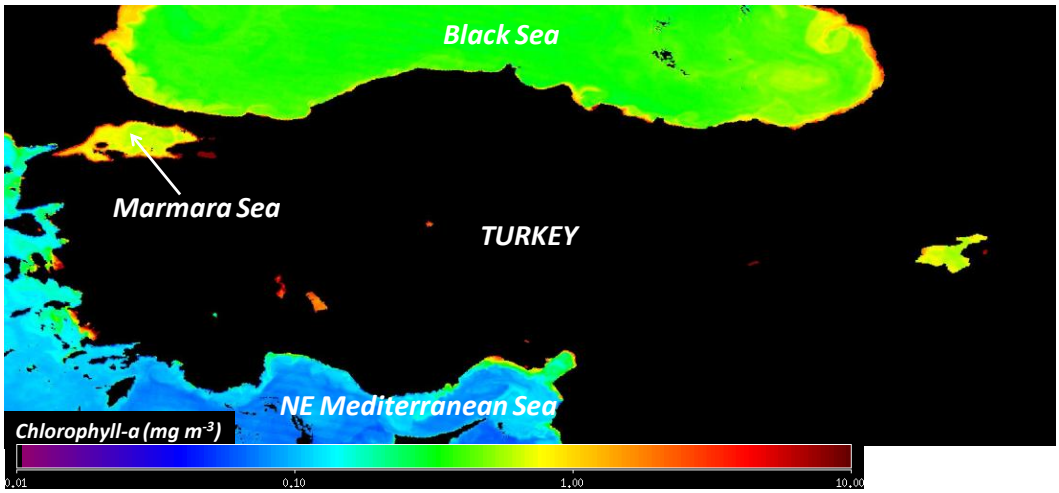

Figure 1.1. Surface water chlorophyll-*a* distributions obtained by Satellite MODIS Aqua in the NE Mediterranean, Marmara and Black Seas in September 2019.

1.2 Scope of the Study

The main objectives of this study are:

- To uncover the biogeochemical processes occurring in the seafloor sediment derived from sediment porewater profiles in the oxic NE Mediterranean and suboxic Marmara Sea,
- To determine redox dependent benthic nutrient fluxes in the NE Mediterranean and Marmara Sea,
- To reveal how sedimentary phosphorus (P) fractions (loosely bound-P, iron bound-P, organic-P, aluminum bound-P, calcium bound-P and total phosphorous) in the sediment change with redox conditions,
- To determine the amount of mobile phosphorous in the NE Mediterranean and Marmara Sea sediments,
- To compare nutrient influxes from sediment with the total of river, wastewater and atmospheric inputs to the NE Mediterranean shelf waters.

Chapter 2 investigates porewater and sediment biogeochemistry in the oligotrophic NE Mediterranean Sea. Porewater nutrients and sediment

biogeochemical variables were determined from the five sediment core samples obtained from the NE Mediterranean Sea. The results of this study reveal that a series of redox reactions (oxic respiration, denitrification, iron reduction) take place in the NE Mediterranean subseafloor. Furthermore, it was shown that diffusive nutrient fluxes constitute a remarkable fraction of the total nutrient budget in the NE Mediterranean Sea displaying oxic conditions in the deep waters.

Chapter 3 extends our knowledge of the porewater and sediment biochemistry in the increasingly hypoxic (<50 μM O_2) and eutrophic Marmara Sea. The dissolved oxygen concentrations in the Çınarcık Basin deep waters (eastern Marmara Sea) decreased by almost 90% percent during the last two decades and the hypoxic and anoxic conditions were developed specifically in the eutrophic regions under the influence of Black Sea inflow, domestic and industrial discharges and riverine inputs. In this chapter we discussed the impacts of deoxygenation and coastal eutrophication on the sedimentary biogeochemical processes in the deoxygenating Marmara Sea. This study showed that the dynamics of porewater and solid-state biogeochemistry in the Marmara Sea have been influenced by eutrophication, bottom water hypoxia as well as seismicity in the region. Vertical profiles of biogeochemical variables indicated principal biogeochemical and early diagenetic processes such as anaerobic oxidation of methane (AOM), carbonate precipitation, Fe-reduction, Fe-S precipitation and low-temperature silicate diagenesis in the Marmara Sea subseafloor. This study also showed high rates of organic matter decomposition and limited trapping of nutrients in the benthic interface.

Chapter 4 builds on the findings of previous chapters and further focus on biogeochemical cycling of sedimentary P species and also related variables (porewater nutrients, sediment carbon, nitrogen and iron) in the three interconnected marine basins: Black Sea, Marmara and NE Mediterranean Seas. The pool of "potentially mobile P" was also determined for the studied sites. The study results showed that porewater and sediment biogeochemistry displayed great variability in the studied sites with the maximum concentrations of porewater phosphate, ammonium, reactive silicate, surface sediment organic carbon, nitrogen,

phosphorus and total phosphorus measured in the suboxic Marmara Sea and suboxic/anoxic Black Sea. The decline in the TP concentrations of all sediment core samples indicated P-mobilization to the overlying water. It was also shown that the deoxygenation and eutrophication would further lead to the releases of P in these three interconnected marine basins.

Chapter 5 presents a comparison and synthesis of the redox dependent benthic nutrient fluxes across sea boundaries in the NE Mediterranean and Marmara Sea. The study results indicated that maximum porewater phosphate, ammonium and silicate concentrations and fluxes were recorded in the suboxic Marmara Sea having greater sedimentation rate and surface water primary productivity. The correlation between calculated diffusive nutrient fluxes and the deep waters dissolved oxygen concentrations suggested the redox-dependency on the benthic nutrient dynamics in the NE Mediterranean and Marmara Sea as the lower deep water dissolved oxygen concentration resulted in higher porewater diffusive nutrient fluxes. For the ecosystem health of NE Mediterranean and recently deoxygenating Marmara Sea, studying redox dependent benthic nutrient dynamics and organic matter geochemistry are of critical importance to attain Good Environmental Status (GES) for these distinct marine basins.

CHAPTER 2

POREWATER AND SEDIMENT BIOGEOCHEMISTRY IN THE NORTHEASTERN MEDITERRANEAN SEA: A NEW NUTRIENT BUDGET INCLUDING THE BENTHIC FLUXES

Abstract

The coastal ecosystem of the Northeastern (NE) Mediterranean has been affected by nutrient inputs originated from regional rivers and wastewater discharges leading to development of eutrophication. Atmospheric nutrient inputs have also remarkable contribution to marine nutrient pool in the NE Mediterranean, especially in dry periods. Sediment porewater nutrient fluxes into the deep waters are strongly associated with eutrophic and suboxic/anoxic conditions. There was only limited number of studies performed on the PW and sediment biogeochemistry in the NE Mediterranean Sea having oxic conditions in the deep waters. In this study, therefore, sediment PW nutrient (Si, N, P) and sediment organic matter biogeochemistry were studied. The study results indicated a series of redox reactions (oxic respiration, denitrification, iron reduction) as well as remarkable contribution of porewater diffusive nutrient fluxes to the total nutrient budget in the NE Mediterranean Sea. Lower Si/N and higher N/P molar ratios in the total nutrient inputs are very likely to modify phytoplankton composition and abundance in the phosphorus deficient NE Mediterranean productive shelf waters leading to development of mesotrophic/eutrophic conditions in the NE Mediterranean Sea.

2.1 Introduction

The Mediterranean Sea is a typical example of oligotrophic seas due to limited nutrient inputs from internal and external sources (UNEP, 1989; Yılmaz and Tugrul, 1998; Kress and Herut, 2001; Krom et al., 2004; Tugrul et al., 2016; 2018). Surface dissolved inorganic nutrient concentrations in offshore waters of the Northeastern Mediterranean (NE) (Figure 2.1) are measured as low as for inorganic phosphate and nitrate during the spring-autumn period (Yılmaz and Tugrul, 1998) and increased slightly in winter due to vertical mixing (Yılmaz and Tugrul, 1998; Dogan-Saglamtimur and Tugrul, 2004, Tugrul et al., 2016 and references therein). Furthermore, atmospheric nutrient inputs, both dry and wet deposition, have remarkable contribution to sustain primary productivity in the Northeastern Mediterranean (Kocak et al., 2010; Kocak, 2015). For example, contribution of P fluxes to the algal production was calculated as high as 0.9% in offshore waters of the Cilician Basin of the NE Mediterranean Sea whereas N fluxes would sustain 8.4% of primary production in offshore waters and the contribution of atmospheric nutrient fluxes would become drastically high during the stratified summer-autumn period (Kocak, 2015). In the low-nutrient upper layer waters of the Mediterranean Sea, primary production is mainly limited by phosphorus due to unusually high NO_3/PO_4 molar ratios in the deep waters as ~28/1 (Krom et al., 1991; Yılmaz and Tugrul, 1998) and in atmospheric and regional rivers (Kocak at al., 2010) as also reported recently by the ^{14}C bioassay experiments conducted in the Turkish coastal waters of the Mediterranean and Aegean Seas (Tufekci et al, 2013). Though low nutrient concentrations in offshore waters of the NE Mediterranean (Figure 2.1) are recorded in the upper layer, its coastal ecosystem is highly fueled by terrestrial nutrient and organic matter inputs from the major rivers and wastewater discharges leading to development of coastal eutrophication in the inner bay waters (Dogan-Saglamtimur and Tugrul 2004; Tugrul et al., 2009; 2011; 2016; 2018). In the offshore waters of the NE Mediterranean Sea, for example, concentrations of total phosphorous (TP) and chlorophyll-*a* (Chl-*a*) were as low as 0.05-0.07 μM for TP

and 0.02-0.05 µg/L for Chl-*a*, reaching to peak values in eutrophic coastal waters (Tugrul et al., 2011; 2016; 2018).

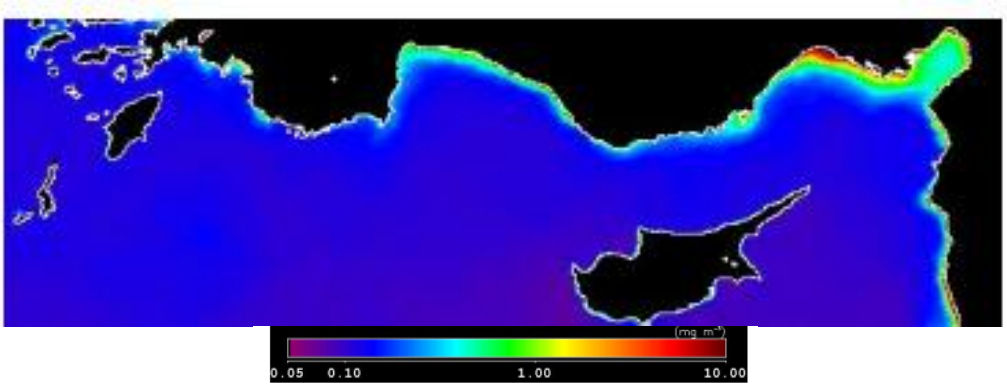

Figure 2.1. Annual surface chlorophyll-*a* distribution of the NE Mediterranean shelf waters, obtained by MODIS Satellite in 2009 (modified after Tugrul et al., 2016).

Biogeochemical cycling of key nutrients (N, P) is highly coupled to oxygen concentrations and metal (Fe, Mn) cycles (Williams, 1987; Jørgensen, 1996). The increase in dissolved inorganic phosphorous and iron concentrations in the oxygen minimum zones (OMZs) is highly related to anoxic conditions in the marine environment as the role of sediments in the OMZs is important for dissolved iron and inorganic phosphate sources to the bottom water (Noffke et al., 2012). Furthermore, in the eutrophic and hypoxic/anoxic Baltic Sea, the intrusion of oxygen-rich North Sea waters into the Eastern Gotland Basin decreased to releases of inorganic phosphate and ammonium from deep sediments (Sommer et al., 2017). Though many studies were performed to understand cycling of key elements (C, N, P, dissolved nutrients, metals (Fe, Mn), trace and major elements) depending on different redox conditions in the suboxic/anoxic marine environments, limited number of studies was carried out to understand porewater and sediment biogeochemistry in the oligotrophic NE Mediterranean Sea having oxic conditions in the deep waters.

Since the cycles of oxygen, phosphorous and nitrogen are highly coupled, ongoing eutrophication in the Baltic Sea induced hypoxia and reduced seafloor resulting in internal phosphorous loading due to changing redox state of the seafloor (Vahtera et al., 2007; Ferreira et al., 2011; Malmaeus et al., 2012; Noffke et al., 2012). Seafloor can, therefore, play a key role in rapid degradation of labile organic matter and nitrification/denitrification processes as well as other abiotic processes in the uppermost millimeters of sediment layer resulting in nutrient releases from the sediments studied extensively during the last decades (Christensen et al., 1988; Ignatieva, 1999; Rasheed, 2004; Al-Rousan et al., 2004; Hille et al., 2005; Rasheed et al., 2006; Rydin et al., 2011; Cheng et al., 2014; Mu et al., 2017). Redox dependent benthic nutrient fluxes would enhance algal production (Christensen et al., 1988; Ignatieva, 1999; Rasheed et al., 2006). In a study conducted on the oligotrophic Eastern Mediterranean Sea continental shelf, the phosphate and nitrate fluxes into the water column supported as much as 11.7 % and 2 % of the phytoplankton P and N demand, respectively (Christensen et al., 1988). Therefore, studying both external (riverine, wastewater, atmospheric inputs) and internal (sediment, submarine groundwater) nutrient fluxes into the oligotrophic and eutrophic marine environments is critical to understand biogeochemical cycling of key elements for further use in biogeochemical modeling and eutrophication management efforts.

Organic matter geochemistry of the sediments has been affected by a series of redox reactions (Jørgensen, 1996) as well as terrestrial inputs of the particulate inorganic/organic matter that might be transported to offshore regions of the continental seas (Middelburg et al., 1993; Yemenicioglu and Tunc, 2013; Erdogan, 2014; Akcay, 2015, Ermiş, 2017; Deininger and Frigstad, 2019; Katz et al., 2020). In the Eastern Mediterranean Sea, surface sediment geochemistry and grain size distributions have been studied extensively during the last decades (Eijsink et al., 2000; Yemenicioglu and Tunc, 2013; Erdogan, 2014, Akcay, 2015; Ermiş, 2017), with the limited number of studies based on sediment core samples to understand organic matter geochemistry (sedimentation, degradation, accumulation and burial

of organic carbon) of the upper 25-40 cm sedimentary column (Van Santvoort et al., 2002; Katz et al., 2020).

The objectives of this study are, therefore, i) to understand porewater nutrient (S, N, P) dynamics, ii) to determine sediment geochemical (Carbon; C, nitrogen; N, reactive iron; r-Fe) properties, iii) to determine sediment porewater diffusive nutrient fluxes, iv) to determine riverine and wastewater nutrient fluxes, v) to compare both external (riverine, wastewater and atmospheric (Kocak et. al., 2010) inputs) and internal (sediment porewater diffusive inputs) nutrient fluxes in the NE Mediterranean shelf waters.

2.2 Methodology

The study area is located at the NE Mediterranean Sea (Figure 2.2). Field studies were carried out using R/V Bilim-2 of METU-IMS. Sediment core samples were obtained from the five stations (

Table 2.1) in March-April 2018 by a multi-corer sediment sampling device, the Multiple Corer (Oktopus, Kiel), which is a novel technique and applied for the first time in the NE Mediterranean Sea. The multicorer is a sediment sampler used in marine research for the transition zone between the sediment and the near bottom water. By using a dampener, the tubes penetrate the sediment slowly and samples can be collected while causing only minimal swirling on the surface layer. For the extraction, lids close the core tubes with special seals and prevent the samples from escaping. The obtained samples were taken out on board and the sediment samples were sliced by layers on board by means of an extruder. Sediment core samples were obtained from the Lamas River influenced region, shelf break and offshore regions in the March 2018 and Goksu River influenced coastal region, shelf break and one deep reference station (Depth: 1165 m) in April 2018 (Figure 2.2,

Table 2.1). Porewater extraction procedure of the collected samples was performed as described by the studies of Christensen et al. (1988), Sundby et al. (1992),

Rasheed et al. (2006), Gao et al. (2008), Noffke et al. (2012), Cheng et al. (2014). Each sediment core was sliced on board under minimum oxygen conditions using N_2 gas and sediment horizons were determined as 0-1 cm, 1-2 cm, 2-3 cm, 3-4 cm, 4-6 cm, 6-8 cm, 8-10 cm, 10-15 cm, 15-20 cm, 20-25 cm, 25-30 cm, 30-35 cm, 35-40 cm and 40-45 cm. After obtaining sliced sediments, each sample was put in a 50 mL falcon tube and centrifuged at 3000 rpm for 30 min. After separation of solids, the porewater samples were extracted using syringe-coupled GF/F filters through 0.45 µm and placed in 15 mL falcon tubes and stored in the freezer (-20 ˚C) for the analysis of nutrients. Sediment samples were also stored at -20 ˚C for the determination of total carbon (TC), total organic carbon (TOC), total nitrogen (TN) and dithionite extractable reactive iron (r-Fe) concentrations. Freshwater samples were collected seasonally at the downstream points of five regional rivers (Ceyhan, Seyhan, Berdan, Lamas, Göksu) in the period of 2008-2015 (Figure 2.2). Furthermore, domestic and industrial wastewater samples were obtained seasonally between 2006 and 2009 from the five major local facilities constructed along the NE Mediterranean region. Volume fluxes of the regional rivers and domestic and industrial wastewater facilities are presented in Table 2.2.

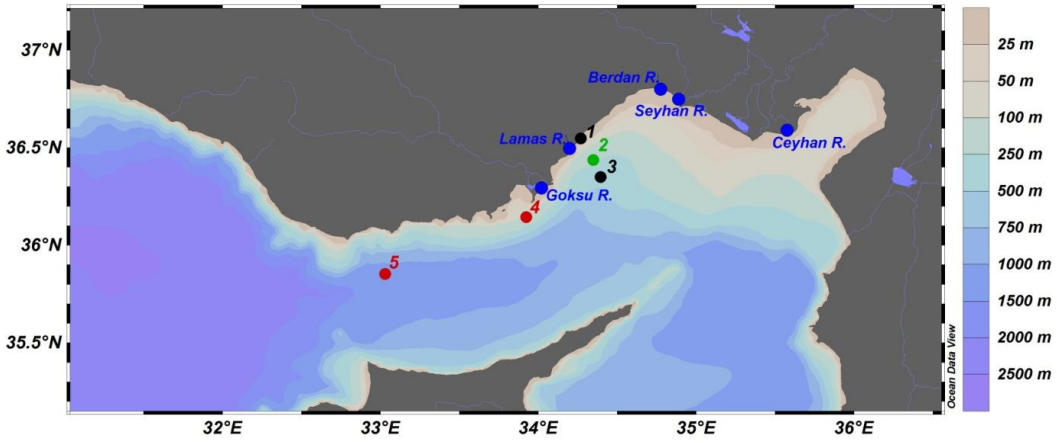

Figure 2.2. Locations of sediment core and river stations (black dots represent March 2018, red dots represent April 2018, one green dot represents both March and April 2018 and blue dots represent river stations).

Table 2.1. Locations of sediment core stations with trophic status and deep water redox state

Date	Station	Latitude (DD)	Longitude (DD)	Depth (m)	Trophic Status	Deepwater Redox State
20.03.2018	1	36.5482	34.2644	52	Mesotrophic to Eutrophic	Oxic
20.03.2018	2	36.4400	34.3458	208	Oligotrophic	Oxic
20.03.2018	3	36.3536	34.3811	323	Oligotrophic	Oxic
17.04.2018	4	36.1379	33.9235	85	Mesotrophic to Eutrophic	Oxic
18.04.2018	5	35.8520	33.0170	1165	Ultra-oligotrophic	Oxic

Table 2.2. Annual mean volume fluxes of the regional rivers (Kocak et al. 2010) and local facilities (Tugrul et al., 2009) in the NE Mediterranean

River	Q (m^3/s)	Wastewater	Q (m^3/s)
Seyhan R.	168	Mersin Discharge	0.60
Ceyhan R.	144	Antalya Discharge	0.45
Goksu R.	45	İskenderun Discharge	0.26
Berdan R.	6	Toros Discharge	0.014
Lamas R.	3	KromSan Discharge	0.006

Dissolved inorganic nutrients (nitrate+nitrite, ammonium, phosphate and silicate) were determined using a Bran+Luebbe Model four-channel autoanalyzer by standardized colorimetric methods (Grasshoff et al., 1983). The detection limits of measured nutrients are 0.02 μM, 0.04 μM, 0.01 μM and 0.04 μM for nitrate, ammonium, phosphate and reactive silicate, respectively. For the measurements of nutrients, the oceanography laboratories of the METU-IMS has successfully participated in the international QUASIMEME Laboratory Performance Studies. TC, TOC and TN concentrations were determined by dry oxidation method using the Vario El Cube Elementar Model CHN Analyzer (UNEP/MAP, 2006). The obtained sediment samples for the TC, TOC and TN measurements were initially freeze-dried. Dry sediments were then powdered and sieved to homogenize the samples. For TOC analysis, nearly 30 mg of dry and homogeneous sediment samples were put into the pre-combusted silver cups. Then, 5-10 μL of distilled water was added into each silver cup to wet the samples. After distilled water addition, 10 μL of 20 % HCl (vol/vol) was added to remove inorganic carbon from the sediment samples. The HCl additions were continued until all the inorganic

carbon was removed in the form of CO_2. Then, the carbonate-free samples were dried at 60 ˚C for one day. After drying the sediment samples, silver cups were compacted and put into autosampler of the CHN analyzer. TC and TN analyses in sediments were performed by the same method as for the TOC analysis, but without acid addition. TN concentrations were also measured on HCl-added samples and there was no significant difference between HCl-treated and untreated samples. The reactive iron (r-Fe) concentrations were determined by colorimetric ferrozine method (Stookey, 1970; Jeitner, 2014) after dithionite (0.3 M solution in a buffer containing 0.35 M sodium acetate and 0.2 M sodium citrate (pH=4.8)) extraction of freeze-dried sediments (Kostka and Luther, 1994; Raiswell et al., 1994, Yücel et al., 2010). In this extraction technique, r-Fe refers to iron oxy(hydr)oxides, but it should be noted that dithionite can also dissolve acid volatile sulfides (ASV)-bound Fe(II) (Yücel et al., 2010).

Porewater dissolved inorganic nutrients (nitrate+nitrite, ammonium, phosphate and silicate) were determined as described method above (Grasshoff et al., 1983). Diffusive nutrient fluxes were calculated based on Fick's First Law of Diffusion as the following equation (Al-Rousan et al., 2004; Cheng et al., 2014; Mu et al., 2017):

$$F = \phi D_s (dC/dz)$$

Where F corresponds to the diffusion flux across sediment-water interface, dC/dz to the concentration gradient of nutrients across sediment-water interface, ϕ to the porosity of sediment, D_s to the actual molecular diffusion coefficient corrected for the sediment tortuosity.

Ullman and Aller (1982) proposed an empirical formula related to the actual diffusion coefficient, D_s, and porosity, ϕ:

$$D_s = \phi D_0 \qquad (\phi < 0.7)$$

$$D_s = \phi^2 D_0 \qquad (\phi > 0.7)$$

where D_0 is the self diffusion coefficient of ions at infinite dilution corrected by *in situ* temperature. For phosphate, nitrate, nitrite and ammonium D_0 values are used from Li and Gregory (1974) and for Si, D_0 values were used from Rebreanu et al. (2008) as $7.34x10^{-6}$ cm^2 s^{-1} for PO_4, $19.0x10^{-6}$ cm^2 s^{-1} for NO_3, $19.1x10^{-6}$ cm^2 s^{-1} for NO_2, $19.8x10^{-6}$ cm^2 s^{-1} for NH_4 and $11.7x10^{-6}$ cm^2 s^{-1} for Si, at 25 ˚C respectively. Porosity of wet sediments was determined by drying the surface layer sediment subsamples at 60 ˚C for 24 h.

Porewater diffusive, riverine and wastewater nutrient fluxes (normalized to NE Mediterranean shelf area) with atmospheric deposition (Kocak et al., 2010) were evaluated to determine quantification of internal and external nutrient sources for the NE Mediterranean shelf waters to understand biogeochemical cycling of key elements for further use in biogeochemical modeling and eutrophication management efforts of the oligotrophic Mediterranean Sea.

2.3 Results and Discussion

2.3.1 Porewater Nutrient Dynamics in the NE Mediterranean Sea

The core samples collected from the selected sites of the NE Mediterranean Sea (Figure 2.2) appeared to represent undisturbed particulate accumulations. Except for the Goksu River influenced region (St. 4), the upper part of the sediment columns was light brown. However, at a depth of 8-10 cm and below this depth, the sediment profile became darker suggested that there is a drop or decrease in redox potential. The sediment core sample obtained from St. 4 has yellowish brown color throughout the sediment column and look like coarse-grained sediment texture. In marine sediments, a number of organisms, such as bacteria, fungi, micro- or macro-fauna, are responsible for the aerobic degradation of organic matter (Jørgensen, 1996; Fenchel et al., 1998; Kristensen, 2000) in the uppermost sedimentary column where oxygen is used as electron acceptor. In general, in this redox zone, aerobic respiration, nitrification and sulfide reduction reactions take

place. In the suboxic zone and anoxic zone, anaerobic degradation of organic matter occur step wise by different functional types of bacteria (Fenchel et al., 1998; Kristensen, 2000). In these redox zones, manganese oxide reduction, denitrification, iron oxide reduction reactions in the suboxic zone and sulfate reduction, hydrolysis/fermentation, and carbon dioxide reduction reactions in the anoxic zone take place, respectively.

Biogeochemical cycling of key nutrients (N, P) is highly coupled to oxygen concentrations and metal (Fe, Mn) cycles (Williams, 1987; Jørgensen, 1996). The increase in dissolved inorganic phosphorous and iron concentrations in the Oxygen Minimum Zones (OMZs) is highly related to anoxic conditions in the marine environment as the role of sediments in the OMZs is important for dissolved iron and inorganic phosphate sources to the bottom water (Noffke et al., 2012). In the oligotrophic NE Mediterranean Sea with highly oxygenated deep waters and surface sediments, porewater nutrient concentrations displayed great variability within the obtained sediment core samples. Porewater reactive PO_4, NO_3, NH_4 and reactive Si concentrations throughout the sediment column ranged between 0.06 and 2.30 μM for reactive PO_4, 1.40 and 67.62 μM for NO_3, 0.45 and 120.55 μM for NH_4 and 1.22 and 154.30 μM for reactive Si, respectively (Figure 2.3). Porewater nutrient concentrations measured in the NE Mediterranean were greater than deep water nutrient values (Yılmaz and Tugrul., 1998) but comparable with the riverine nutrient concentrations in the studied region which will further be discussed below.

Seafloor can play a key role in rapid degradation of labile organic matter and nitrification/denitrification processes as well as other abiotic processes in the uppermost millimeters of sediment layer resulting in nutrient releases from the sediments (Christensen et al., 1988; Ignatieva, 1999; Rasheed, 2004; Al-Rousan et al., 2004; Hille et al., 2005; Rasheed et al., 2006; Rydin et al., 2011; Cheng et al., 2014; Mu et al., 2017). Expectedly, nutrient concentrations (PO_4, NH_4, Si) increased with depth throughout the sediment column indicating organic matter degradation processes took place in the first 3-10 centimeters of the sediment column in the NE Mediterranean Sea. The decrease in the nitrate concentrations

with depth within the sediment column suggested denitrification process (Jørgensen, 1996) in the coastal zone (St. 1) having eutrophic properties (Tugrul et al., 2018). Though coastal zone (St. 4) influenced by the Goksu River (Figure 2.2), having greater volume fluxes than Lamas River (Tugrul et al., 2009; Kocak et al., 2010), displayed eutrophic properties (Tugrul et al., 2018), there was no apparent decrease in nitrate concentrations within the sediment column suggested oxic respiration throughout the sediment column as also recorded in the sediment core samples obtained from shelf break (St. 3), offshore (St. 4) and reference station (St.5) (Figure 2.3).

The porewater was found oxic throughout the sediment column in the low chlorophyll regions of South Pacific Gyre having low primary production, low sedimentation rate and low organic carbon content in the uppermost centimeters of the sediment column (D'Hondt et al., 2009). In a recent study performed in the oligotrophic Eastern Mediterranean Sea, oxygen microprofiles indicated the oxygenated surficial (0-30 cmbs) sediments (Van Santvoort et al., 2002) as also inferred from the NO_3 profiles obtained in this study (Figure 2.3) suggesting the availability of oxic sediment column in the uppermost 30-45 centimeters of the NE Mediterranean subseafloor having low chlorophyll concentrations in the surface layer (Tugrul et al., 2018) as also recorded in the South Pacific Gyre (D'Hondt et al., 2009).

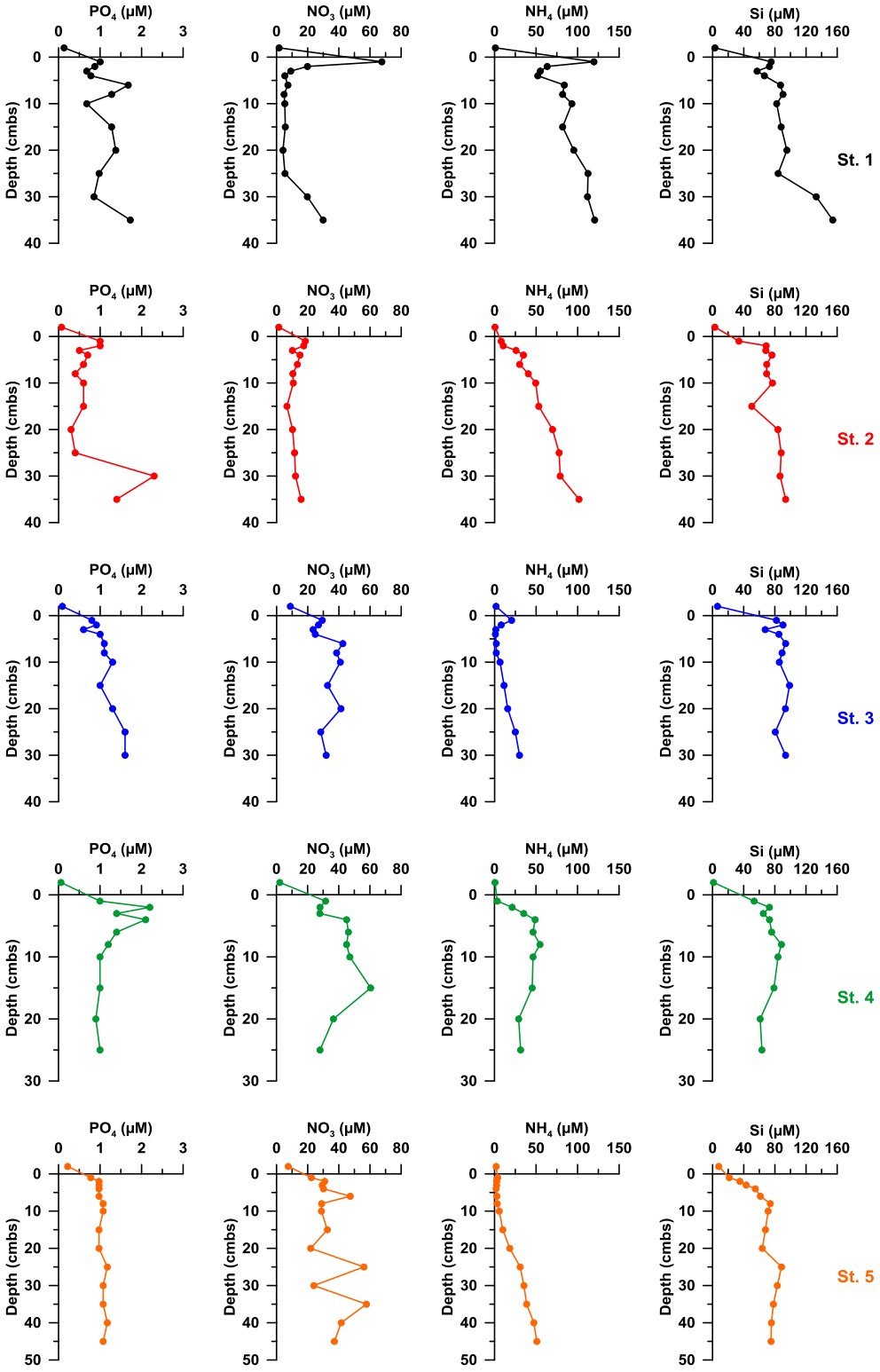

Figure 2.3. Sediment porewater nutrient concentrations in the NE Mediterranean Sea.

2.3.2 Solid-phase Sediment Geochemistry in the NE Mediterranean Sea

Organic matter geochemistry of the sediments has been affected by a series of redox reactions (Jørgensen, 1996) as well as terrestrial inputs of the particulate inorganic/organic matter that might be transported to offshore regions of the continental seas (Middelburg et al., 1993; Yemenicioglu and Tunc, 2013; Erdogan, 2014; Akcay, 2015, Ermiş, 2017; Deininger and Frigstad, 2019; Katz et al., 2020). In the Eastern Mediterranean Sea, surface sediment geochemistry and grain size distributions have been studied extensively during the last decades (Eijsink et al., 2000; Yemenicioglu and Tunc, 2013; Erdogan, 2014, Akcay, 2015; Ermiş, 2017), with the limited number of studies based on sediment core samples to understand organic matter geochemistry (sedimentation, degradation, accumulation and burial of organic carbon) of the upper 25-40 cm sedimentary column (Van Santvoort et al., 2002; Katz et al., 2020). Surface sediment TC (TOC+TIC) concentrations obtained in this study varied between 3.31 and 6.79 mmol/g dw (dry weight) with maximum concentrations recorded in the uppermost centimeters of the core sample obtained from Goksu River influenced area (Figure 2.4) having minimum porosity at the sediment surface. On the contrary to TC distributions, lower TOC concentrations were measured in uppermost 1-2 centimeters of the core sample obtained from Goksu River influenced area (0.26-0.32 mmol/g dw). TOC concentrations in the surface sediments of other core samples ranged from 0.51 to 0.70 mmol/g dw with the greatest value recorded in the St.2 (Figure 2.4). Regional variations of TN distributions in the study region were very similar to TOC distributions and ranged between 0.02-0.07 mmol/g dw. Terrestrial inputs of nutrients and organic matter modify the organic matter composition and concentrations and grain size distributions of the sediment layer (Yemenicioglu and Tunc, 2013; Akcay, 2015). Moreover, differences in the sedimentation rates and currents and wave energy affect distributions of geochemical properties (De Falco et al., 2004; Katz et al., 2020). According to results of the five major river data, maximum concentrations of suspended matter (TSS) were recorded in the Goksu

River among the other regional rivers (Tugrul et al., 2009) and fine-grained sediments were carried to the central and offshore regions due to regional wave actions and currents (De Falco et al., 2004; Katz et al., 2020) resulting in carbonate-rich sediment column in the Goksu River influenced coastal area (Figure 2.4).

The TOC and TN concentrations measured in this study agreed with the organic matter geochemical properties from the previous studies performed in the oligotrophic Eastern Mediterranean Sea (Eijsink et al., 2000; Erdogan, 2014, Akcay, 2015; Ermiş, 2017; Katz et al., 2020). The TOC concentrations of the sediment column (0.28-0.84% in the 1-45 cmbs) recorded in this study were in agreement with the TOC contents obtained from South Pacific Gyre sediment core samples (0.17-0.52% in the 3 cmbs-1.47 mbsf) by the study of D'Hondt et al. (2009) having similar biochemical properties with the oligotrophic NE Mediterranean Sea with low chlorophyll and nutrient concentrations (Tugrul et al., 2018) suggesting that oxic respiration is the major organic matter degradation process in the uppermost sedimentary column of the oligotrophic marine environments as also observed from the oxygen microprofiles obtained from the surficial (0-30 cmbs) Eastern Mediterranean sediments (Van Santvoort et al., 2002).

Vertical profiles of TOC concentrations and vertical profiles (in St.2 and 5) suggested that organic matter degradation occurred in the uppermost centimeters of the sediment column reaching a constant value down to 8-10 cm indicating refractory organic matter pool below this layer. The r-Fe concentrations varied between 12.7-47.8 μmol/g dw throughout the sediment column of the obtained core samples. The results of r-Fe concentrations of this study were very similar to the recent studies performed in the NE Mediterranean surface sediments (Ermis, 2017) and Eastern Black Sea core samples (Yucel et al., 2010). Vertical profiles of r-Fe concentrations were very similar to observed in the TOC profiles; high concentrations in the upper sedimentary column which decreased with sediment depth suggesting organic matter degradation by iron reduction in the NE

Mediterranean subseafloor. These findings strongly suggested the coupling between reactive iron and organic carbon in the NE Mediterranean as recently explored from the studies of Ermiş (2017) and Katz et al. (2020) in the region. Further studies should be performed about sediment iron speciation and its coupling with the redox sensitive elements (Mn, P, S, U, V, Mo) to understand the intersections between sediment geochemistry (organic carbon degradation and burial) and redox sensitive porewater macro- and micro-nutrients, available for the marine organisms in the NE Mediterranean Sea. As a result, sediment porewater nutrients and solid state geochemical parameters should be measured and integrated to marine monitoring programmes to attain Good Environmental Status (GES) of the Eastern Mediterranean Sea.

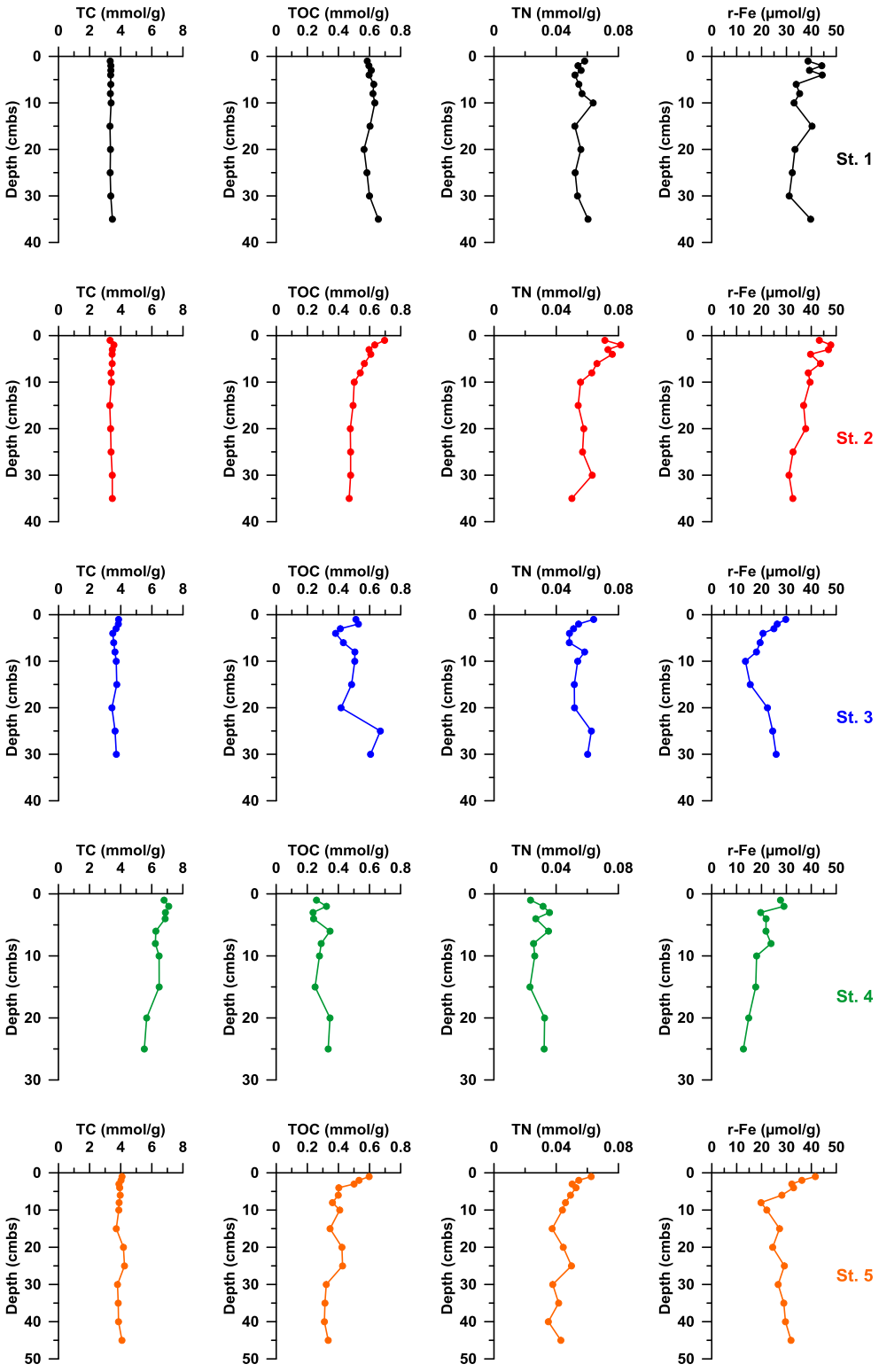

Figure 2.4. Solid state total carbon (TC), total organic carbon (TOC), total nitrogen (TN) and reactive iron (r-Fe) concentrations in the NE Mediterranean Sea.

Vertical profiles of porewater nutrients (Figure 2.3) and also solid-phase sediment organic matter (C, N) and reactive iron concentrations (Figure 2.4) revealed that organic matter mineralization was occurred by oxic/aerobic respiration in the upper 30-45 cmbs in the offshore regions of the NE Mediterranean Sea having low chlorophyll concentrations in the surface layer (Tugrul et al., 2018) and also low sedimentation rate (0.005-0.014 cm/y) (Katz et al., 2020) which are typical for (ultra-)oligotrophic and deep-sea environments. On the other hand, denitrification process occurred in the coastal zone (St. 1) where nitrate concentrations decreased with increasing sediment depth. On the other hand, there was no apparent decrease in nitrate concentrations within the sediment column suggested oxic respiration throughout the sediment core samples obtained from shelf break (St. 3), offshore (St. 4) and reference station (St. 5) (Figure 2.3). Moreover, vertical profiles of r-Fe and TOC concentrations indicated high concentrations in the upper sedimentary column which decreased with sediment depth suggesting organic matter degradation by iron reduction in the NE Mediterranean subseafloor. In order to understand past and future implications of the sediment biogeochemistry and the distributions of key elements incorporated into biomass (C, N, P, metals), voltammetric determination of redox dependent elements (oxygen, hydrogen sulfide, manganese and iron) by micro-sensors should be needed for a better understanding of the NE Mediterranean Sea ecosystem dynamics.

2.3.3 Riverine, Wastewater, Atmospheric and Sediment Porewater Nutrient Dynamics in the NE Mediterranean Sea

The seasonal and regional averages of nutrient concentrations measured in the five regional rivers (Figure 2.2) for the 2008-2015 period are presented in Table 2.3, showing remarkable seasonal and regional variations with the peak values reached in the wet winter-spring seasons. Rivers often transport nutrients that can enrich coastal plankton communities (Farrow et al., 2019). The development of eutrophication in the coastal sites of the NE Mediterranean shelf waters has been

experienced due to riverine and wastewater discharges (Dogan-Saglamtimur and Tugrul 2004; Tugrul et al., 2009; 2011; 2016; 2018). Atmospheric nutrient inputs, both dry and wet deposition, have also remarkable contribution to sustain primary production in the Northeastern Mediterranean Sea (Kocak et al., 2010; Kocak, 2015), especially in dry summer-autumn period when the volume fluxes of the regional rivers decrease. The results of riverine nutrient concentrations indicated that maximum nutrient concentrations were measured in the contaminated Seyhan and Ceyhan Rivers whilst lowest concentrations were determined in the least contaminated Lamas River having the lowest volume flux. Nutrient inputs increased in the winter-spring periods due to enhanced flow rates and nutrient contents of the major rivers. Maximum concentrations of seasonal TP (12-33 μM) and PO_4 (3-29 μM) were recorded in Seyhan and Ceyhan Rivers. The least contaminated small Lamas River waters contained lower nutrient concentrations (TP: 0.1-9.6 μM; PO_4: 0.02-1.37 μM). Nitrate and reactive silicate contents of the five rivers are seasonally variable (NO_3: 64.1-167 μM; Si: 84.2-169 μM) with the Si/NO_3 ratio ranging seasonally between 0.73-2.0.

Table 2.3. Average concentrations of dissolved inorganic nutrients in the five regional rivers between 2008 and 2015

River (Discharge; m^3/s*)	Season	PO_4 (μM)	NO_3 (μM)	NH_4 (μM)	Si (μM)	Si/NO_3	NO_3/PO_4
Ceyhan (144)	Autumn	0.97	118.76	12.06	145.27	1.27	170.9
	Winter	3.23	167.07	17.28	141.29	1.01	147.0
	Spring	1.05	141.05	18.82	135.3	1.05	218.2
	Summer	0.97	125.13	7.94	169.01	1.45	167.5
Seyhan (168)	Autumn	6.32	166.73	40.00	98.84	0.73	43.5
	Winter	2.04	92.80	39.89	91.23	1.57	75.2
	Spring	4.04	117.82	14.89	93.68	1.28	99.6
	Summer	4.31	93.88	8.72	89.92	1.55	97.7
Berdan (6)	Autumn	2.48	95.86	12.68	87.55	1.01	87.5
	Winter	1.57	97.36	23.03	127.74	1.47	115.8
	Spring	1.34	100.44	12.9	87.35	0.97	113.6
	Summer	2.22	84.35	8.39	88.82	1.12	69.5
Lamas (3)	Autumn	0.12	94.46	1.08	86.28	0.95	932.1
	Winter	0.08	102.98	0.69	99.49	1.04	1631.6
	Spring	0.28	93.37	1.84	84.17	0.96	991.9
	Summer	0.11	83.96	1.54	110.14	1.51	1303.4
Göksu (45)	Autumn	0.64	64.11	10.29	126.94	2.0	140.8
	Winter	0.53	66.72	2.82	101.75	1.74	171.0
	Spring	0.69	68.17	3.77	118.26	1.96	152.9
	Summer	1.05	72.97	4.24	108.46	1.67	237.7

* Discharge rates were retrieved from Kocak et al. (2010).

Wastewater nutrient concentrations were much greater than measured in the regional rivers and showed marked spatial variability (Table 2.4). Maximum concentrations of PO_4 and NH_4 were measured in the Mersin Discharge. KromSan and Toros Discharges had moderately low concentrations. Minimum nutrient concentrations were recorded in Antalya Discharge showing effective biochemical treatment in this region. Though high concentrations of wastewater nutrients recorded in the studied regions, volume fluxes of wastewater discharges were lower than riverine volume fluxes (Table 2.2), but still resulting in local pollution and eutrophication in the coastal areas of the NE Mediterranean as experienced in İskenderun and Mersin inner bays (Tugrul et al., 2009; 2011; 2016).

Table 2.4. Concentrations of wastewater dissolved inorganic nutrients between 2006 and 2009

Wastewater (Discharge; m^3/s*)	Season	PO_4 (μM)	NO_3 (μM)	NH_4 (μM)	Si (μM)	Si/NO_3	NO_3/PO_4
İskenderun Discharge (0.26)	Autumn	147.10	259.73	42.04	634.67	7.26	1.9
	Winter	52.58	666.70	22.88	320.10	0.59	13.6
	Spring	46.00	550.30	12.19	482.90	0.89	33.4
	Summer	97.60	621.40	207.03	665.75	1.18	9.7
KromSan Discharge (0.006)	Autumn	0.25	602.25	110.40	428.00	0.72	5613.1
	Winter	0.15	708.40	69.50	104.65	0.14	5520.8
	Spring	0.29	327.50	101.50	142.10	0.76	2043.0
	Summer	0.09	663.50	49.89	203.60	1.11	7372.2
Toros Discharge (0.014)	Autumn	2.36	1937.50	193.10	455.15	0.25	1331.1
	Winter	2.02	1628.50	158.81	369.00	0.23	901.6
	Spring	1.52	2021.00	60.25	539.40	0.27	2607.0
	Summer	2.40	2026.90	216.73	321.65	0.15	847.6
Mersin Discharge (0.60)	Autumn	171.00	4.30	1828.50	258.50	64.04	0.03
	Winter	135.55	94.96	2151.00	276.70	11.48	1.7
	Spring	188.00	34.25	2707.00	281.60	11.84	0.2
	Summer	174.33	20.79	1890.00	278.33	27.04	0.1
Antalya Discharge (0.45)	Autumn	31.40	360.46	3.38	350.50	115.97	17.6
	Winter	83.39	84.40	155.23	365.10	13.45	1.3
	Spring	88.25	500.20	559.33	319.25	2.58	14.1
	Summer	73.53	653.20	97.23	307.33	4.77	14.6

* Discharge rates were retrieved from Tugul et al. (2009).

Atmospheric nutrient concentrations in aerosols determined from a long-term observation (Kocak et al., 2010) showed that water soluble reactive PO_4 and Si concentrations ranged from 0.03 to 6.40 nmol m^{-3} for PO_4 and 0.04 to 26.27 nmol m^{-3} for Si. Water soluble NO_3 and NH_4 concentrations varied between 0.2-258.8 nmol m^{-3} and 0.1-473.2 nmol m^{-3}, respectively. For rainwater samples obtained from the same study, the volume weighted mean values for PO_4, Si, NO_3 and NH_4 were calculated as 0.7, 1.9, 44 and 46 μM, respectively. comparison of atmospheric deposition (dry+wet) (Kocak et al., 2010) showed that aerosol and rainwater reactive Si concentrations measured in the NE Mediterranean were much lower than measured Si concentrations in the riverine and wastewater concentrations, but PO_4 and NO_3 concentrations were comparable to those measured in the rivers. Aerosol and wastewater samples were highly enriched by NH_4 compared to riverine NH_4 concentrations.

2.3.4 Comparison of Internal and External Nutrient Fluxes and Their Elemental Compositions (Si/N/P) in the Northeastern Mediterranean Sea

In this study, the quantification of all source terms of nutrients (rivers, wastewaters, porewater diffusive nutrient fluxes, atmospheric inputs (based on the study performed by Kocak et al. (2010)) was made to assess nutrient loads for the NE Mediterranean Sea having oligotrophic properties in its offshore waters (UNEP, 1989; Yılmaz and Tugrul, 1998; Kress and Herut, 2001; Krom et al., 2004; Tugrul et al., 2016; 2018). Since riverine and wastewater inputs have highly affected coastal zones of the NE Mediterranean Sea, fluxes were normalized to the area of shelf regions of the NE Mediterranean Sea.

It should be noted that the total nutrient fluxes were assumed to be greater than diffusive nutrient fluxes due to other processes at sediment-water interface such as bioturbation-irrigation (Barbanti et al., 1992) and also biotic/abiotic processes for the organic matter degradation in the uppermost millimeters of sediment layer (Christensen et al., 1988; Ignatieva, 1999; Rasheed, 2004; Al-Rousan et al., 2004; Hille et al., 2005; Rasheed et al., 2006; Rydin et al., 2011; Cheng et al., 2014; Mu et al., 2017). In this study, calculated diffusive nutrient fluxes based on the Fick's First Law of Diffusion presented in Table 2.5 indicated remarkably high nutrient fluxes from the sediment into the deep waters of the NE Mediterranean Sea. Maximum nutrient fluxes were calculated in the river-influenced coastal region indicated that human-induced pressures not only affect the coastal surface waters, but also affect sediment porewater nutrient dynamics due to increase in primary productivity and hence sedimentation in the eutrophic coastal areas. Expectedly, lower porewater diffusive nutrient fluxes were calculated in the oligotrophic offshore regions of the NE Mediterranean Sea (Table 2.5).

Table 2.5. Diffusive nutrient fluxes from sediment layer to the deep waters in the NE Mediterranean

Station	PO_4 (mmol m^{-2} yr^{-1})	NO_3 (mmol m^{-2} yr^{-1})	NH_4 (mmol m^{-2} yr^{-1})	Si (mmol m^{-2} yr^{-1})
1	0.57	66.87	46.23	77.20
2	0.36	18.55	12.79	50.77
3	0.42	50.11	22.30	60.81
4	0.35	26.50	11.71	36.62
5	0.36	43.43	2.81	28.48

Redox dependent benthic nutrient fluxes would enhance algal production (Christensen et al., 1988; Ignatieva, 1999; Rasheed et al., 2006). In a study conducted in the oligotrophic Eastern Mediterranean continental shelf, the phosphate and nitrate fluxes into the water column supported as much as 11.7% and 2% of the phytoplankton P and N demand, respectively (Christensen et al., 1988). Furthermore, it was observed that porewater nutrient concentrations revealed reduced conditions in these shelf sediments where nitrate depletion was seen in the uppermost centimeters of the collected sediment cores (Jørgensen, 1996) as also experienced in NE Mediterranean shelf region by this study. In this study, calculated diffusive nutrient fluxes were very similar to the study of Christensen et al. (1988) and Rasheed et al. (2006) performing their studies in the oligotrophic regions, but much lower than the studies by Ignatieva (1999) and Noffke et al. (2012) where the studies were conducted in the highly eutrophic regions having suboxic and anoxic/sulfidic deep waters.

Mean annual nutrient fluxes in the NE Mediterranean shelf region were calculated (Table 2.6) for both external and internal sources and the contribution of each source term was quantified in the NE Mediterranean Sea (Figure 2.5). In the NE Mediterranean shelf waters, total nutrient fluxes for PO_4, NO_3, NH_4 and Si were calculated as 6.80, 303.71, 88.90 and 221.94 mmol m^{-2} yr^{-1}, respectively. The results of the source assessment of nutrient fluxes to the NE Mediterranean Sea indicated that the major contribution of nutrients to the NE Mediterranean coastal area was assigned as riverine nutrient inputs for phosphate, nitrate and reactive

silicate. Atmospheric inputs (Kocak et al., 2010) have remarkable contribution for the ammonium fluxes to the NE Mediterranean having limited inputs in terms of reactive silicate (Figure 2.5). Contribution of wastewater phosphate and ammonium fluxes to the NE Mediterranean was also markedly high and much greater than wastewater nitrate and silicate inputs. In this study, contribution of porewater diffusive nutrient fluxes to the total nutrient fluxes in the NE Mediterranean was calculated as 5.8% for PO_4, 12% for NO_3, 19% for NH_4 and 22% for reactive Si, respectively (Figure 2.5). The increase in dissolved inorganic phosphorous and iron concentrations in the eutrophic and suboxic/anoxic/sulfidic regions is highly related to redox conditions in the marine environment as the role of sediments in these regions has important for dissolved iron, inorganic phosphate and ammonium sources to the bottom water (Noffke et al., 2012). Furthermore, in the eutrophic and hypoxic/anoxic/sulfidic Baltic Sea, the intrusion of oxygen-rich North Sea waters into the Eastern Gotland Basin decreased to releases of inorganic phosphate and ammonium from deep sediments (Sommer et al., 2017) which also showed the redox-dependency on the benthic nutrient dynamics in this region. Though dissolved oxygen concentrations were at saturation levels in the NE Mediterranean upper layer (Tugrul et al., 2016; 2018) with highly oxygenated deep waters, the contribution of porewater diffusive nutrient fluxes was markedly high. Contribution of diffusive nutrient inputs was much greater than wastewater nutrient inputs for nitrate, ammonium and reactive silicate, but lower than phosphate due probably to adsorption of phosphate onto metal oxides (Mortimer, 1942 as referenced in Nteziryayo and Danielsson, 2018) in the oxygenated surface sediments of the NE Mediterranean Sea.

Table 2.6. External and internal nutrient sources for the NE Mediterranean (Atmospheric nutrient fluxes were retrieved from the study of Kocak et al. (2010).)

Source	PO_4 (mmol m^{-2} yr^{-1})	NO_3 (mmol m^{-2} yr^{-1})	NH_4 (mmol m^{-2} yr^{-1})	Si (mmol m^{-2} yr^{-1})	Si/NO_3 (Molar)	NO_3/PO_4 (Molar)
Sediment	0.39	36.3	17.2	48.0	1.32	91.8
Atmospheric	0.69	125.0	38.0	1.43	0.01	181.2
River	4.45	139.4	22.4	168.9	1.21	31.3
Wastewater	1.27	3.1	11.3	3.66	1.19	2.4
Total	6.80	303.71	88.90	221.94	0.73	44.7

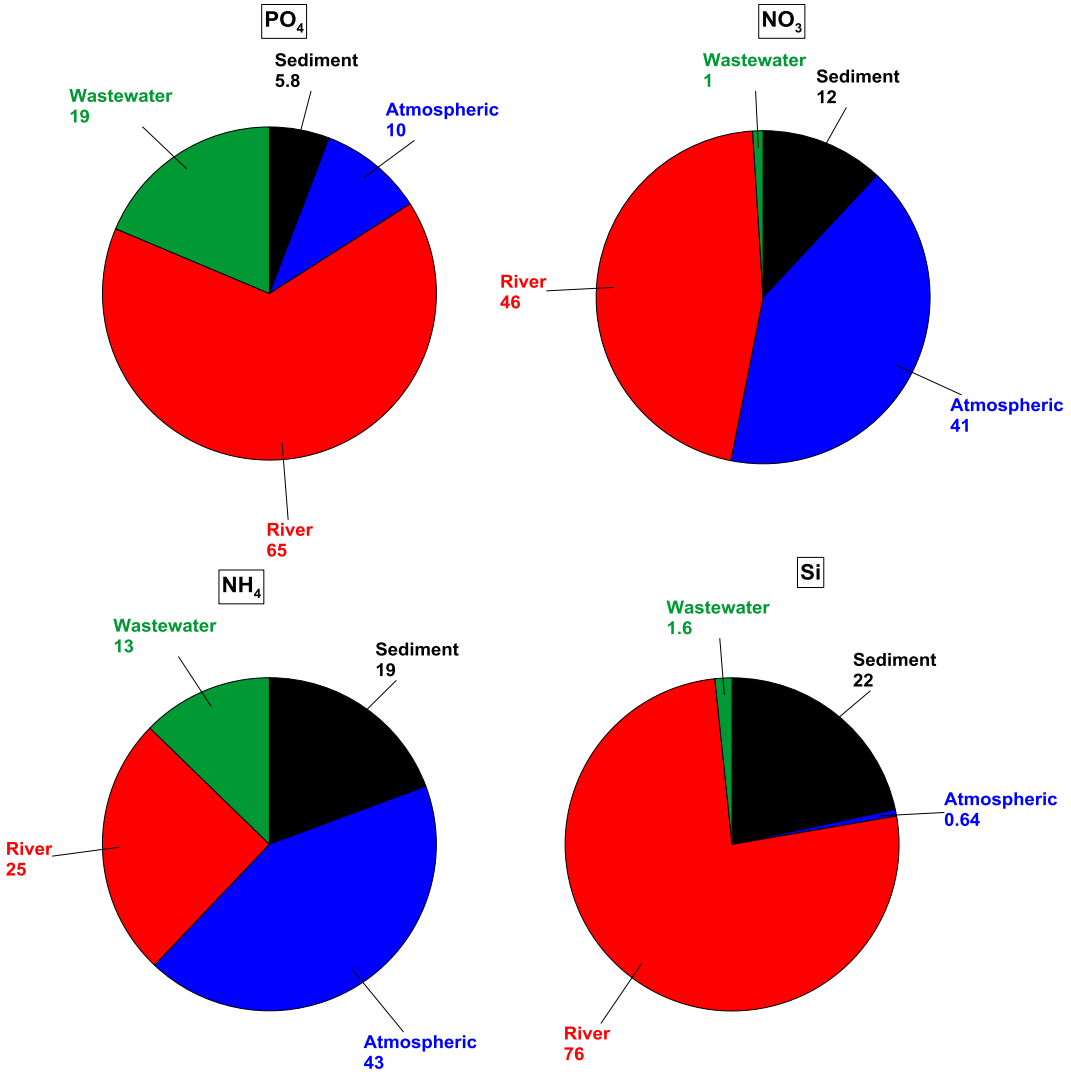

Figure 2.5. Contribution of sources of nutrients for the NE Mediterranean shelf waters (%).

The eastern Mediterranean deep water is characterized by high N/P molar ratios (Krom et al., 1991, Yılmaz and Tugrul, 1998) due to internal and external sources with high N/P molar ratios (Krom et al., 2004; Kocak et al., 2010) as well as lack of feedback mechanisms for bio-available N through denitrification in the sediment and water column (Krom et al., 2004). Positive nutrients (Si, N, P) fluxes indicated sediment layer in the NE Mediterranean shelf acts as a source for nutrients. The N/P molar ratios calculated for the source terms of nutrients (Table 2.6, Figure 2.6), except for wastewaters (riverine, atmospheric and sediment diffusive inputs), were greater than classical Redfield Ratio (N/P=16), reflecting high N/P molar ratios in the Mediterranean deep waters (Krom et al., 1991, Yılmaz and Tugrul, 1998). As a result, it can be concluded benthic nutrient fluxes with high N/P molar ratios and the nutrient dynamics at the sediment-water interface in the NE Mediterranean shelf region might be also one of the reasons addressing why the eastern Mediterranean is P-limited as also experienced in the previous studies (Krom et al., 1991; 2004; Yılmaz and Tugrul, 1998; Tufekci et al., 2013; Tugrul et al., 2011; 2016; 2018). It should be also noted that lower Si/N (Si/NO_3=0.73) and high N/P (NO_3/PO_4=44.7) molar ratios in the total nutrient inputs and also from the linear regressions of the Si/N/P plots compared to classical Redfield Ratio are very likely to modify phytoplankton composition and abundance in the phosphorus deficient NE Mediterranean productive shelf waters leading to development of mesotrophic/eutrophic conditions in the NE Mediterranean Sea. Therefore, quantification of nutrients is needed for further use in biogeochemical modeling of the oligotrophic Mediterranean Sea and its ecosystem dynamics which are of critical importance to attain Good Environmental Status (GES) for the Eastern Mediterranean Sea.

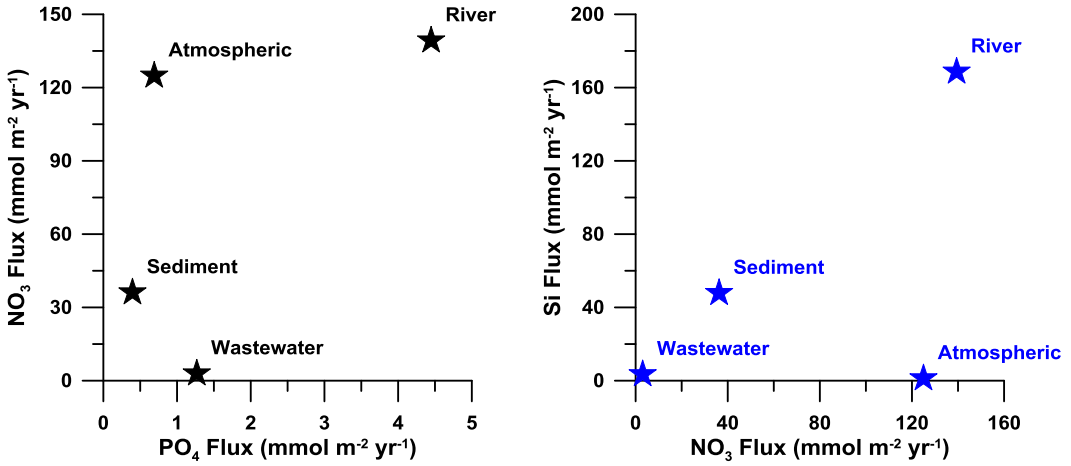

Figure 2.6. N vs. P and Si vs. N plots of the nutrient fluxes in the NE Mediterranean Sea.

2.4 Conclusions

Sediment porewater nutrient (Si, N, P) and sediment organic matter biogeochemistry were studied in the NE Mediterranean Sea. Porewater diffusive nutrient fluxes were also calculated for the comparison with the external nutrient inputs in the NE Mediterranean shelf region. The study results indicated a series of redox reactions; organic matter mineralization was occurred by oxic/aerobic respiration in the upper 30-45 cmbs in the offshore regions of the NE Mediterranean Sea having low surface water chlorophyll concentrations and low sedimentation rates which are typical for (ultra-)oligotrophic and deep-sea environments whilst denitrification process dominated in the river influenced coastal region. Vertical profiles of the reactive iron concentrations also suggested microbial iron reduction in the NE Mediterranean subseafloor. Determination of redox dependent benthic nutrient fluxes is critical for the management of eutrophication status of coastal marine ecosystems since high nutrient inputs from the surface sediment can support benthic community and productivity in highly polluted sites of the inner bays. Riverine and wastewater nutrient fluxes were also determined in the NE Mediterranean and using atmospheric (wet+dry deposition)

nutrient fluxes, all the external inputs were quantified and compared with the benthic nutrient fluxes. Results of this study indicated remarkable contribution of porewater diffusive nutrient fluxes to the total nutrient budget in the NE Mediterranean Sea. Lower Si/N and higher N/P molar ratios in the total nutrient inputs are very likely to modify phytoplankton composition and abundance in the phosphorus deficient NE Mediterranean productive shelf waters leading to development of mesotrophic/eutrophic conditions. Another important source term of allochthonous nutrients is the submarine groundwater discharge which is not determined in the scope of this study though its contribution was markedly high in the Mediterranean Sea (Rodellas et al., 2015). The magnitude of volume fluxes, the nutrient concentrations and composition of the submarine groundwater discharge in the NE Mediterranean Sea located on one of the widest shelf areas should be needed for further use in biogeochemical modeling of the oligotrophic Mediterranean Sea and its ecosystem dynamics. It is also important that sediment porewater nutrients and solid-phase geochemical parameters should be determined and integrated to marine monitoring programmes to attain Good Environmental Status (GES) of the Eastern Mediterranean Sea.

Acknowledgements

This study has been supported by DEKOSIM (Centre for Marine Ecosystem and Climate Research, Project Code BAP-08-11-DPT.2012K120880) Project and TUBA-GEBIP Program of the Turkish Academy of Sciences. Riverine and wastewater samples were obtained by the projects (107G066, 111G152) supported by the Scientific and Technological Research Council of Turkey (TUBITAK). We would like to thank the cruise participants, crew of R/V Bilim-2 and METU-IMS technical personnel for helping biogeochemical sampling and analyses.

CHAPTER 3

IMPACTS OF EUTROPHICATION AND DEOXYGENATION ON THE POREWATER AND SEDIMENT BIOGEOCHEMISTRY IN THE MARMARA SEA

Abstract

Seafloor biogeochemistry can dramatically shift in response to deoxygenation and eutrophication-driven organic carbon production. In such conditions, biogeochemical cycling of key nutrients can be highly coupled to oxygen concentrations and metal redox cycles, often leading to the increase in dissolved nutrients and metals concentrations in the deep waters. This chapter aims to understand impacts of deoxygenation and coastal eutrophication on the sedimentary biogeochemical processes in the deoxygenating Marmara Sea, rapidly changed due to the pressure of anthropogenic impacts. Therefore, porewater concentrations of nutrients, dissolved iron, hydrogen sulfide and major elements were measured from the obtained core samples in the Marmara Sea. The study results indicated maximum concentrations of porewater reactive silicate, phosphate and ammonium were measured in the eutrophic and suboxic/anoxic/sulfidic İzmit Bay. Lower concentrations were recorded in the Southern Marmara Sea having lower surface water primary productivity and more oxygenated deep waters. Porewater nitrate, sulfate and hydrogen sulfide profiles showed organic matter degradation processes in the upper 20-30 cmbs have been mediated by oxic respiration, denitrification and sulfate reduction whilst organic matter decomposition was limited by oxic respiration in the upper sedimentary column in the southern Marmara Sea. Moreover, the distribution of porewater sulfate, hydrogen sulfide, and major elements throughout the sediment cores obtained specifically from the İzmit Bay, suggested principal biogeochemical and early

diagenetic processes such as anaerobic oxidation of methane (AOM), carbonate precipitation, Fe-reduction, Fe-S precipitation and low-temperature silicate diagenesis. Sediment total organic carbon distributions throughout the sediment column and the calculated redox dependent benthic nutrient fluxes in the Marmara Sea suggested high rates of organic matter decomposition and limited trapping of nutrients in the benthic interface, which would further enhance eutrophication in the Marmara Sea, analogous to benthic 'vicious cycle' in the much shallower Baltic Sea.

3.1 Introduction

The oxygen minimum zones (OMZs) are referred to the portion of the water column that have volume or depth interval in which oxygen concentrations are less than 0.15 mL/L (6.7 μM) (Cline and Richards, 1972). Biogeochemical cycling of key nutrients (N, P) is highly coupled to oxygen concentrations and metal (Fe, Mn) cycles (Williams, 1987; Jørgensen, 1996). For example, OMZs play an essential role in the global nitrogen cycle where different forms of nitrogen, having different oxidation states as ammonium, nitrite, nitrate, nitrous oxide, molecular nitrogen, may be processed by different bacterial processes (Paulmier and Ruiz-Pino, 2009 and references therein).

The Marmara Sea, a typical example of two-layer enclosed seas, connects the Black Sea to the Mediterranean via the two shallow and narrow straits, called İstanbul (Bosporus) and Çanakkale (Dardanelles) Straits and this oceanographic system is also called the Turkish Straits System (TSS) (Ünlüata et al. 1990; Beşiktepe et al. 1994; Ediger et al., 2016 and references therein). Marmara Sea's distinctly two-layer ecosystem has distinct biogeochemical properties due to water exchanges between the Black Sea and the Mediterranean Sea through TSS (Polat, and Tugrul, 1995; Tugrul and Polat, 1995, Tugrul et al., 2002). Marmara Sea ecosystem has been highly polluted by the Black Sea inflow and direct discharges mainly from the İstanbul city in recent decades (Tuğrul and Morkoç, 1989; Tugrul

and Polat, 1995; Ediger et al., 2016; Yalçın et al., 2017; Tan and Aslan, 2020). The eutrophication problem in the Northwestern Black Sea collapsed Black Sea ecosystem and fisheries (Mee, 1992; Tuğrul et al., 2014), leading to similar changes in the Sea of Marmara during the last two decades (Polat and Tugrul, 1995; Ediger et al., 2016; Yalçın et al., 2017). Marmara Sea two-layer ecosystem has also particular importance due to strong density gradient between water masses highly influencing physical mixing processes (Beşiktepe et al. 1994) and dynamics of dissolved nutrients and oxygen (Tugrul et al., 2002; Ediger et al., 2016; Yalçın et al., 2017). Recent studies performed in the Marmara Sea indicated that dissolved oxygen (DO) concentrations are at saturation levels in the thin upper layer of Black Sea origin and decreased rapidly in the permanent pycnocline coinciding with nutricline since primary production is confined to upper mixed layer for most of the year. The major source of the DO in the Marmara Sea lower layer is Mediterranean waters highly enriched in DO and transported by Dardanelles undercurrent. However, the steep halocline limits ventilation of deep waters by the DO rich surface waters. Therefore, DO deficiency in the Marmara Sea deep waters increases from the Dardanelles to Bosporus Strait (Tugrul and Polat, 1995; Tugrul et al., 2002; Ediger et al., 2016; Yalçın et al., 2017). The increasing organic matter inputs in the upper layer and limited ventilation of deep waters have dramatically reduced DO concentrations in the deep waters of Marmara Sea in the last decades, detected by the vertical profiles of DO in the Çınarcık Basin, eastern Marmara Sea (Figure 3.1).

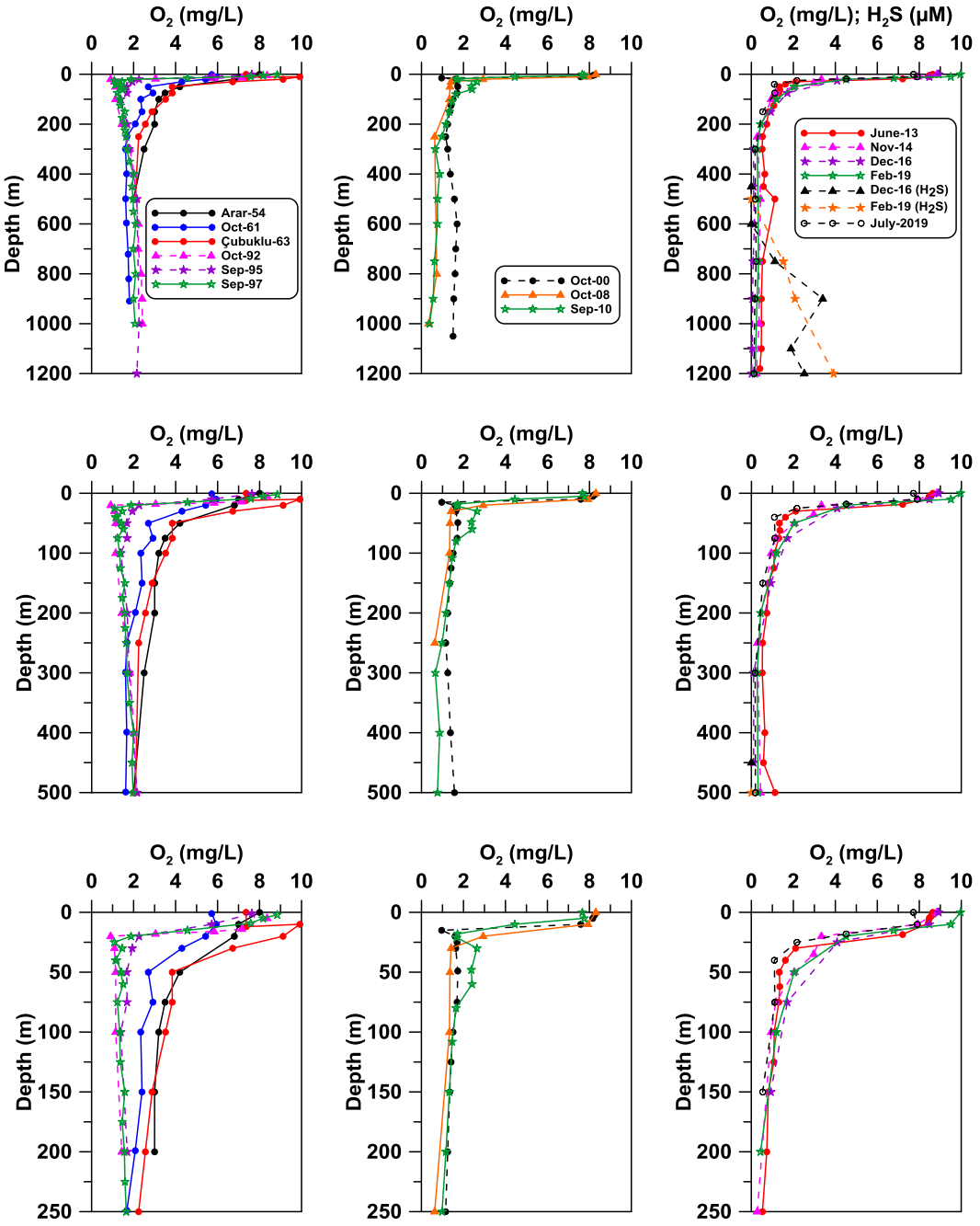

Figure 3.1. Vertical profiles of dissolved oxygen and hydrogen sulfide (in 2019) concentrations in the eastern Marmara Sea in 1954-2019 period (Historical data were taken from the METU-IMS database).

Marmara Sea is also a region of particular importance since it is a tectonically active marine basin, intersected in an east-west direction by the northern branch of

the North Anatolian Fault (N.A.F.) (Le Pichon et al. 2001; Géli et al., 2008) enabling the Marmara Sea to host multiple gas seeps (or cold seeps), emitting fluids into seawater at the seafloor (Ruffine et al., 2018; Hélène et al., 2020). The anaerobic oxidation of methane (AOM) was firstly determined in the 1970s and highly coupled to sulfur cycle as sulfate reduction mediated by anaerobic methanotrophic archaea (ANME) and sulfate-reducing bacteria (SRB) (Reeburgh, 1976; 1980; Cui et al., 2015) as well as two more different processes of AOM depending on the different electron acceptors: (a) nitrate/nitrite and (b) metal ions (Mn^{4+} and Fe^{+3}) (Cui et al., 2015). In the Marmara Sea, high concentrations of methane in the sediment column of the gas emission sites lead to depletion of sulfate by the AOM as the following reaction (Halbach et al., 2002; Çağatay et al., 2004; Tryon et al., 2010; Ruffine et al., 2018; Çağatay et al., 2018):

$$CH_4 + SO_4^{2-} => HCO_3^- + HS^- + H_2O$$

Recent studies in different basins of the Marmara Sea indicated that the emissions of gases in the Western and Central Highs were thermogenic whilst the gases emitted from the Eastern Marmara Sea were primarily microbial activities in the sediment column (Yang et al., 2018 and references therein).

Historical data sets obtained by METU-IMS with the results of this study indicated that, in the eastern Marmara Sea, dissolved oxygen concentrations of deep waters (>1000 m) decreased from 2.3 mg/L (72 μM) in 1995 to <0.25 mg/L (<7.8 μM) in 2019, indicating a rapid deoxygenation during the last two decades (Figure 3.1) due to organic and inorganic matter inputs from the natural (Black Sea) and anthropogenic sources in recent decades (Tugrul and Polat, 1995; Ediger et al., 2016 and references therein). The aims of this part of my Ph.D. dissertation are, therefore, (i) to determine the impacts of eutrophication and deoxygenation on the porewater nutrient dynamics, (ii) to understand organic matter (C, N) geochemistry of the recently obtained sediment core samples, (iii) to describe early diagenetic processes in the porewaters and sediments and (iv) to determine the porewater

diffusive nutrient (Si, N, P) fluxes in the three different regions of the Marmara Sea: İzmit Bay, Çınarcık Basin and the southern Marmara Sea.

3.2 Methodology

3.2.1 Study Area

Principal physical and biochemical parameters were measured at 97 stations in the Marmara Sea (Figure 3.2) in the winter and summer of 2019 using R/V Bilim-2 of METU-IMS. Sediment core samples were obtained from the 13 selected stations in the İzmit Bay, Çınarcık Basin and southern Marmara Sea to measure porewater nutrients (PO_4, Si, NO_3+NO_2, NH_4), major ions (Cl, SO_4, Br, Li, Na, K, Mg, Ca), hydrogen sulfide (H_2S), dissolved iron (dFe), and solid state total carbon/organic carbon (TC/TOC) and nitrogen (TN) concentrations in different regions of the Marmara Sea.

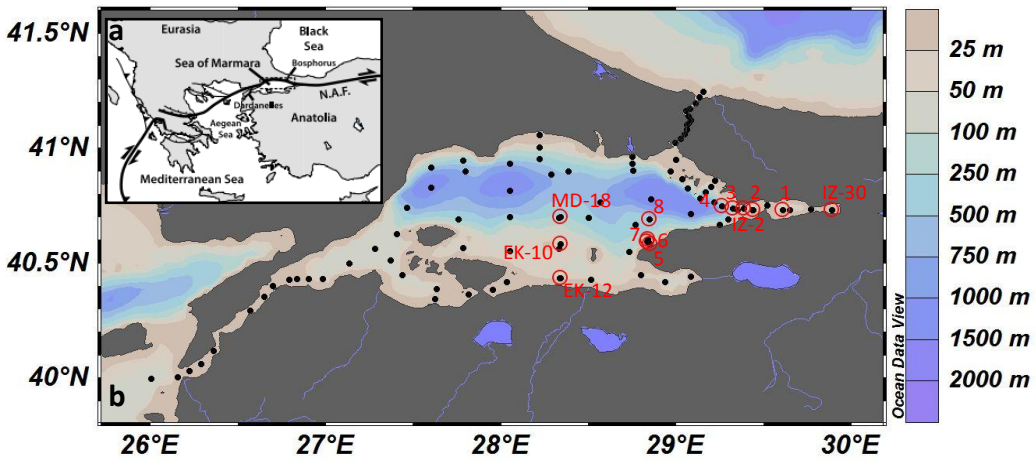

Figure 3.2. Marmara Sea with the tectonic framework (a; Tryon et al., 2010) and (b) the sampling locations in winter and summer of 2019 (red dots represent sediment core stations).

3.2.2 Sampling and Analysis

Physical data (temperature, salinity, density) were measured *in situ* by a SEABIRD model CTD probe that is coupled to a 12-Niskin bottle Rosette System in which seawater samples were collected from the selected depths by remote control. The Secchi Disk Depth (SDD), an estimation of water transparency, was measured by lowering a disk into the seawater until it can no longer be seen. Dissolved oxygen measurements were carried out by the automated Winkler titration method (UNEP/MAP, 2005). Total phosphorus concentrations were determined by the conventional colorimetric method at 880 nm wavelength (Strickland and Parsons, 1972; Grasshoff et al., 1983) after persulfate oxidation of seawater samples (Menzel and Corwin, 1965). Seawater and porewater dissolved inorganic nutrients (nitrate+nitrate, ammonium, phosphate and silicate) were measured using a Bran+Luebbe Model four-channel Autoanalyzer by standardized methods (Grasshoff et al., 1983). The detection limits of dissolved nutrients are 0.05 μM, 0.04 μM, 0.01 μM, 0.04 μM and 0.03 μM for nitrate+nitrite, ammonium, phosphate, silicate and total phosphorus, respectively. Chlorophyll-*a* (Chl-*a*) measurements were carried out by the conventional spectrofluorometric method after digestion of filtered samples by 90% (v/v) acetone solution using a HITACHI model F-2500 Fluorescence Spectrophotometer (Strickland and Parsons, 1972; UNEP/MAP, 2005). Hydrogen sulfide (H_2S/HS^-) concentrations in seawater and porewater samples were measured on board by the spectrophotometric methylene blue method at 670 nm wavelength (Cline, 1969). Porewater dissolved iron (sum of Fe^{2+} and Fe^{3+}) concentrations were measured on board by the spectrophotometric determination of Fe with ferrozine-based assay at 562 nm wavelength (Stookey, 1970; Jeitner, 2014).

Sediment core samples were obtained by a multiple-corer sediment sampling device, the Multi Corer (Oktopus, Kiel), which was applied for the first time in the Marmara Sea. Each sediment core was sliced on board under minimum oxygen conditions using N_2 or Ar gas. After obtaining sliced sediments, each sample was

put in a 50 mL falcon tube and centrifuged at 6000 rpm for 20 minutes. Then, the porewater samples were extracted using syringe-coupled GF/F filters through 0.45 μm. Dissolved iron and hydrogen sulfide concentrations of porewater sub-samples were immediately determined on board by the methods mentioned above and the remained sub-samples were placed in 15 mL falcon tubes and stored in the freezer for the analysis of dissolved nutrients and major ions. Analyses of porewater nutrients were carried out by the automated method mentioned above. Analysis of major ions (Cl, SO_4, Li, Na, K, Mg, Ca) in porewater samples were conducted by Ion Chromatography. Porewater-free sediment samples were also stored for the determination of TC, TOC and TN concentrations and surface sediment porosity measurements. Sediment samples for the TC, TOC and TN measurements were initially freeze-dried. Dry sediments were then powdered and sieved on 63 μm pore size for the homogenization of the samples. For TOC analysis, nearly 30 mg of dry and homogeneous sediment samples were put into the silver cups (pre-combusted at 400 ^{o}C for 6 hours). Then, 10 μL of distilled water was added into each silver cup to wet the samples. After distilled water addition, 10 μL of 20 % HCl (v/v) was added to remove inorganic carbon from the sediment samples. The HCl additions were continued until all the inorganic carbon was removed in the form of CO_2. Then, the samples were dried at 60-70 ^{o}C for one day. After drying the sediment samples, silver cups were compacted and put into autosampler of the CHN analyzer. TC and TN analyses in sediments were performed by the same method as for the TOC analysis, but without acid addition. TN concentrations were also determined on HCl-added sediment samples and there was no significant difference between HCl-treated and untreated samples indicating significant fraction of TN pool was in the organic nitrogen form. Therefore, TN concentrations of HCl-untreated sediment samples were reported in this study. Total carbon (TC), organic carbon (TOC) and nitrogen (TN) concentrations were determined by dry oxidation method using the Vario El Cube Elementar Model CHN Analyzer (UNEP/MAP, 2006). Porosity of wet sediments was determined by the displacement method as described by Mu et al. (2017).

3.2.3 Calculation of Diffusive Nutrients (Si, N, P) Fluxes

In this study, diffusive nutrient fluxes were calculated based on Fick's First Law of Diffusion using porewater nutrient concentrations and porosity as the following equation (Cheng et al., 2014; Mu et al., 2017):

$$F = \phi D_s (dC/dz)$$

Where F corresponds to the diffusion flux across sediment-water interface, dC/dz to the concentration gradient of nutrients across sediment-water interface, ϕ to the porosity of sediment, D_s to the actual molecular diffusion coefficient corrected for the sediment tortuosity.

Ullman and Aller (1982) proposed an empirical formula related to the actual diffusion coefficient, D_s, and porosity, ϕ:

$$D_s = \phi D_0 \qquad (\phi < 0.7)$$

$$D_s = \phi^2 D_0 \qquad (\phi > 0.7)$$

where D_0 is the self diffusion coefficient of ions at infinite dilution corrected by *in situ* temperature. For phosphate, nitrate, nitrite and ammonium D_0 values are used from Li and Gregory (1974) and for silicate, D_0 values were used from Rebreanu et al. (2008) as 7.34×10^{-6} cm^2 s^{-1} for PO_4, 19.0×10^{-6} cm^2 s^{-1} for NO_3, 19.1×10^{-6} cm^2 s^{-1} for NO_2, 19.8×10^{-6} cm^2 s^{-1} for NH_4 and 11.7×10^{-6} cm^2 s^{-1} for Si at 25 °C, respectively.

3.3 Results and Discussion

3.3.1 Variations of Physical and Biochemical Variables in the Marmara Sea

In order to determine spatio-temporal variations of physical and eutrophication-related biochemical variables, two field studies were performed in the Marmara

Sea (including the Bosporus and Dardanelles straits) in the summer and winter periods of 2019. The physical and chemical oceanography of the Marmara Sea are significantly affected by the inputs from the Black and Aegean Seas (Ünlüata et al., 1990; Beşiktepe et al., 1994; Polat and Tuğrul, 1995; Tuğrul and Polat, 1995; Polat et al., 1998; Tuğrul et al., 2002). According to surface water distributions of physical parameters (Table 3.1), temperature values seasonally ranged from 6.93-10.98 ˚C in winter to 19.06-26.17 ˚C in summer with the minimum values recorded in the surface waters of the Bosporus strait. The surface water salinity values ranged spatio-temporally from 17.29 to 29.40 in the Marmara Sea. Regional variability of the salinity values in the summer and winter periods were very similar to spatial variability of the temperature values with the lowest values recorded in the Bosporus strait due to brackish Black Sea waters (Table 3.1, Figure 3.3) increasing in the surface waters of the Dardanelles strait. However, seasonal variations of salinity values for the surface waters of the Marmara Sea indicated moderately higher salinity values in winter (Table 3.1) due to wind-induced mixing processes in the region (Beşiktepe et al., 1994). Similar spatio-temporal variability in the physical (temperature and salinity) variables was experienced in a recent study performed in the Marmara Sea (Yalçın et al., 2017). The Secchi Disk Depth (SDD) values, a rough estimation of water transparency, measured in the study region varied from 4.5-17.5 m in summer to 4.0-11 m in winter (Table 3.1). Lowest values were recorded in the Çınarcık Basin and semi-enclosed İzmit Bay influenced by brackish Black Sea inflow and anthropogenic wastewater inputs and southern Marmara Sea affected by regional rivers (Figure 3.3). Lower SDD values, as an indicator of eutrophication, in these regions were due to nutrients enrichment and hence phytoplankton production (in terms of Chl-*a*) in the surface waters of the study region decreasing the water clarity in the hot points. These findings suggested the signal of eutrophication in these regions due to combined effect of brackish Black Sea inflow and land-based sources (rivers and wastewater inflows) in the Marmara Sea as also presented in the previous studies performed in the

region (Polat and Tuğrul, 1995; Tuğrul and Polat, 1995; Polat et al., 1998; Ediger et al., 2016; Yalçın et al., 2017).

Marmara Sea ecosystem has been highly polluted by the Black Sea inflow and wastewater discharges in recent decades (Tuğrul and Morkoç, 1989; Tugrul and Polat, 1995; Ediger et al., 2016; Yalçın et al., 2017; Tan and Aslan, 2020). The eutrophication problem in the Northwestern Black Sea collapsed Black Sea ecosystem and fisheries (Mee, 1992; Tuğrul et al., 2014), leading to similar changes in the Sea of Marmara during the last two decades (Polat and Tugrul, 1995; Ediger et al., 2016; Yalçın et al., 2017). Dissolved nutrient concentrations in the Marmara Sea displayed regional and seasonal variability as also experienced in distributions of physical variables (Table 3.1, Figure 3.3). Surface water NO_x (NO_x: NO_2+NO_3) concentrations ranged spatio-temporally from 0.05 to 9.97 µM in the study region whilst PO_4 concentrations varied between 0.02 and 3.27 µM. Higher concentrations of NO_x and PO_4 in winter period were due to enrichment of brackish Black Sea inflow by nitrate and phosphate (Tuğrul et al., 2002). Similar seasonal variations were also recorded in the concentrations of NH_4 and reactive Si with the maximum values recorded in the Bosporus strait and eastern Marmara Sea; İzmit Bay and Çınarcık Basin. Variations in the nutrient fluxes from the Black Sea and in anthropogenic nutrient inputs have affected the nutrient dynamics in the Marmara Sea (Yalçın et al., 2017 and references therein). Moderately high nutrient concentrations in the surface waters of the Çınarcık Basin, İzmit Bay and also southern Marmara Sea were due to combined effects of nutrient inputs from the Black Sea via Bosporus strait, riverine inputs and domestic and wastewater discharges carrying significant amount of organic and inorganic matter inputs (Tuğrul and Morkoç, 1989; Tugrul and Polat, 1995; Polat and Tugrul, 1995; Polat et al., 1998; Ediger et al., 2016; Yalçın et al., 2017). This excessive amount of nutrient inputs from natural (Black Sea) and terrestrial sources into the Marmara Sea enhanced phytoplankton production and the development of eutrophication (Figure 3.3). The surface water chlorophyll-*a* (Chl-*a*) concentrations ranged from 0.01-1.81 µg/L in summer to 0.26-3.77 µg/L in winter. High nutrient inputs in

winter increased phytoplankton abundance (in terms of Chl-*a*) compared to those in summer. According to eutrophication assessment based on the Chl-*a* values (Simboura et al., 2005), trophic status of the most areas located at the Marmara Sea were characterized from "mesotrophic/moderate" to "dystrophic/bad". The degree of eutrophication is more pronounced in winter due to high nutrient inputs from the Black Sea and terrestrial inputs increasing the measured Chl-*a* concentrations. The recent nutrient data obtained from this study and also from the historical data set of METU-IMS indicated that the accumulation of nutrients enhancing primary productivity (in terms of Chl-*a*) leads to development of eutrophication, subsurface hypoxia (<150 μM O_2) and deep water anoxia in the Marmara Sea (Figure 3.1, Figure 3.3). In the Çınarcık Basin (eastern Marmara Sea), dissolved oxygen concentrations in the deep waters (>1000 m) decreased from 2.3 mg/L (72 μM) in 1995 to <0.25 mg/L (<7.8 μM) in 2019, indicating a rapid deoxygenation during the last two decades (Figure 3.1). In January 2019, Hydrogen sulfide was also detected in deep waters, with concentrations ranging from 3.92 μM at 1200 m in the Çınarcık Basin to 0.52 μM at 29 m in the eastern part of the İzmit Bay indicating a regime shift in the organic matter degradation, from oxic respiration to denitrification and sulfate reduction.

Table 3.1. Values of surface water physical and eutrophication-related biochemical parameters in the Marmara Sea in winter and summer periods of 2019 (N: # of observations)

Winter	Temperature (˚C)	Salinity	TP (μM)	PO_4 (μM)	NO_x (μM)	NH_4 (μM)	Si (μM)	DO (μM)	Chl-*a* (μg/L)	SDD (m)
Mean	8.80	24.15	0.48	0.19	2.19	1.11	5.56	296.3	1.24	8.2
Std. Dev.	1.28	4.39	0.23	0.18	2.55	1.46	4.10	31.6	0.79	1.8
Min.	6.93	17.96	0.16	0.02	0.09	0.15	0.85	195.3	0.26	4.0
Max.	10.98	28.83	1.11	0.72	9.97	8.84	16.19	344.4	3.77	11.0
N	39	39	39	39	39	39	39	39	39	12

Summer	Temperature (˚C)	Salinity	TP (μM)	PO_4 (μM)	NO_x (μM)	NH_4 (μM)	Si (μM)	DO (μM)	Chl-*a* (μg/L)	SDD (m)
Mean	24.27	23.00	0.53	0.14	0.92	0.30	1.54	235.0	0.23	11.9
Std. Dev.	1.37	2.73	0.46	0.40	2.16	0.10	1.26	9.7	0.24	2.9
Min.	19.06	17.29	0.14	0.02	0.05	0.02	0.20	188.1	0.01	4.5
Max.	26.17	29.40	3.45	3.27	9.28	0.64	7.08	254.1	1.81	17.5
N	84	84	84	84	84	84	84	84	84	45

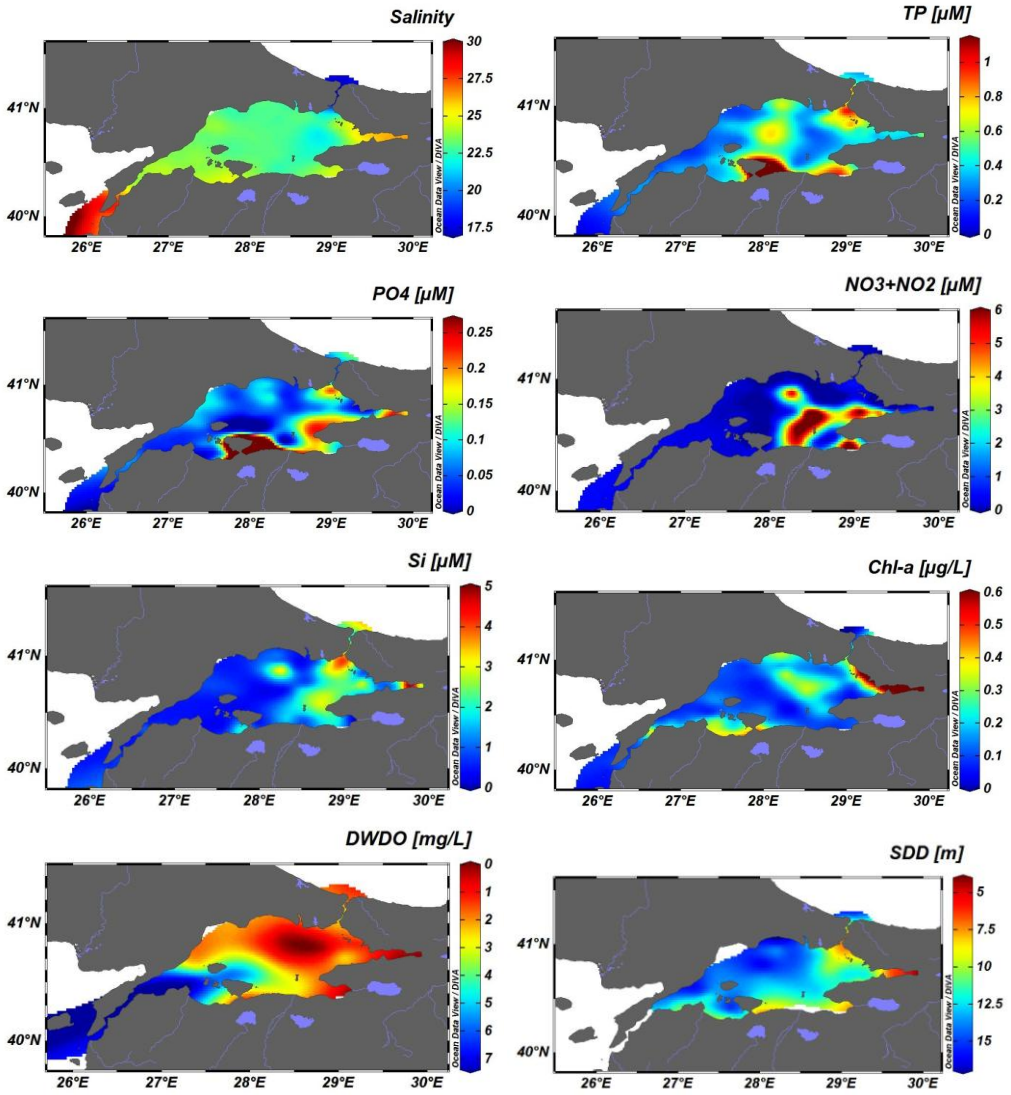

Figure 3.3. Distributions of surface water salinity, concentrations of dissolved nutrients, Secchi Disk Depth (SDD) values and deep water dissolved oxygen content (DWDO) in the Marmara Sea in the summer of 2019.

3.3.2 Sediment Organic Matter Geochemistry in the Marmara Sea

Solid-state total carbon (TC), total organic carbon (TOC) and TN concentrations in sediment cores from different regions of the Marmara Sea displayed spatial variability (Figure 3.4). Maximum concentrations were found in the surface

sediments of the highly eutrophic (dystrophic) İzmit Bay sediment core samples displaying anoxic/sulfidic conditions in the deep waters (Figure 3.4). TC concentrations ranged regionally between 1.97 and 4.12 mmol/g dw (dry weight) in the upper 3 cm of the obtained core samples decreased to 0.92-3.25 mmol/g dw levels below 30 cmbs (Figure 3.4). TOC and TN contents within the sediment core samples were also displayed same spatial variability in the study region; maximum concentrations were measured in the İzmit Bay where maximum phytoplankton production (in terms of Chl-*a*) were recorded (Figure 3.3). Vertical profiles of TOC and TN distributions were very similar to TC distributions throughout the sediment column. TOC values were in the range of 0.47-2.70 mmol/g dw whilst TN values varied between 0.04 and 0.23 mmol/g dw throughout the sediment column in the obtained core samples (Figure 3.4). The decrease in the TOC and TN concentrations with the increasing depth throughout the sediment column indicated organic matter decomposition processes. The organic matter mineralization took place in the upper 10-20 cmbs of the studied sites, below this depth, TOC and TN profiles were relatively constant and not changed regionally suggesting the availability of refractory organic matter below 20 cmbs buried in the Marmara Sea. The TOC concentrations of the obtained core samples measured in this study were in agreement with the previous studies performed in different regions of the Marmara Sea (Evans et al., 1989; Çağatay et al., 2004; Sarı and Çağatay, 2010; Ruffine et al., 2018; Yang et al., 2018; Tan and Aslan, 2020) with the relatively higher values measured in Çınarcık Basin and İzmit Bay displaying anoxic/sulfidic properties in the deep waters. Expectedly, the maximum organic matter (C, N) concentrations were detected in the surface sediments of the eastern İzmit Bay with highly eutrophic conditions and the accumulation of H_2S (0.52 μM at 29 m) in the bottom waters due to anthropogenic inputs indicating a regime shift in the organic matter degradation, from oxic respiration to denitrification and sulfate reduction. Therefore, the development of eutrophication in the İzmit Bay due to terrestrial and natural nutrient and organic matter inputs (Tuğrul and Morkoç, 1989; Yalçın et al.,

2017; Tan and Aslan, 2020) have led to increase in the accumulation rates of the organic matter sedimented on the İzmit Bay.

Maximum sediment TOC and TN concentrations (Figure 3.4) in the İzmit Bay will further enhance eutrophication in the Marmara Sea, analogous to benthic 'vicious cycle' in the much shallower Baltic Sea due to release of increased amount of dissolved nutrients, biologically available for the phytoplankton. In the Çınarcık Basin, relatively lower concentrations of TC, TOC and TN were measured compared to eastern İzmit Bay, but comparable to those measured in the western İzmit Bay having similar deep water physical and biochemical properties (Table 3.2), indicating redox-dependency on the benthic organic matter dynamics. In the southern Marmara Sea, however, minimum concentrations of TOC and TN were measured though TC concentrations were comparable with the İzmit Bay and Çınarcık Basin. The lower primary productivity (in terms of Chl-*a*) and also lower sedimentation rate (Çağatay et al., 2004) in the southern Marmara Sea resulted in low organic matter accumulation at the sediment and the higher deep water DO concentrations (Figure 3.3, Table 3.2) prevented the release of reactive phosphate, silicate and ammonium fluxes from the surface sediments. Therefore, development of eutrophication and deep water hypoxia/anoxia in the Çınarcık Basin and İzmit Bay caused to accumulation of excess amount of organic matter in the upper sediment column highly enhancing the release of dissolved nutrients whereas in the oxic southern Marmara Sea, lower sediment organic matter (C, N) concentrations resulted in lower porewater nutrients concentrations and their diffusive fluxes due to high concentrations of deep water dissolved oxygen.

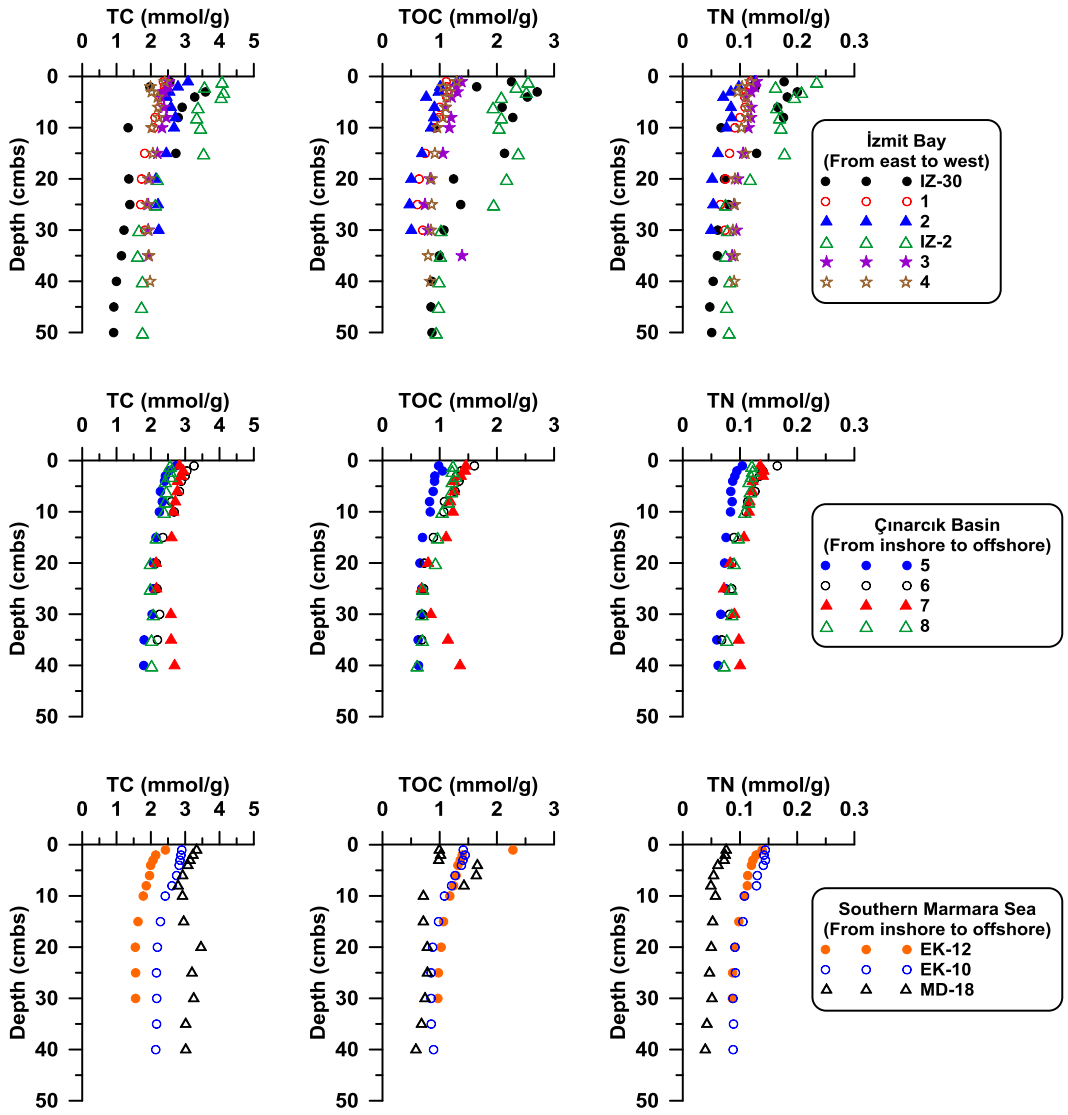

Figure 3.4. Vertical profiles of TC, TOC and TN in the sediment cores from the Marmara Sea.

3.3.3 Porewater Nutrient Dynamics in the Marmara Sea

In the euphotic zone, CO_2 is fixed accompanied by sunlight and particulate organic carbon is produced from the inorganic constituents of seawater (nutrients). Between 1 and 40% of primary production is sinking below the euphotic zone and it exponentially attenuates to the base of the mesopelagic zone at around 1000 m.

In the water column, organic matter is remineralized, converting organic matter to CO_2. Therefore, only 1% of the surface production is buried in seafloor (Herndl and Reinthaler, 2013). The long-term development of eutrophication in the Marmara Sea resulted in high particulate organic matter concentrations (Ediger et al., 2016 and references therein) being exported to the deep water and eventually to the sediment resulting in a gradual decrease in the deep-water oxygen concentrations during the last two decades (Figure 3.1). Vertical profiles of dissolved oxygen concentrations between 1954 and 2019 indicated an upward shift in the oxycline depth as well as the formation of hydrogen sulfide in near-bottom waters (Figure 3.1) due to response of anthropogenic pressures. Therefore, dissolved oxygen concentrations in the Çınarcık Basin deep waters (eastern Marmara Sea) decreased by almost 90% percent during the last two decades (Figure 3.1, Figure 3.5) and the suboxic and anoxic conditions developed specifically in the eutrophic regions under the influence of Black Sea inflow, domestic and industrial discharges and riverine inputs (Figure 3.3). Though the Marmara Sea ecosystem health is of particular importance, only few studies were performed to understand seawater nutrients and organic matter dynamics (Tuğrul and Morkoç, 1989; Tugrul and Polat, 1995; Polat and Tugrul, 1995; Polat et al., 1998; Tuğrul et al., 2002; Ediger et al., 2016; Yalçın et al., 2017). Since the region is a tectonically active marine basin, intersected in an east-west direction by the northern branch of the North Anatolian Fault (N.A.F.) (Le Pichon et al. 2001; Géli et al., 2008), the porewater geochemistry and the organic carbon and metal distributions were also determined by a number of studies (Evans et al., 1989; Halbach et al., 2002; Çağatay et al., 2004; Sarı and Çağatay, 2010; Tryon et al., 2010; Ruffine et al., 2018; Yang et al., 2018). However, this study is the first process-based study performed in the Marmara Sea to understand the impacts of eutrophication and the rapid deoxygenation on the porewater nutrient dynamics as biogeochemical cycling of key nutrients (N, P) is highly coupled to oxygen concentrations and metal (Fe, Mn) cycles (Williams, 1987; Jørgensen, 1996). The obtained data from this study with the historical data of METU-IMS indicated the

accumulation of reactive Si and PO_4 and consumption of NO_x (denitrification) in the deep waters of the Çınarcık Basin (Figure 3.5) suggested high rates of organic matter decomposition and release of reactive silicate and phosphate at the sediment-water interface. In this study, therefore, sediment core samples were obtained from the selected stations to determine the impacts of eutrophication and deoxygenation on the porewater nutrient dynamics and on the sediment organic matter (C, N) geochemistry of the Marmara Sea. Sediment core samples were obtained from eutrophic to highly eutrophic (dystrophic) İzmit Bay and eutrophic Çınarcık Basin displaying suboxic to anoxic/sulfidic properties in the deep waters, and from the mesotrophic/eutrophic southern Marmara Sea displaying oxic properties. Deep water physical and biochemical variables of the core stations presented in Table 3.2 and also surface water spatial variability of the parameters (Figure 3.3) indicated that the selected regions displayed significantly different physico-chemical and biochemical properties.

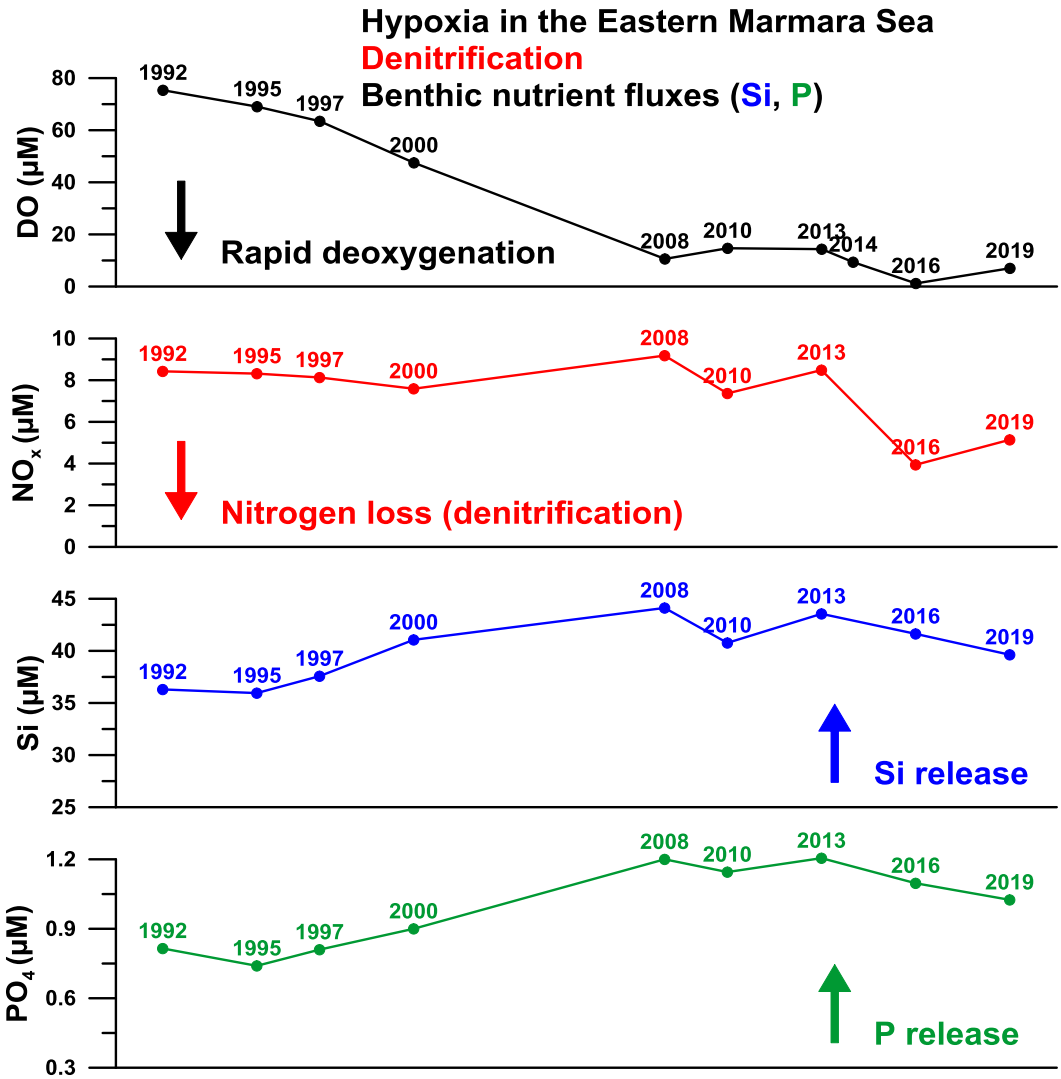

Figure 3.5. Deep water (>1000 m) biochemical properties of the Çınarcık Basin, eastern Marmara Sea (Historical data were taken from the METU-IMS database).

Table 3.2. Deep water physico-chemical properties of the sediment core stations

Region	Station	Date	Depth (m)	Temperature (˚C)	Salinity	TP (µM)	PO_4 (µM)	NO_x (µM)	Si (µM)	NH_4 (µM)	DO (µM)
İzmit Bay	IZ-30	05.01.2019	29	15.88	38.63	0.99	0.96	8.44	20.35	0.78	54.1
	1	24.07.2019	63	15.41	38.72	1.15	1.06	9.45	21.39	0.54	45.6
	2	24.07.2019	111	15.27	38.77	1.76	1.03	10.32	23.08	0.43	35.9
	IZ-2	05.01.2019	157	15.63	38.76	1.34	1.13	8.34	26.75	1.18	30.3
	3	24.07.2019	238	14.56	38.71	1.52	1.04	7.66	33.34	0.40	7.8
	4	24.07.2019	425	14.46	38.70	1.28	0.85	5.42	26.12	0.28	10.3
Çınarcık Basin	5	25.07.2019	98	15.32	38.80	0.95	0.85	9.06	20.79	0.22	57.5
	6	25.07.2019	190	14.73	38.73		0.97	9.62	31.02	0.36	17.2
	7	25.07.2019	288	14.51	38.70		1.06	8.32	35.69	0.17	7.2
	8	25.07.2019	407	14.47	38.70		1.29	7.00	40.02	0.24	6.3
Southern MS	EK-12	06.01.2019	45	16.22	38.68	0.53	0.40	4.31	8.65	0.47	164.1
	EK-10	06.01.2019	56	15.80	38.84	0.78	0.66	6.49	15.69	0.56	118.4
	MD-18	06.01.2019	145	15.24	38.80	1.09	0.69	6.49	17.21	0.19	51.6

All the core samples obtained in this study appeared to represent undisturbed accumulations in the upper 40-50 cm as also shown in the lithological studies performed in the Çınarcık Basin and southern Marmara Sea (Çağatay et al., 2004), and in the İzmit Bay (Sarı and Çağatay, 2010). The measured porewater nutrients (Si, N, P) concentrations (Figure 3.6) showed spatial variations in the studied sites as also observed surface water nutrient distributions (Figure 3.3). Porewater nutrient concentrations throughout the obtained sediment core samples ranged between 0.47 and 58.2 µM for PO_4, 0.34 and 91.5 µM for NO_3, 0.17 to 666 µM for NH_4 and 9.02 to 335 µM for Si, respectively (Figure 3.6). Biogeochemical cycling of key nutrients (N, P) is highly linked to dissolved oxygen concentrations and metal (Mn, Fe) cycles due to rapid degradation of labile organic matter by the redox-processes as denitrification, manganese and iron reduction as well as sulfate reduction and methanogenesis in the uppermost centimeters of sediment column resulting in nutrient releases from the sediments (Williams, 1987; Christensen et al., 1988; Jørgensen, 1996; Ignatieva, 1999; Rasheed, 2004; Al-Rousan et al., 2004; Hille et al., 2005; Rasheed et al., 2006; Rydin et al., 2011; Cheng et al., 2014; Mu et al., 2017). Expectedly, maximum porewater PO_4, NH_4 and Si concentrations were measured in the highly eutrophic (dystrophic) İzmit Bay (Figure 3.6) with the vertical profiles increasing with increasing sediment depth throughout the sediment

column suggested organic matter remineralization processes. Porewater NO_3 concentrations were highest in the porewaters of core samples obtained from southern Marmara Sea having oxic conditions in the deep waters and lower surface water primary productivity (in terms of Chl-*a*) (Figure 3.3). Vertical profiles of porewater NO_3 concentrations in the studied sites suggested that denitrification process took place in the uppermost millimeters of sediment core samples obtained from the İzmit Bay and Çınarcık Basin whilst oxic respiration was the major process for the organic matter remineralization in the southern Marmara Sea.

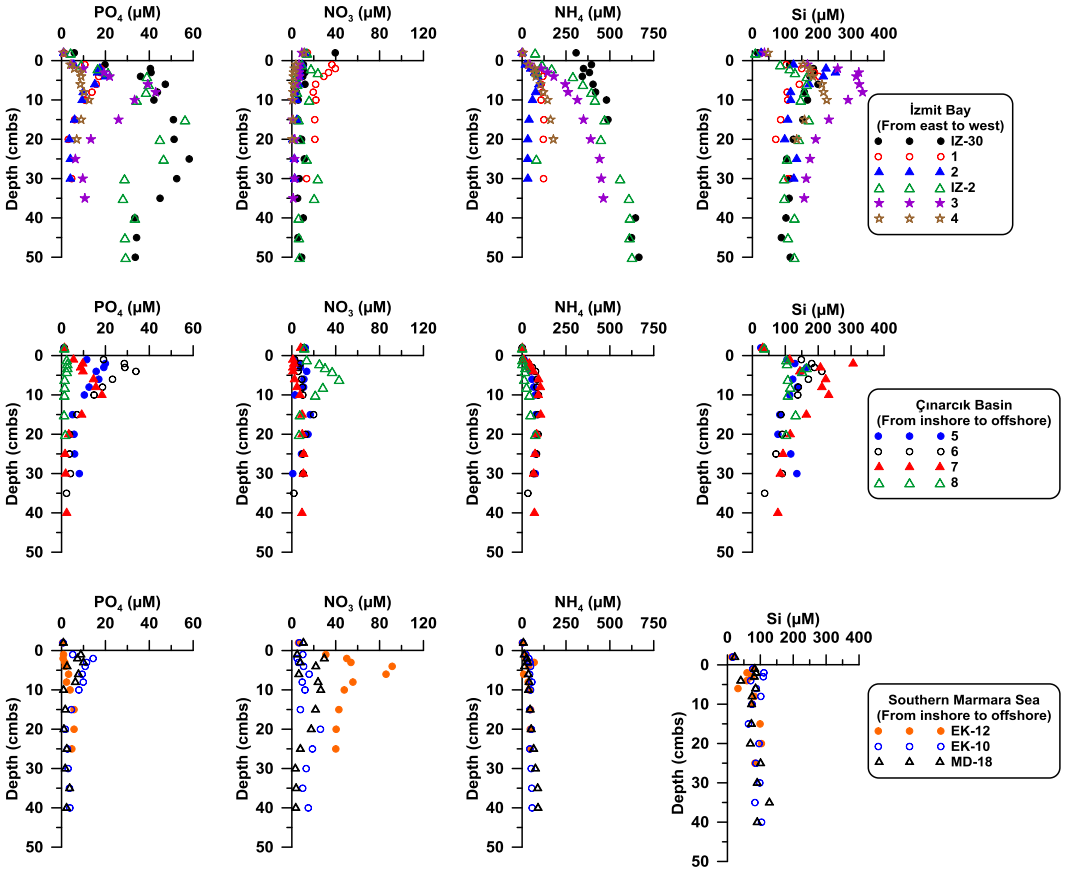

Figure 3.6. Porewater nutrient concentrations in the sediment cores from the Marmara Sea.

In order to understand the impacts of eutrophication and rapid deoxygenation on the porewater nutrient dynamics in the sediment of Marmara Sea, diffusive nutrient fluxes were calculated based on Fick's first law of diffusion for the southern

Marmara Sea, Çınarcık Basin and İzmit Bay having different deep water redox state from oxic to anoxic/sulfidic (Table 3.3). A flux with a positive sign indicated that sediment acts a source of that particular constituent whereas a negative sign indicated that sediment acts as a sink. Calculated porewater diffusive fluxes showed spatial variability in the Marmara Sea. In the all sites, sediments act as a source for PO_4, NH_4 and Si, whilst sediments in the highly eutrophic and sulfidic sites of the İzmit Bay act as a sink for NO_x (referred to NO_3+NO_2) due to rapid utilization of NO_3 ion as a terminal electron acceptor by denitrification process. Porewater diffusive PO_4, NH_4 and Si fluxes were highest in the İzmit Bay having eutrophic to dystrophic trophic status whereas minimum diffusive NO_x fluxes were calculated in this region due to NO_x loss by denitrification. In the Çınarcık Basin, higher porewater diffusive PO_4, NH_4 and Si fluxes were calculated. In the southern Marmara Sea, however, the calculated PO_4, NH_4 and Si fluxes were lowest whilst the highest porewater diffusive NO_x fluxes were calculated in this region having mesotrophic to eutrophic status and displaying oxic conditions in the deep waters (Table 3.3). The increase in dissolved inorganic nutrients (PO_4, NH_4, Si), iron and manganese concentrations in the eutrophic and suboxic/anoxic/sulfidic regions is highly coupled to redox state in the marine environment since the role of sediments in these regions has important for dissolved iron, manganese, inorganic phosphate, ammonium and reactive silicate sources to the bottom waters (Konovalov et al., 2007; Noffke et al., 2012; Mu et al., 2017). The correlation between calculated diffusive nutrient fluxes and the deep water dissolved oxygen concentrations indicated the redox-dependency on the benthic nutrient dynamics in the Marmara Sea (Figure 3.7) as the lower deep water dissolved oxygen concentration resulted in higher porewater diffusive PO_4, NH_4 and Si fluxes in the Marmara Sea which is in agreement with the high rates of organic matter decomposition and release of reactive silicate and phosphate, and nitrate loss at the sediment-water interface in the Çınarcık Basin during the last two decades (Figure 3.1, Figure 3.5). Furthermore, the calculated diffusive nutrient fluxes with the other results performed in oligotrophic (oxic) and highly eutrophic (anoxic/sulfidic) sites

showed that the organic matter decomposition with limited trapping of nutrients in the benthic interface might further enhance eutrophication in the Marmara Sea, analogous to benthic 'vicious cycle' in the much shallower Baltic Sea (Table 3.3). Furthermore, the calculated Si/N and N/P molar ratios in the deep waters ranged between 1.8 and 5.5 for Si/N and 5.6-12 for N/P, respectively. Though Si/N molar ratios of the diffusive nutrient fluxes (Si/N: 1.0-5.5) were similar to calculated in the deep waters of studied sites, N/P molar ratios of diffusive nutrient fluxes (8.4-31) were greater than deep water N/P molar composition, but comparable with the N/P molar ratios calculated in the diffusive nutrient fluxes in the suboxic/anoxic Baltic Sea (N/P: 20-30) (Ignatieva, 1999; Van Helmond et al., 2020). The change in the nutrient dynamics in the eastern Marmara Sea during the last two decades is, therefore, caused by the rapid deoxygenation and eutrophication in the region and should be under focus for future implementation plan for the ecosystem health of Marmara Sea.

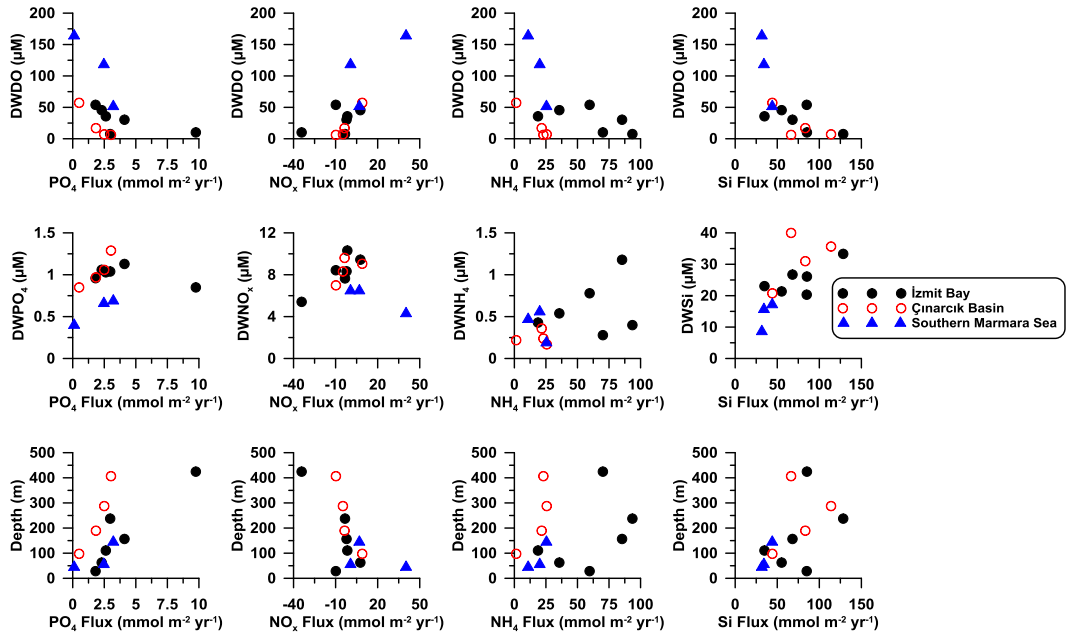

Figure 3.7. Relationship between calculated diffusive nutrient fluxes and deep water concentrations of dissolved oxygen and nutrients in the Marmara Sea.

Table 3.3. Diffusive nutrient fluxes estimated from the porewater profiles of different regions having distinct trophic and redox states

Region	Trophic Status	Deep Water Redox State	PO_4 (mmol m^{-2} yr^{-1})	NO_x (mmol m^{-2} yr^{-1})	NH_4 (mmol m^{-2} yr^{-1})	Si (mmol m^{-2} yr^{-1})
İzmit Bay[1]	Eutrophic to Dystrophic	Suboxic/Anoxic/Sulfidic	1.81-9.76	-34.2-7.65	18.7-93.5	34.8-128.4
Çınarcık Basin[1]	Eutrophic	Suboxic/Anoxic	0.51-3.03	-9.78-8.98	1.45-25.6	44.1-114
Southern MS[1]	Mesotrophic to Eutrophic	Oxic	0.11-3.22	0.65-40.2	10.93-25.4	31.7-44.0
Eastern Mediterranean[2]	Oligotrophic	Oxic	0.60	4.14	6.79	34.51
Red Sea[3]	Oligotrophic	Oxic	1.28	6.32	2.08	20.04
Peruvian OMZ[4]	Eutrophic to Dystrophic	Suboxic/Anoxic	2.3-227.6			
Baltic Sea[5]	Eutrophic to Dystrophic	Suboxic/Anoxic/Sulfidic	0.47-67.82		15.64-1441.23	
Çınarcık Basin[6]	Mesotrophic to Eutrophic	Suboxic	0.60		2.04	

[1]This study; [2]Christensen et al., 1988; [3]Rasheed et al., 2006; [4]Noffke et al., 2012; [5]Ignatieva, 1999; [6]Çağatay et al., 2004

3.3.4 Porewater Geochemistry and Early Diagenesis in the Marmara Sea

Marmara Sea is a tectonically active marine basin, intersected in an east-west direction by the northern branch of the North Anatolian Fault (N.A.F.) (Le Pichon et al. 2001; Géli et al., 2008) making the Marmara Sea a preferential site for the occurrence of multiple seeps, emitting fluids into seawater at the seafloor (Ruffine et al., 2018). In a recent study, based on the five remotely operated vehicle dives along the N.A.F. and inherited faults, CO_2 and oil-rich seeps were found at Tekirdağ Basin while amphipods, anemones and coral populated in the Çınarcık Basin of the Marmara Sea. Furthermore, it was found that methane is the dominant component of the gases releasing from the seafloor, resulting in very high concentrations (up to >370 μM) in the Marmara Sea water column. The methane seeps in the Marmara Sea is, therefore, favors sulfate depleting processes and carbonate precipitation (Ruffine et al., 2018). In order to describe early diagenetic processes from the recently obtained sediment core samples in the Marmara Sea, concentrations of Cl, SO_4, H_2S, Li, Na, K, Mg, Ca and dFe in porewaters of the collected core samples were determined. Though the measured concentrations of

the selected ions did not show significant spatial variability within the study region, they displayed variations with depth (Figure 3.8). The ranges of the measured concentrations throughout the sediment column were 326-747 mM for Cl, 0.84-32.6 mM for SO_4, 1.6-3204 μM for H_2S, 8.64-31.7 μM for Li, 313-614 mM for Na, 9.2-15.2 mM for K, 43.9-77 mM for Mg, 3.3-15.8 mM for Ca and 0.2-31.8 μM for dFe, respectively (Figure 3.8) as also recorded in the previous studies performed in the Marmara Sea (Çağatay et al., 2004; Tryon et al., 2010; Ruffine et al., 2018). The variations in the porewater concentrations of dissolved nutrients (Figure 3.6) and major ions (Figure 3.8) throughout the sediment column were affected by a series of bacterially mediated diagenetic reactions modifying geochemical composition of the porewaters in the studied sites. It was shown that there is a freshening gradient of major ions (specifically Cl and Na) in the Marmara Sea sediment porewaters due to mixing with the buried brackish water from the Marmara Lake which is observed at all sites in the Marmara Sea with the exception of Western High and this freshening was more pronounced below 250-300 cmbs in the Marmara Sea (Tryon et al., 2010). Relatively low concentrations of major ions, specifically Cl and Na, measured in the porewaters of the obtained core samples in this study and vertical profiles of these ions throughout the sediment column also indicated a downcore freshening in the Marmara Sea (Figure 3.8).

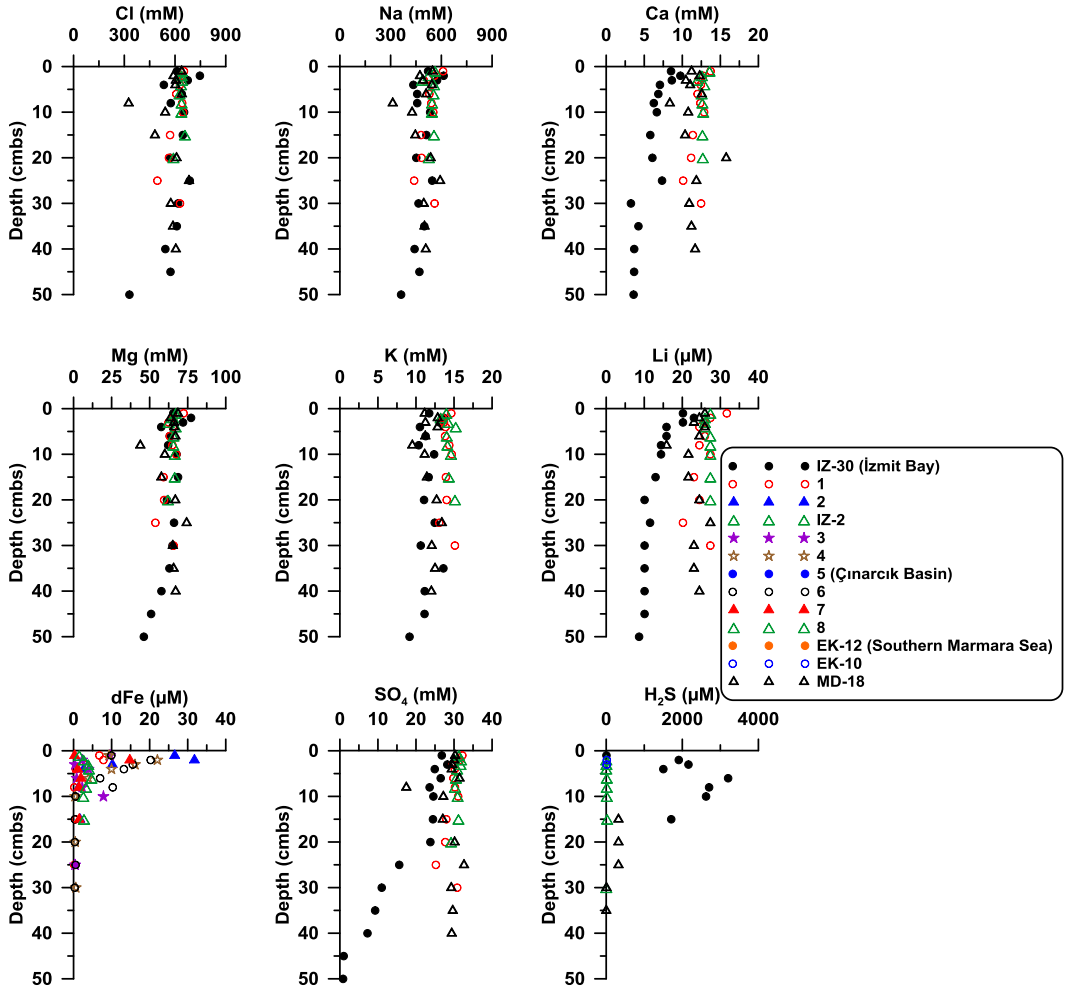

Figure 3.8. Vertical profiles of Cl, Na, Ca, Mg, K, Li, dFe, SO_4 and H_2S in the sediment porewaters from the obtained core samples in the Marmara Sea.

The series of bacterially mediated diagenetic reactions were mainly from the result of organic matter degradation by NO_3 (denitrification), Fe/Mn oxides and SO_4, as well as the processes of the SO_4 depletion by AOM, of the carbonate precipitation and of the silicate diagenesis changing porewater concentrations of major ions measured in the Marmara Sea. Vertical profiles of porewater nutrients (Figure 3.6) and solid state TOC/TN (Figure 3.4) concentrations indicated that organic matter degradation processes take place in the upper 10-20 cmbs, introducing high concentrations of porewater reactive Si, PO_4 and NH_4 and removing oxidized nitrogen (NO_3) called denitrification. The decrease in SO_4 concentrations with

depth in the sediments was due to sulfate reduction as well as the AOM, releasing H_2S, Mg and Ca in the eastern İzmit Bay. The release of Mg and Ca, then, results in carbonate precipitation reactions reducing the porewater concentrations of these ions with depth throughout the sediment column in the eastern İzmit Bay (Figure 3.8). Similar chemical composition and diagenetic reactions in the porewaters in different regions of the Marmara Sea have been observed by the studies performed by Halbach et al. (2002), Çağatay et al. (2004), Tryon et al. (2010), Ruffine et al. (2018) and the strong correlation between gas emissions and fast depletion of sulfate in the upper sedimentary column of the Marmara Sea suggested the important role of AOM for preventing complete releases of methane originating from the N.A.F. and inherited faults (Ruffine et al., 2018). The porewater geochemistry of the obtained core samples from this study and previous studies in different regions of the Marmara Sea (mainly Çınarcık, Central and Tekirdağ Basins, southern Marmara Sea, İzmit Bay) revealed that the sulfate-depletion zone, corresponding to the sulfate-methane transition zone (SMTZ), shifted from a few meters in 1999 to less than 15 centimeters below seafloor in 2014. The observed SMTZ was recorded a few meters below seafloor in the Marmara Sea by the studies in which scientific expeditions were performed before 2010 (Halbach et al., 2004; Çağatay et al., 2004; Tryon et al., 2010), the shallower SMTZ, from less than 15 to 40 centimeters below seafloor, were reported in a recent study carried by Ruffine et al. (2018) when the core samples were collected in 2014. The findings of this study also showed a shallower SMTZ, less than 50 cm, in the eastern İzmit Bay (Figure 3.8) due to increase in AOM reaction rates by intense emissions of methane resulting in fast depletion of sulfate in the upper sedimentary column (Ruffine et al., 2018). It should be also noted that the techniques and equipments to obtain core samples were distinct for the each study performed in the Marmara Sea. Gravity core samples were used in the studies of Halbach et al. (2002) and Çağatay et al. (2004), piston core samples were obtained by Tryon et al. (2010), ROV-assisted push core samples were obtained by the study of Ruffine et al. (2018) and the core samples were taken in this study using by multiple corer (Oktopus, Kiel),

respectively. All these discrepancies of sampling operations might also cause different profiles of porewater geochemistry in the Marmara Sea, but the porewater geochemistry from the results of this study and previous studies showed that there was an apparent upward shift in the SMTZ and should be under focus for future works focusing on sediment biogeochemistry in the Marmara Sea.

Organic matter degradation by the Fe/Mn oxides released the reduced forms of these metals into the sediment porewaters according to redox-ladder proposed by Jørgensen (1996). Though the dissolved manganese was not measured in this study, previous studies performed in the oxic, suboxic and anoxic regions showed that anoxic conditions support accumulation of dissolved manganese whereas oxic sediments become depleted in manganese (Jørgensen, 1996). In the oxic region of the Black Sea, for example, redox transformations and physical processes caused to redistribution of manganese from its initial sources across the bottom waters and leading to accumulation of manganese in oxidized form in the upper sedimentary column (Konovalov et al., 2007). A similar process was observed with the relative depletion of reduced iron in sediments in the Southern Marmara Sea having oxic deep waters and its accumulation in the sediments under hypoxic conditions in the Çınarcık and İzmit Bay as also experienced in the oxic, suboxic and anoxic marine environments (Jørgensen, 1996; Konovalov et al., 2007; Yücel et al., 2010) (Figure 3.8). According to a study performed in the sediment cores obtained from oxic, suboxic, anoxic/sulfidic parts of the Black Sea (Konovalov et al., 2007), FeS production is faster than pyrite reacting with zerovalent sulfur or H_2S to form FeS_2. If the Fe(III) is available in the sulfidic sediments, Fe(III) reacts with the H_2S to form Fe(II) which in turn reacts with H_2S to form FeS phases. In the Marmara Sea, the obtained geochemical profiles indicated that the producing H_2S by AOM formed iron-sulfide precipitates in the presence of reduced iron (Halbach et al., 2002). In this study, dFe (referred to sum of Fe(II)+Fe(III)) concentrations ranged from 0.2 to 31.8 μM in the porewaters of the obtained sediment core samples displaying a maximum in the upper sedimentary column decreasing to undetectable values below 10-15 cmbs indicating iron-sulfur precipitation reactions as also

experienced in the anoxic/sulfidic sediments of the Marmara Sea (Halbach et al., 2002) and Black Sea (Konovalov et al., 2007). The decrease in SO_4 concentrations with depth in the sediments was due to sulfate reduction as well as the AOM, releasing H_2S, Mg and Ca, specifically in the eastern İzmit Bay as discussed above. The release of Mg and Ca, then, result in carbonate precipitation reactions reducing the porewater concentrations of these ions with depth throughout the sediment column in the Marmara Sea (Figure 3.8). However, the release of Ca might also be the result of low-temperature silicate diagenetic processes as also shown in a recent study performed in the Marmara Sea (Tryon et al., 2010) since low-temperature silicate diagenetic processes depend not only on the availability of the silicate minerals but also available cations such as K, B, Li, Mg and Na. The end products of these diagenetic reactions, Ca and Sr, are released to the porewaters in the Marmara Sea (Tryon et al., 2010 and references therein). The downcore decreases in the concentrations of Mg, K, Na and Li obtained from this study were also associated with the low-temperature silicate diagenetic processes in the Marmara Sea.

The results of this study showed that the dynamics of porewater nutrients, redox-sensitive elements, major ions involved in the diagenetic processes and also solid-state geochemistry in the Marmara Sea have been influenced by eutrophication, bottom water hypoxia/anoxia. High concentrations of nutrients enhanced surface water primary productivity and hence increased the organic matter (C, N) concentrations accumulated at the sediment. Maximum porewater nutrients (Si, PO_4, NH_4) and sediment TOC and TN concentrations were measured in the anoxic and sulfidic İzmit Bay and Çınarcık Basin of the Marmara Sea having sedimentation rates ranging between 70 and 190 cm/1000 y (Ergin and Yörük, 1990; Ergin et al., 1994; Çağatay et al., 2004). In the southern Marmara Sea with the lower Chl-*a* concentrations in the surface waters and more oxygenated deep waters, relatively low concentrations of porewater nutrients and sediment organic matter were measured with moderately low sedimentation rate of 45 cm/1000 y (Çağatay et al., 2004). It should be also noted that the sediment organic matter

degradation processes differed in the three distinct regions where denitrificiation and sulfate reduction were observed in the Çınarcık Basin and İzmit Bay whilst oxic respiration was the major process for the organic matter remineralization in the uppermost sedimentary column of the southern Marmara Sea characterizing the sediment of the corresponding regions as sink and source for nitrate/nitrite, respectively. Moreover, the distribution of porewater sulfate, hydrogen sulfide, and major elements throughout the sediment column obtained specifically from the İzmit Bay, suggested principal biogeochemical and early diagenetic processes such as anaerobic oxidation of methane (AOM), carbonate precipitation, Fe-reduction, Fe-S precipitation and low-temperature silicate diagenesis.

3.4 Conclusions

The dynamics of porewater nutrients, redox-sensitive elements, major ions involved in the diagenetic processes and also solid-state geochemistry in the Marmara Sea was found to be clearly influenced by eutrophication and the subsequent bottom water hypoxia/anoxia. Development of eutrophication and deep water suboxia/anoxia has been experienced in the Çınarcık Basin and İzmit Bay due to natural and terrestrial pressures. Porewater nutrients (Si, N, P) results indicated that maximum concentrations of porewater reactive silicate, phosphate and ammonium were measured in the eutrophic and suboxic/anoxic İzmit Bay and Çınarcık Basin having higher primary production (in terms of chlorophyll-*a*) resulted in higher diffusive fluxes of nutrients to the deep waters. Lower porewater nutrients concentrations were recorded in the Southern Marmara Sea (Susurluk Shelf) having lower primary production and more oxygenated deep waters. Porewater nitrate, sulfate and hydrogen sulfide concentrations showed that organic matter degradation processes in the upper 20-30 cmbs have occurred by denitrification and sulfate reduction whilst organic matter decomposition was limited by oxic respiration in the upper centimeters of sedimentary column in the southern Marmara Sea. Moreover, the distribution of porewater sulfate, hydrogen

sulfide, and major elements throughout the sediment cores obtained specifically from the İzmit Bay, suggested principal biogeochemical and early diagenetic processes such as anaerobic oxidation of methane (AOM), carbonate precipitation, Fe-reduction, Fe-S precipitation and low-temperature silicate diagenesis. Sediment total organic carbon contents throughout the sediment column and the calculated redox dependent benthic nutrient fluxes in the Marmara Sea suggested high rates of organic matter decomposition and limited trapping of nutrients in the benthic interface, which would further enhance eutrophication in the Marmara Sea, analogous to benthic 'vicious cycle' in the much shallower Baltic Sea. The nitrate loss and the higher rates of diffusive fluxes of phosphate, ammonium and reactive silicate in the Çınarcık Basin and İzmit Bay may affect the water column nutrients concentrations and compositions leading to further ecological problems such as enhanced eutrophication, deep water anoxia, changes in phytoplankton abundance and composition, and mucilage formation recently observed in the Marmara Sea.

Acknowledgements

This study has been supported by DEKOSIM (Centre for Marine Ecosystem and Climate Research, Project Code BAP-08-11-DPT.2012K120880) Project, the Scientific and Technological Research Council of Turkey (TUBİTAK-2247, 119C027) Project and TUBA-GEBIP Program of the Turkish Academy of Sciences. We would like to thank the scientific cruise participants, crew of R/V Bilim-2 and METU-IMS technical personnel for helping biogeochemical sampling and analysis.

CHAPTER 4

BIOGEOCHEMICAL DYNAMICS OF PHOSPHORUS IN SEDIMENTS OF THE THREE DISTINCT BASINS: BLACK SEA, MARMARA AND MEDITERRANEAN SEAS

Abstract

Phosphorus (P) is a key element to all life that is used for structural and functional component of all organisms. The cycling of sedimentary P may differ depending on the redox-conditions of the overlying waters affecting the dynamics, and distribution of P-fractions and the elements that are highly coupled to P cycle. In this study, the biogeochemical cycling of sedimentary P and also related variables (porewater nutrients, sediment carbon, nitrogen and iron) were studied in the three interconnected marine basins: Black, Marmara and Northeastern (NE) Mediterranean Seas. The pool of "potentially mobile P" was also determined for the studied sites. The study results showed that porewater and sediment biogeochemistry displayed great variability in the studied sites with the maximum concentrations of porewater phosphate, ammonium, reactive silicate, surface sediment organic carbon, nitrogen, phosphorus and total phosphorus measured in the hypoxic Marmara Sea and suboxic/anoxic Black Sea. The decline in the TP concentrations of all sediment core samples indicated P-mobilization to the overlying water. The pool of "potentially mobile P" varied between 0.023 and 0.148 mol/m^2 in the studied sites with the maximum values recorded in suboxic and anoxic/sulfidic parts of the Black Sea. This study predicts that the deoxygenation and eutrophication would further lead to the preferential release of P in these three interconnected marine basins, hence changing the remineralization, N/P molar ratios and eventually transform the deep-water nutrient stocks with implications for internal N/P control on marine ecosystems.

4.1 Introduction

Phosphorus (P) is a fundamental element with utilization in different structural and functional component of all organisms. As well as being structural constituent in many cell components in cell membranes, teeth, and bones, it is an element of particular importance for the DNA and RNA which is crucial in the chemical energy transmission through the ATP molecule (Paytan and McLaughlin, 2007 and references therein). P is also an essential nutrient regulating primary production and ecosystem structure in the marine environment. Unlike N, P does not have any redox cycle at the surface pressures and temperatures of the Earth, but its cycling is highly coupled to that of carbon, oxygen, nitrogen (N) and metals (Fe, Mn) (Williams, 1987; Sundby et al., 1992; Jørgensen, 1996; Ruttenberg, 2003; Hille et al., 2005; Paytan and McLaughlin, 2007; Noffke et al., 2012; Mu et al., 2017). Total phosphorus (TP) pool in the marine environment is composed of inorganic and organic phosphorus compounds. In the upper layer, TP pool is fed by inorganic- and organic-P inputs from anthropogenic sources, atmospheric deposition and also by inorganic-P inputs from deep waters by physical processes. Therefore, the organic and inorganic constituents of TP pool are determined by rates of P-inputs and removal by photosynthetic and heterotrophic activities and sinking of particulate-P (Butcher et al., 1992; Paytan and McLaughlin, 2007). The only long-term removal mechanism of P in the marine environment is the burial in sediments (Ruttenberg, 2003; Paytan and McLaughlin, 2007; Dijkstra et al., 2014; Van Helmond et al., 2020). The removal mechanism of P in the buried marine sediments can be P bound to iron (Fe) (oxyhydr)oxides, P incorporated into authigenic carbonate fluorapatite and vivianite and P associated with organic matter (Ruttenberg and Berner, 1993; Dijkstra et al., 2014; Van Helmond et al., 2020).

The cycling of sedimentary P may differ depending on the redox-conditions of the overlying waters affecting the dynamics, and distribution of P-fractions and the elements that are highly coupled to P cycle such as carbon, nitrogen, iron and

manganese (Foster and Fulweiler, 2019; Schroller-Lomnitz et al., 2019; Lenstra et al., 2021; Song et al., 2021). In the regions having oxic deep waters, for example, organic P, Fe-bound P and the authigenic Ca-P are the dominant P forms buried in sediments (Ruttenberg, 2003; Ruttenberg and Berner, 1993; Paytan and McLaughlin, 2007). In these marine sediments, dissolved inorganic phosphate (PO_4) can be adsorbed or bound to iron (oxyhydr)oxides (Fe-bound P) in the uppermost centimeters of the sediment column. Upon burial of Fe-bound P throughout the deeper anoxic sedimentary column, PO_4 is released due to organic matter degradation by iron (oxyhydr)oxides (Jørgensen, 1996) resulting in precipitation of the released PO_4 ions with authigenic carbonate fluorapatite (authigenic Ca-P), or upward diffusion of PO_4 ions where it is again adsorbed or bound the iron (oxyhydr)oxides in the oxic surface sediment (Ruttenberg and Berner, 1993; Slomp et al., 1996; Paytan and McLaughlin, 2007). In the marine environment having anoxic/sulfidic deep waters, however, organic P is the dominant P-fraction of total phosphorus pool buried in the sediments. In these sediments, Fe-bound P is generally lower than expected due to organic matter degradation by iron reduction leading to inefficient cycling of Fe and P. During the organic matter remineralization processes, the dissolved inorganic phosphate is released to the deep waters or sediment porewaters due to degradation of organic P (Ruttenberg, 2003; Paytan and McLaughlin, 2007) leading to depletion of PO_4 in the surface sediments which limits the formation of authigenic Ca-P in the uppermost sedimentary column (Ruttenberg and Berner, 1993; Slomp et al., 1996; Dijkstra et al., 2014; Van Helmond et al., 2020).

Since the 1960s, dead zones in the many coastal areas have spread due to anthropogenic nutrient (N, P) inputs that dramatically increased primary productivity, lead to development of eutrophication and depletion of deep water oxygen in the coastal zones (Diaz and Rosenberg, 2008). Recent studies showed that the N and P releases from the estuarine and coastal marine sediments are considered to be important sources for phytoplankton production as the sediments supply an average of 15-32% of N and 17-100% of P for phytoplankton demand

and in some regions, specifically eutrophic and anoxic marine basins, the N and P releases from sediments are larger than terrestrial nutrient inputs (Boynton et al., 2018). In a study recently performed in the Baltic Sea, for example, annual release of P ranged between 100-1330 tonnes yr^{-1} from the sediment which is in the same order of magnitude as the regional P input from the terrestrial inputs (Malmaeus et al., 2012). Biogeochemical cycling of key nutrients (N, P) is highly coupled to oxygen concentrations and metal (Fe, Mn) cycles (Williams, 1987; Jørgensen, 1996). The increase in dissolved inorganic phosphorous and iron concentrations in the oxygen minimum zones is highly related to anoxic conditions in the marine environment as the role of sediments in the low-oxygen areas is important for dissolved iron and inorganic-P sources to the bottom water (Noffke et al., 2012; Mu et al., 2017; Schroller-Lomnitz et al., 2019; Ballagh et al., 2020; Spiegel et al., 2021; Moncelon et al., 2021).

Though biogeochemistry of water column in the three interconnected marine basins of Black, Marmara and Mediterranean Seas have been studied previously, relatively few studies were performed in the sedimentary P-dynamics in these regions having distinct biogeochemical properties. This chapter of my dissertation therefore aims (i) to determine P-fractions (loosely bound-P, iron bound-P, organic-P, aluminum bound-P, calcium bound-P, residual-P) in the subseafloor sediments, (ii) to quantify "potentially mobile P" that is the term used for the stock of sedimentary P to be eventually released (Rydin, 2000), (iii) to present concentrations of porewater nutrients (Si, N, P) and geochemical (C, N, r-Fe) parameters from the recently collected sediment core samples in the three distinct basins: Black, Marmara and Northeastern Mediterranean Seas. The results of this study also indicated the redox-dependency on the sedimentary P-fractions and mobilization of P as well as distributions of geochemical (C, N, r-Fe) variables in the Black, Marmara and Mediterranean Seas displaying distinct biogeochemical properties.

4.2 Methodology

4.2.1 Study Area

The study area covers three interconnected marine basins displaying distinct biogeochemical properties in the water column and sediment. The Black Sea (Figure 4.1) is situated between Europe, Anatolia and Caucasus. It is connected to the Mediterranean Sea through the Bosporus Strait which is the only connection of the Black Sea to the Global Ocean (Toderascu and Rusu, 2013). It is known as the largest anoxic water body in the world (Oguz, 2005) that has a permanently euxinic marine basin (Ross and Degens, 1974) making the Black Sea an excellent site to study redox-driven biogeochemical processes under oxic, suboxic and anoxic/sulfidic conditions in the water column (Murray et al., 1995; Tugrul et al., 2014). Since the 1970s, the Black Sea marine ecosystem, specifically its northwestern shelf, has been subject to anthropogenic pressures due to terrestrial organic and inorganic matter inputs carried by regional rivers, mainly Danube, Dnieper, Dniester and Bug as well as many other small rivers, leading to development of eutrophic conditions in the basin (Konovalov and Murray, 2001; Mee, 1992; Tugrul et al., 2014). Therefore, primary productivity rates measured in the northwestern shelf exceeded 400 g C m^{-2} y^{-1} decreasing by 2-4 fold in the offshore waters of the Black Sea (Vedernikov and Demidov, 1993; Bologa et al., 1999; Yılmaz, 2002).

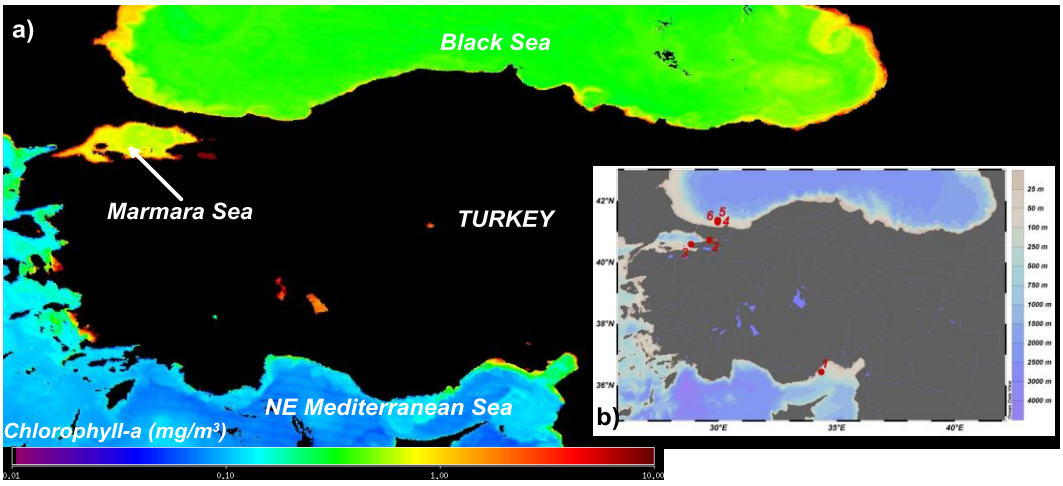

Figure 4.1. (a) Surface water chlorophyll-*a* distributions obtained by Satellite MODIS Aqua in the Northeastern (NE) Mediterranean, Marmara and Black Seas in September 2019 and (b) the sampling locations.

The Marmara Sea (Figure 4.1) is a typical example of two-layer enclosed seas connecting the Black Sea to the Mediterranean Sea via the two shallow and narrow straits, called Bosporus and Dardanelles and this oceanographic system is called Turkish Straits System (TSS) (Ünlüata et al. 1990; Beşiktepe et al. 1994; Ediger et al., 2016 and references therein). Marmara Sea ecosystem has distinct biogeochemical properties due to water exchanges between the Black Sea and the Mediterranean Sea through TSS (Polat, and Tugrul, 1995; Tugrul and Polat, 1995, Tugrul et al., 2002; Yalçın et al., 2017). Marmara Sea ecosystem has also been affected by anthropogenic pressures by direct discharges mainly from the İstanbul city (Tuğrul and Morkoç, 1989; Tugrul and Polat, 1995; Ediger et al., 2016; Yalçın et al., 2017; Tan and Aslan, 2020). The development of eutrophication in the Northwestern Black Sea (Konovalov and Murray, 2001; Mee, 1992; Tugrul et al., 2014) also adversely affected Marmara Sea ecosystem (Polat and Tugrul, 1995; Ediger et al., 2016; Yalçın et al., 2017). Recent studies in the Marmara Sea indicated dissolved oxygen deficiency in the deep waters due to increasing organic matter inputs in the upper layer (Ediger et al., 2016; Yalçın et al., 2017) and limited ventilation of deep waters by strong density gradient between water masses

(Beşiktepe et al. 1994; Tugrul and Polat, 1995; Tugrul et al., 2002; Ediger et al., 2016).

The Eastern Mediterranean Sea (Figure 4.1) is one of the world's oligotrophic seas due to principally the limited nutrient supply from external and internal sources having low primary productivity throughout its surface waters (UNEP, 1989; Yılmaz and Tugrul, 1998; Kress and Herut, 2001; Krom et al., 2004; Tanhua et al., 2013; Tugrul et al., 2016, 2018). The sedimentation rates in the oligotrophic Eastern Mediterranean Sea ranges from 0.003 to 0.014 cm y^{-1} (Van Santvoort et al., 2002; Katz et al., 2020) much lower than recorded in the open Black Sea (0.23 cm y^{-1}) (Dijkstra et al., 2018) and the Marmara Sea (0.008 to 0.19 cm y^{-1}) (Ergin and Yörük, 1990; Ergin et al., 1994; Çağatay et al., 2004). The primary production in the surface waters of the oligotrophic Eastern Mediterranean is also as low as 12-88 g C m^{-2} y^{-1} (Van Santvoort et al., 2002) compared to measurements reported in the Black Sea and Marmara Sea (Ergin et al., 1994; Yılmaz, 2002). However, increased inputs of nutrients from terrestrial sources (rivers, wastewaters) to the NE Mediterranean coastal areas have enhanced primary production and biodegradable particulate organic matter production (Coban-Yıldız et al., 2000; Yılmaz, 2002; Dogan-Saglamtimur and Tugrul, 2004), leading to eutrophication in the inner bays (Tugrul et al., 2011, 2016, 2018, Kaptan, 2013).

4.2.2 Sampling and Analysis

In this study, *in situ* physical (temperature, salinity, density) measurements, biochemical measurements (dissolved oxygen, hydrogen sulfide) and sampling (nutrients, chlorophyll-*a*) in the water column and sediment core sampling were performed from the six stations in the Black, Marmara and NE Mediterranean Seas (Figure 4.1), displaying distinct deep water redox-state (Table 4.1). Three sediment core samples were obtained from three different locations in the Black Sea having redox-state from oxic to anoxic/sulfidic. Two sediment core samples were obtained from the hypoxic parts of Marmara Sea whilst one sediment core sample was

obtained from the NE Mediterranean Sea having oxic condition in the deep waters. Sediment core sampling in the NE Mediterranean Sea was performed in spring 2018 while sediment core samples were obtained from the Black Sea in summer 2019. Marmara Sea core samples were collected in winter and summer of 2019 (Table 4.1).

Table 4.1. Locations of sediment core stations with deep water dissolved oxygen (DWDO) and hydrogen sulfide (DWH_2S) concentrations and deepwater redox state

Date	Station	Region	Depth (m)	DWDO (µM)	DWH_2S (µM)	Deepwater Redox State
20.03.2018	1	NE Mediterranean Sea	208	207.4	0.00	Oxic
05.01.2019	2	İzmit Bay, Marmara Sea	157	30.31	<1.00	Suboxic
25.07.2019	3	Çınarcık Basin, Marmara Sea	190	17.09	<1.00	Suboxic
23.07.2019	4	Black Sea	85	177.0	0.00	Oxic
23.07.2019	5	Black Sea	152	26.92	<1.00	Suboxic
23.07.2019	6	Black Sea	330	0.000	70.1	Anoxic/Sulfidic

Physical variables (temperature, salinity, density) were measured *in situ* by a SEABIRD model CTD probe, coupled to a 12-Niskin bottle Rosette System. Sediment core samples were collected by using the Multi Corer (Oktopus, Kiel). Each sediment core was sliced on board under minimum oxygen atmosphere using inert nitrogen (N_2) or argon (Ar) gas. Horizons of the collected sediment samples were 0-1 cm, 1-2 cm, 2-3 cm, 3-4 cm, 4-6 cm, 6-8 cm, 8-10 cm, 10-15 cm, 15-20 cm, 20-25 cm, 25-30 cm, 30-35 cm, 35-40 cm, 40-45 cm and 45-50 cm. Sliced sediment subsamples was put in a 50 mL falcon tube and centrifuged at 6000 rpm for 20 minutes. Then, the porewater samples were collected by syringe-coupled GF/F filters having 0.45 µm pore size. Hydrogen sulfide (H_2S) concentrations of porewater subsamples were immediately measured on board and the remained subsamples were placed in 15 mL falcon tubes and stored in the freezer (at -20 ˚C) for the analysis of dissolved nutrients. Porewater-free sediment samples were also stored (at -20 ˚C) for the determination of organic content and concentrations of TC, TOC, TN and P-fractions.

Seawater dissolved oxygen (DO) concentrations were determined on board by the automated Winkler titration method (UNEP/MAP, 2005). Seawater and porewater hydrogen sulfide (H_2S) concentrations were also measured on board by the spectrophotometric methylene blue method at 670 nm wavelength (Cline, 1969). Porewater nutrients (nitrate+nitrate, ammonium, phosphate and silicate) were determined by the conventional colorimetric method using a Bran+Luebbe Model four-channel Autoanalyzer (Grasshoff et al., 1983). The detection limits of measured nutrients are 0.05 μM, 0.04 μM, 0.01 μM and 0.04 μM for nitrate+nitrite, ammonium, phosphate and silicate, respectively. Sediment samples for the measurements of total carbon (TC), organic carbon (TOC), nitrogen (TN) and P-fractions were initially freeze-dried. Organic content of sediment subsamples was determined by the method of loss on ignition (LOI) after ignition at 550 ˚C in a muffle furnace for two hours. For TOC analysis, inorganic carbon forms were firstly removed from the sediment samples using 20% HCl (v/v). TC, TOC and TN concentrations were determined by dry oxidation method using the Vario El Cube Elementar Model CHN Analyzer (UNEP/MAP, 2006). The dithionite (0.3 M solution in a buffer containing 0.35 M sodium acetate and 0.2 M sodium citrate (pH=4.8) (Kostka and Luther, 1994; Raiswell et al., 1994, Yücel et al., 2010)) extractable reactive iron (r-Fe) concentrations were determined by colorimetric ferrozine method (Stookey, 1970; Jeitner, 2014). Replicate measurements of TC, TOC, TN and r-Fe concentrations showed that relative errors were less than 5%.

4.2.3 P-Fractions and Calculation of Potentially Mobile P

The forms of P extracted and the time and chemicals for the corresponding extraction procedure were presented in Figure 4.2. The weak acid extraction method was followed to determine total phosphorus (TP) of sediments after combusted at 550 ˚C for 3 hours as described in Berner and Rao (1994) and Fang et al. (2007). Concentrations of different P-fractions were determined sequentially as described in Psenner et al. (1988) (Figure 4.2). In this sequential extraction

procedure, loosely bound-P, P associated with iron (oxyhydr)oxides (Fe-P), aluminum bound P (Al-P), organic P (Org-P), calcium bound P (Ca-P) were determined and residual P (Res-P) was calculated by subtracting extracted phosphorus forms from TP, considered as the refractory organic P forms (Rydin et al., 2011). Concentrations of TP and P-fractions of extracted sediment samples were measured by manual colorimetric method (Strickland and Parsons, 1972, Grasshoff et al., 1983). Based on duplicate measurements, relative errors were less than 10% for TP and all P-fractions. In order to determine potentially mobile P, "background sedimentary P" was determined from the vertical profiles of TP which is the sediment TP concentrations being constant and stabilized throughout the sediment column. The average TP concentration below stabilization depth was subtracted from the TP concentration in the layers above and the resulting concentration was multiplied with the dry matter content for the calculation of P amount in each layer. The amount of potentially mobile P per square area was then calculated by depth integration (Rydin et al., 2011; Malmaeus et al., 2012; Van Helmond et al., 2020).

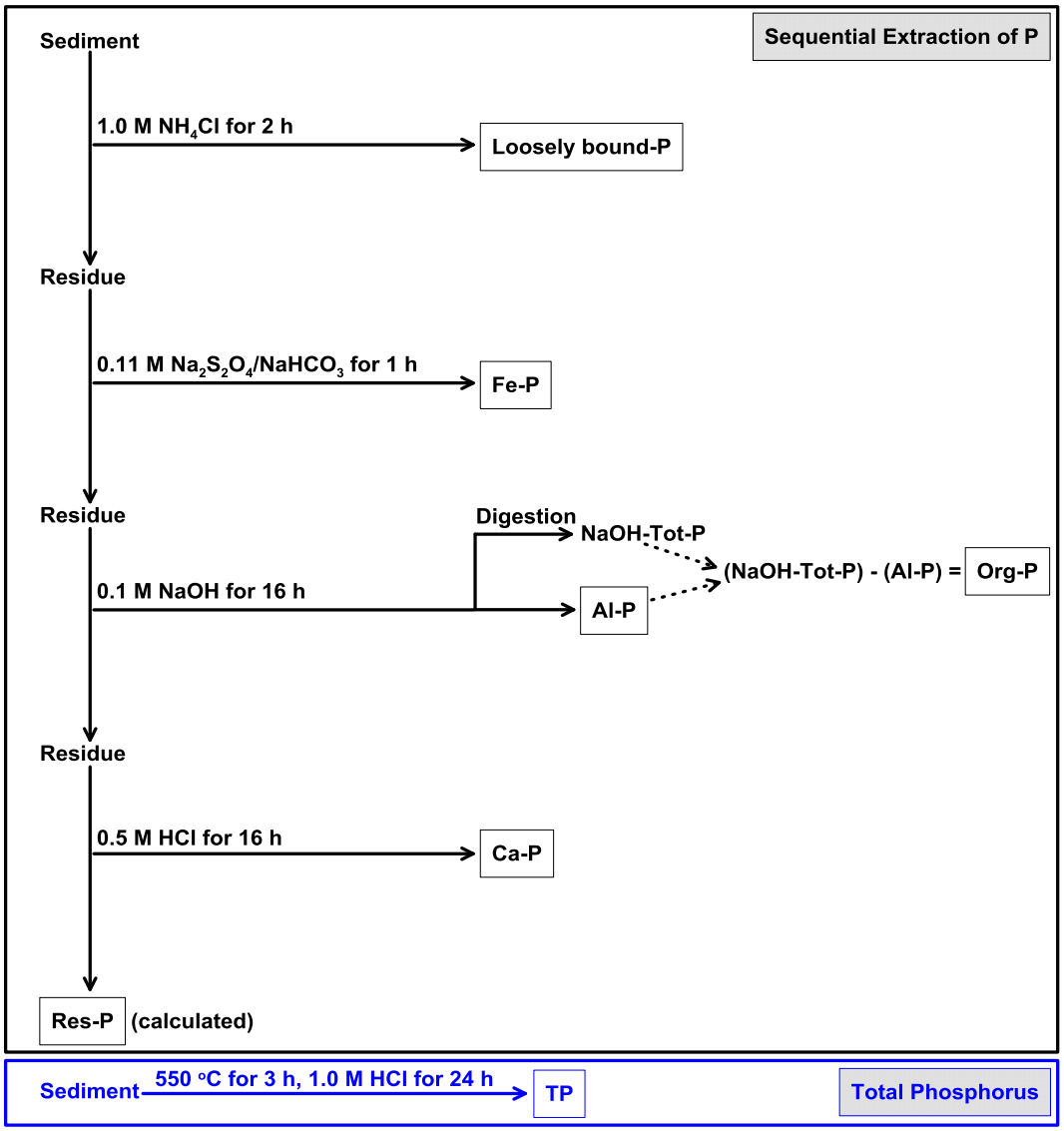

Figure 4.2. Method for the determination of P-fractions and total phosphorus (TP) in the obtained sediment core samples (modified after Rydin, 2000) in the Black, Marmara and NE Mediterranean Seas.

4.3 Results and Discussion

4.3.1 Sediment Porewater Nutrient (Si, N, P) Distributions

Sediment porewater nutrient concentrations displayed great spatial variability in the NE Mediterranean, Marmara and Black Seas having distinct biochemical properties in the water column (Figure 4.3). Reactive phosphate (PO_4), nitrate (NO_3), ammonium (NH_4) and reactive silicate (Si) concentrations throughout the sediment column ranges between 0.07 and 189 μM for PO_4, between 0.00 and 23.8 μM for NO_3, between 0.17 and 1233 μM for NH_4, and between 2.96 and 717 μM for Si, respectively. Expectedly, maximum porewater PO_4, NH_4 and Si concentrations were measured in the suboxic Marmara Sea and suboxic/anoxic Black Sea (Figure 4.3). Porewater PO_4, NH_4 and Si concentrations in the sediment core sample obtained in the NE Mediterranean Sea had lower concentrations due to its oxic and oligotrophic nature with low sedimentation and primary production rates (Van Santvoort et al., 2002; Katz et al., 2020). Porewater PO_4, NH_4 and Si concentrations increased with sediment depth whilst NO_3 concentrations decreased with depth at all stations suggesting degradation of organic material. The downcore decreases in the NO_3 concentrations in the suboxic and anoxic parts of the Black Sea sediments suggested denitrification (Jørgensen, 1996).

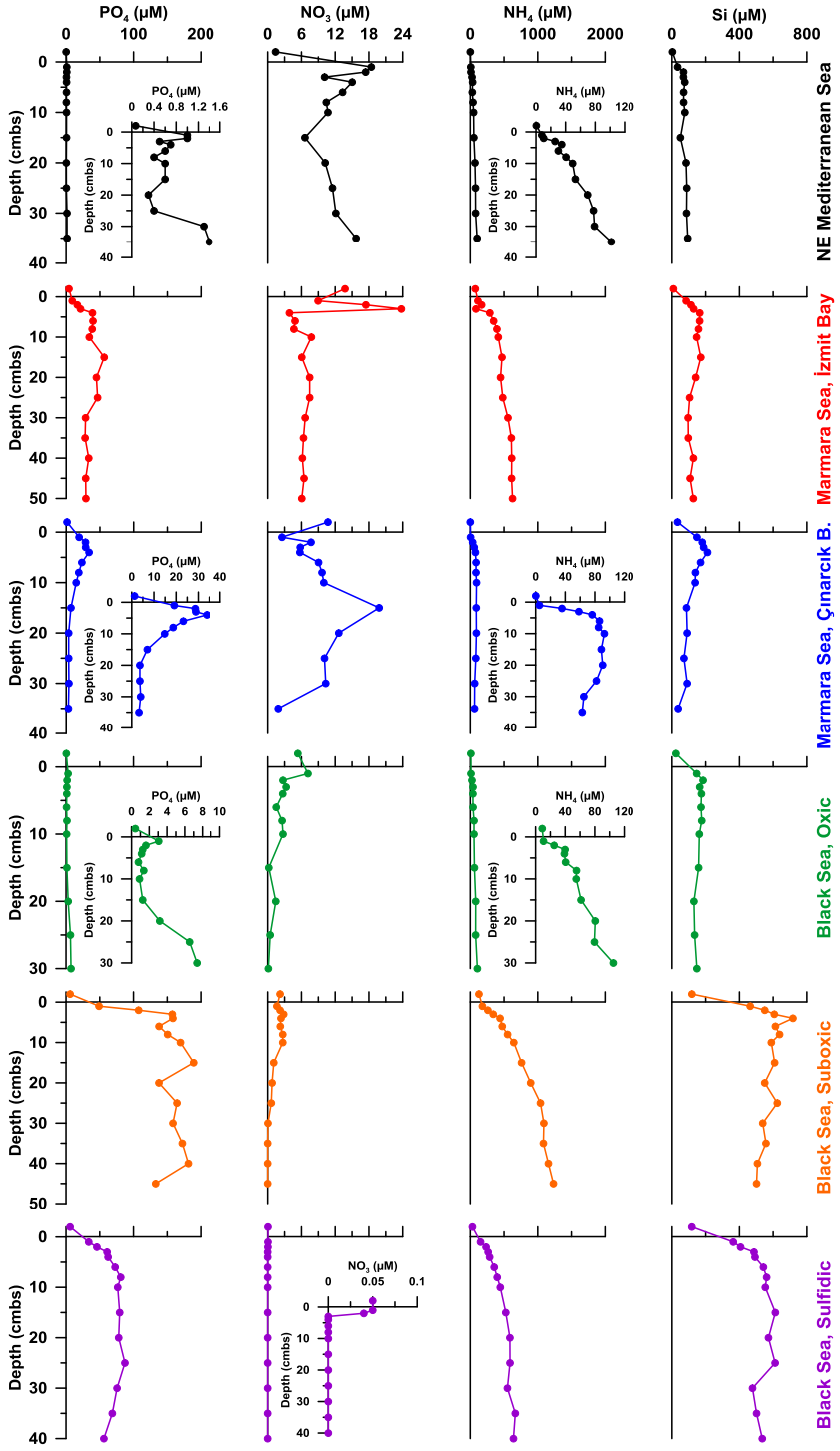

Figure 4.3. Sediment porewater nutrient (PO_4, NO_3, NH_4, Si) profiles in the 6 stations from the NE Mediterranean, Marmara and Black Seas selected for the P-fractionation study.

4.3.2 Sediment Organic Matter Biogeochemistry (C, N, P)

Organic matter biogeochemistry of the coastal and/or deep sea sediments has been affected by a series of redox reactions (Jørgensen, 1996; Foster and Fulweiler, 2019; Schroller-Lomnitz et al., 2019; Lenstra et al., 2021; Song et al., 2021), environmental (T, S) conditions (Dijkstra et al., 2014) and terrestrial inputs of the particulate inorganic/organic matter (Middelburg et al., 1993; Yemenicioglu and Tunc, 2013; Deininger and Frigstad, 2019; Katz et al., 2020). While the water column biochemistry in the Mediterranean, Marmara and Black Seas has been studied extensively, only few studies of sediment biogeochemistry in these three interconnected marine basins have been published. In this study, the measured TC (TOC+TIC) concentrations ranged from 19.4 mg/g dw (dry weight) to 49.5 mg/g dw (Figure 4.4). Except for the NE Mediterranean Sea core sample, TC concentrations decreased with sediment depth. It is well known that from 1 to 40% of primary production is sinking below the euphotic zone and it exponentially attenuates to the base of the mesopelagic zone at around 1000 m. In the water column, organic matter is remineralized, converting organic matter to CO_2. Therefore, only 1% of the surface production is buried in seafloor (Herndl and Reinthaler, 2013). However, this proportion of organic matter sedimented at the seafloor might change due to terrestrial inputs of nutrients and organic matter modifying the organic matter composition and concentrations and grain size distributions of the sediment column (Yemenicioglu and Tunc, 2013; Akcay, 2015). Differences in the sedimentation rates and currents and wave energy also affect distributions of sediment organic matter biogeochemistry (De Falco et al., 2004; Katz et al., 2020). TOC concentrations from the all core samples decreased with sediment depth throughout the sediment column indicated organic matter degradation processes. The TOC concentrations throughout the sediment column ranged from 5.63-8.36 mg/g dw in the NE Mediterranean Sea to 11.3-30.6 mg/g dw in the İzmit Bay, Marmara Sea (Figure 4.4). Expectedly, the spatial and downcore distributions of TN concentrations were very similar to recorded in TOC

concentrations and ranged between 0.67 and 3.28 mg/g dw in the studied core samples (Figure 4.4). The lower primary production and sedimentation rates in the oligotrophic NE Mediterranean Sea resulted in lower particulate organic matter flux and burial at the seafloor. Therefore, the TOC and TN concentrations in the NE Mediterranean core sample was 3-4 fold lower than measured in the core samples of Marmara and Black Seas. The r-Fe concentrations varied between 3.04-63.1 μmol/g dw throughout the sediment column of the obtained core samples with the minimum values measured below 10 cmbs in the oxic and anoxic/sulfidic parts of the Black Sea. The results of r-Fe concentrations of this study were in agreement with the recent studies performed in the NE Mediterranean surface sediments (Ermis, 2017) and Black Sea core samples (Yucel et al., 2010; Dijkstra et al., 2014) highly coupled to organic matter geochemistry (C, N, P) in the studied sites.

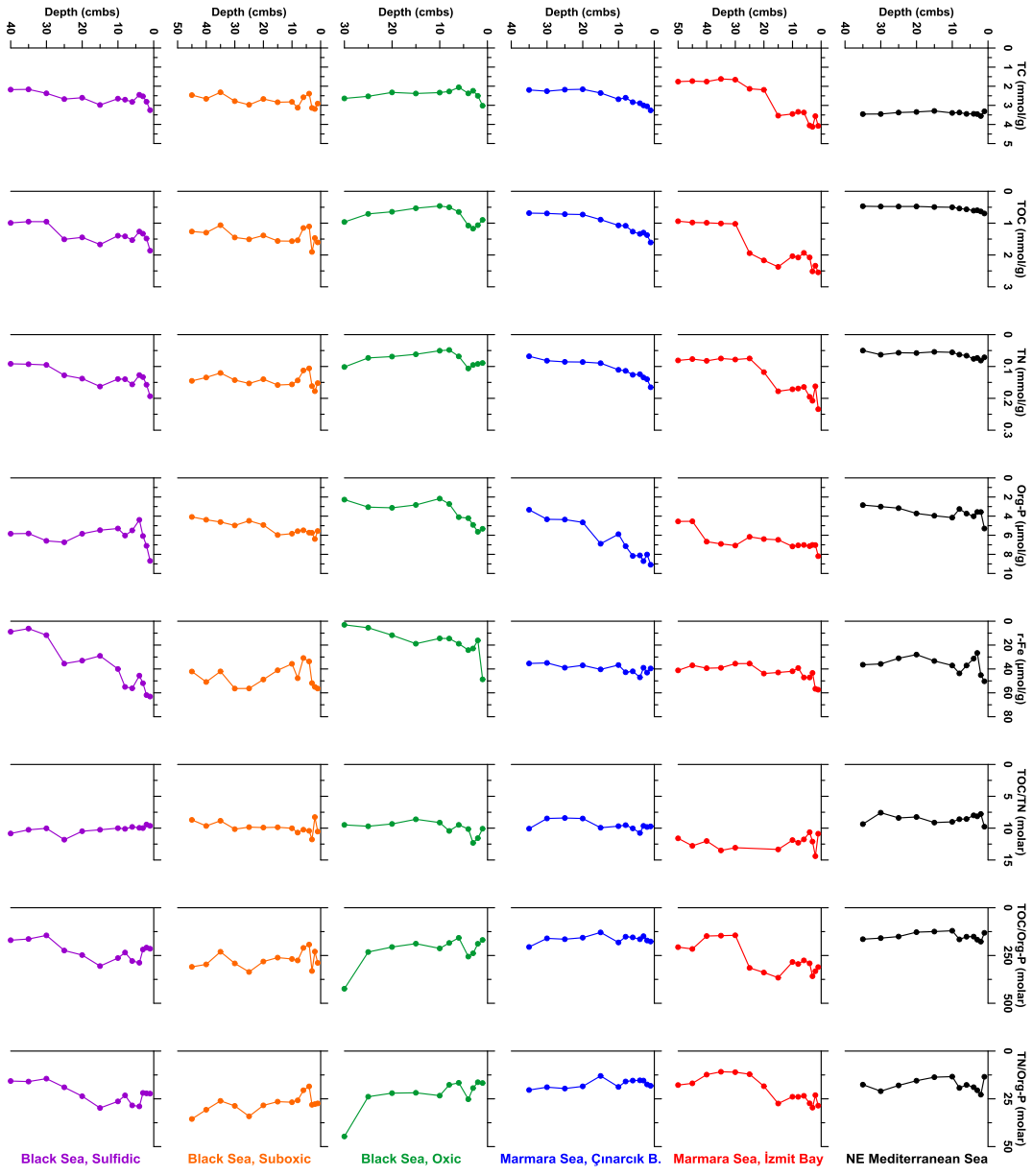

Figure 4.4. Solid-phase depth profiles of total carbon (TC), total organic carbon (TOC), total nitrogen (TN), organic phosphorus (Org-P), reactive iron (r-Fe), and molar ratios of TOC/TN, TOC/Org-P and TN/Org-P in the NE Mediterranean, Marmara and Black Seas.

From the sediment organic C, N and P content, molar ratios of C/N and N/P were calculated and presented in Figure 4.4. The calculated C/N molar ratios in surface sediments varied between 9.6 and 10.9 and did not significantly change with

sediment depth. Spatial variability in the calculated organic matter N/P molar ratio was more pronounced ranging from 13 to 29 in the surface sediments decreased with sediment depth in the NE Mediterranean Sea, Marmara Sea and anoxic/sulfidic Black Sea (Figure 4.4). A low C/N molar ratio in marine sediments is an indicative of relatively fresh and undegraded organic matter. Nitrogen and phosphorus are deposited to the seafloor bounding algal cells or organic detritus which undergo decomposition in the water column with faster loss of organic nitrogen and phosphorus, than of carbon, resulted in higher C/N and N/P molar ratios relative to Redfield molar ratio C/N/P (Jørgensen, 1996). In this study, both C/N and N/P molar ratios calculated for the obtained sediment core samples were greater than the classical Redfield Ratio of C/N/P. The study of Boynton et al. (2018) showed that the calculated molar ratios (C/N/P) from the surface sediment data suggested phytoplankton to be the primary source of organic matter based on Redfield ratios of phytoplankton composition (C/N/P=106/16/1) since surface sediment C/N molar ratios mostly ranged from 6.6 to 20 and this distribution suggests a preferential loss of N to denitrification or anammox. Except for the İzmit Bay core sample, the calculated sediment TOC/TP ratios were equal to or less than the Redfield ratio of 106/1 suggesting that phosphorus is preferentially retained in shallow marine sediments relative to organic carbon, possibly as P adsorbed to iron-rich sediments and the lower TN/TP ratios indicates either preferential loss of N (Jørgensen, 1996) or retention of P in sediments (Rydin et al., 2011; Malmaeus et al., 2012; Dijkstra et al., 2014; Boynton et al., 2018; Van Helmond et al., 2020). In the NE Mediterranean Sea, sediment organic matter (C, N, P) concentrations were lower compared to Marmara and Black Seas, typical for the oligotrophic offshore and deep sea regions having low primary productivity and sedimentation rates. Measurements from the sediment of NE Mediterranean Sea indicated that TOC concentrations were less than 1.0% (10 mg/g dw), TN concentrations were less than 0.12% (1.2 mg/g dw) and TP concentrations were less than 0.05% (0.5 mg/g dw) throughout the sediment column with slightly lower molar ratios (TOC/TN: 8-10 and TOC/TP: 45-59, TOC/Org-P: 121-177) compared

to eutrophic coastal marine sediments (Eijsink et al., 2000; Van Santvoort et al., 2002; Aydın et al., 2009; Yemenicioglu and Tunc, 2013; Erdogan, 2014; Escobar-Briones and García-Villalobos, 2009; Katz et al., 2020). The calculated TOC/TP and TOC/Org-P ranged from 34 to 160 and from 129 to 424 in the Marmara and Black Sea sediments in line with the recent works performed in the anoxic/sulfidic regions of the Black Sea (Dijkstra et al., 2014; Van Helmond et al., 2020).

4.3.3 P-Fractions and the Potentially Mobile P in Sediments

Concentrations of surface sediment TP and P-fractions varied considerably in the NE Mediterranean, Marmara and Black Seas (Figure 4.5). The measured TP concentrations in the surface sediments of the studied sites varied between 13.9 and 21.7 μmol/g dw decreasing with sediment depth for all the obtained core samples (Figure 4.5). Expectedly, minimum values were recorded in the oligotrophic NE Mediterranean surface sediments having lower primary productivity and lower sedimentation rate compared to those measured in the Marmara and Black Seas. The Org-P concentrations in the Çınarcık Basin and İzmit Bay surface sediments were comparable with the measured Org-P concentrations in the anoxic/sulfidic part of the Black Sea (Figure 4.5) though sedimentation rates in the open Black Sea (0.23 cm y^{-1}; Dijkstra et al., 2018) were greater than calculated in the Marmara Sea (from 0.008 to 0.19 cm y^{-1}; Ergin and Yörük, 1990; Ergin et al., 1994; Çağatay et al., 2004). This organic matter enrichment in the Marmara Sea is possibly due to the development of eutrophication from terrestrial and natural nutrient and organic matter inputs (Tuğrul and Morkoç, 1989; Ediger et al., 2016; Yalçın et al., 2017; Tan and Aslan, 2020) leading to increase in the accumulation rates of organic matter with high P content in the Marmara Sea, specifically in the İzmit Bay. With the exception of surface sediment from the oligotrophic NE Mediterranean Sea having minimum TOC and TN concentrations, Org-P was found to major P-fraction of sediment TP pool in the studied sites (Figure 4.6). The Fe-bound P concentrations in the surface sediments ranged from 0.37 to 4.94 μmol/g dw with

the maximum values measured in the suboxic İzmit Bay and suboxic part of the Black Sea, exceeding 20% of the sediment TP pool (Figure 4.6). In the marine environment having anoxic/sulfidic deep waters, org-P is the dominant P-fraction of TP pool buried in the sediments. In these sediments, Fe-bound P is generally lower than expected due to organic matter degradation by iron reduction leading to inefficient cycling of Fe and P (Slomp et al., 1996; Ruttenberg, 2003; Paytan and McLaughlin, 2007). However, recent studies showed that Fe-bound P is an important P-fraction of TP pool in anoxic basins such as Black and Baltic Seas exceeding 20% of the sediment TP (Jilbert and Slomp, 2013; Dijkstra et al., 2014). It was assumed that the possible source of Fe-bound P is in the form of reduced Fe-P minerals formed as inclusions in sulfur-disproportionating *Deltaproteobacteria* recently observed in bacterial mats in the anoxic/sulfidic Black Sea performing anaerobic oxidation of methane (Basen et al., 2011; Milucka et al., 2012).

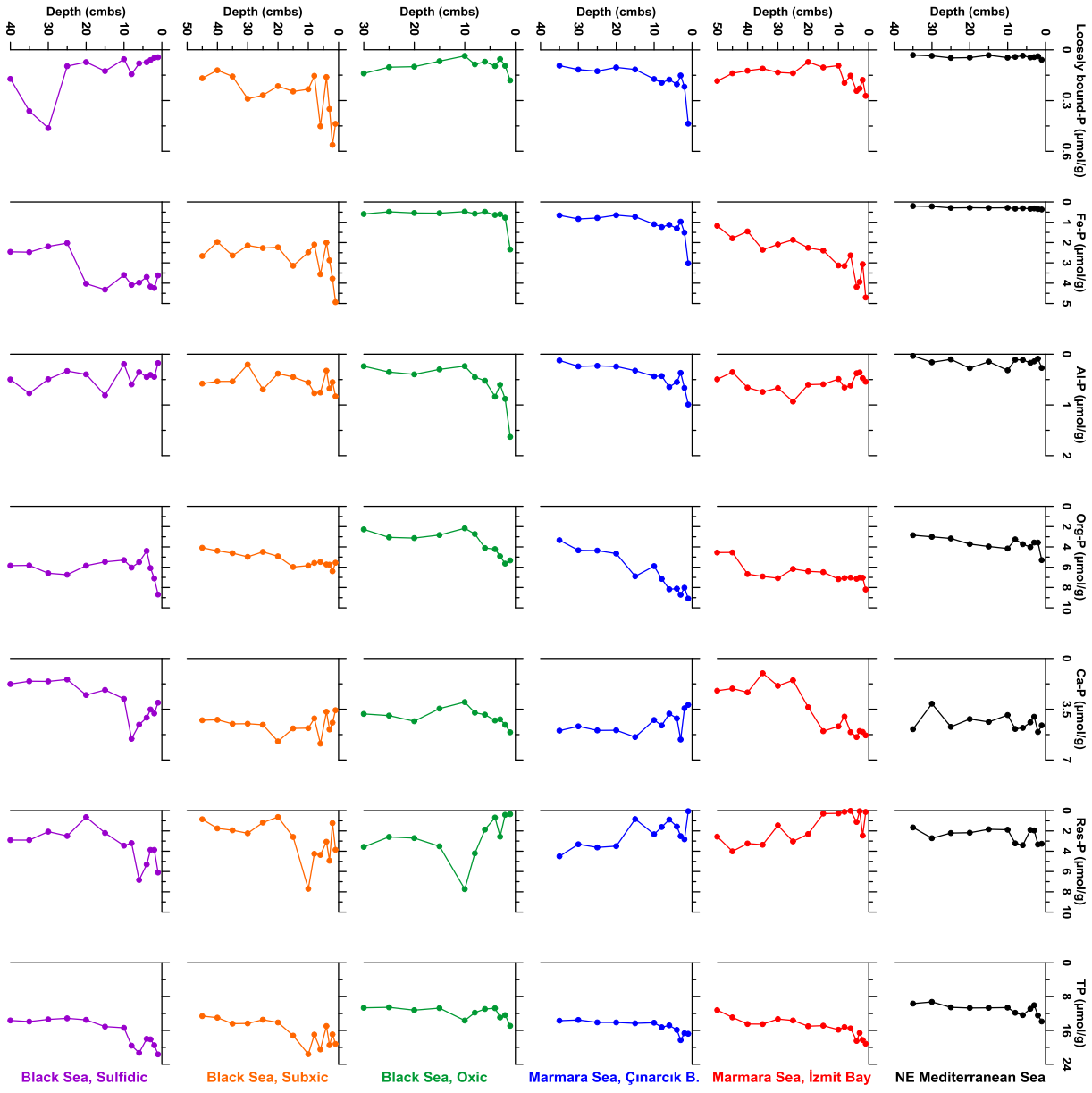

Figure 4.5. Solid-phase depth profiles of P-fractions and TP in the NE Mediterranean, Marmara and Black Seas.

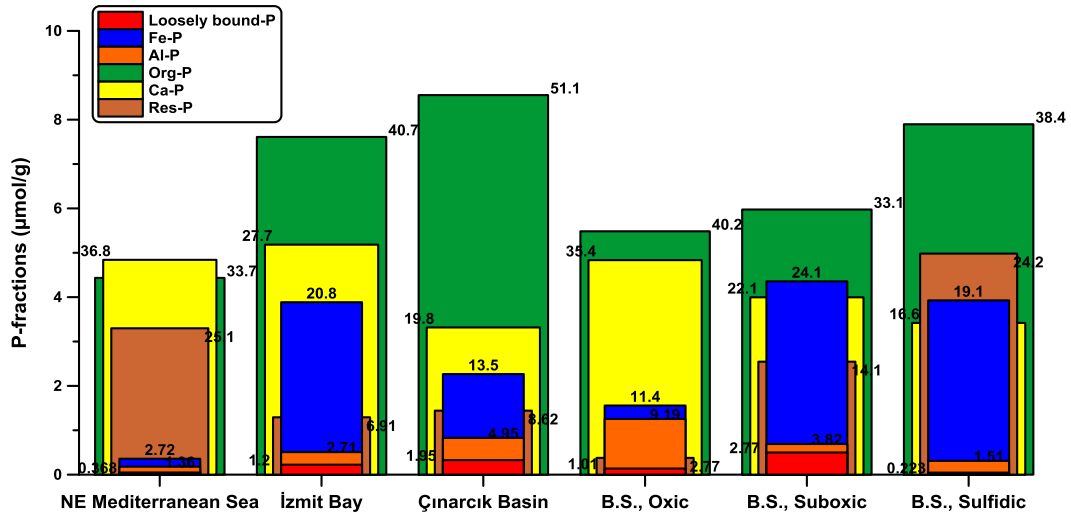

Figure 4.6. Concentration of P-fractions and their contribution to the TP pool (%) in surface (0-2 cm) sediments of the NE Mediterranean, Marmara and Black Seas.

The Ca-P concentrations in the surface sediments of the studied sites varied 3.05 µmol/g dw in the anoxic/sulfidic Black Sea to 5.30 µmol/g dw in the İzmit Bay, Marmara Sea. Previous studies showed that in surface sediments overlain by oxic deep waters, organic P, Fe-bound P and the authigenic Ca-P are the dominant P forms buried in sediments (Ruttenberg, 2003; Ruttenberg and Berner, 1993; Paytan and McLaughlin, 2007). Expectedly, the Ca-P fraction of the surface sediment TP pool reached maximum levels in the oxic NE Mediterranean and oxic part of the Black Sea having maximum TIC concentrations (Figure 4.6). In the marine environments having anoxic conditions in the deep waters, the released dissolved inorganic phosphate to the deep waters or sediment porewaters by degradation of organic P (Ruttenberg, 2003; Paytan and McLaughlin, 2007) have led to depletion of PO_4 in the surface sediments which limits the formation of authigenic Ca-P in the uppermost sedimentary column (Ruttenberg and Berner, 1993; Slomp et al., 1996; Dijkstra et al., 2014; Van Helmond et al., 2020). The minimum Ca-P concentrations with minimum contribution to TP pool in the surface sediment overlain by anoxic/sulfidic Black Sea were, therefore, mainly caused by the lack of authigenic Ca-P formation in the region.

In this study, amounts of "potentially mobile P" from sediments were determined in the three interconnected marine basins displaying distinct biogeochemical properties in the water column and sediments (Figure 4.7). TP concentrations in all cores decreased with sediment depth and stabilized at 10-15 cmbs suggested that the sediments of the studied sites have limited ability to permanently burial of all the deposited P (Figure 4.7). The decline in the TP concentrations of all sediment core samples, therefore, indicated the mobilization of P to the overlying water as also experienced in the recent studies performed in the oxic, suboxic and anoxic/sulfidic parts of the Black and Baltic Seas (Rydin et al., 2011; Malmaeus et al., 2012; Dijkstra et al., 2014; Van Helmond et al., 2020). The pool of "potentially mobile P" varied between 0.023 and 0.148 mol/m^2 in the studied sites with the maximum values recorded in suboxic and anoxic/sulfidic parts of the Black Sea (Figure 4.7). Since the 1970s, for example, the Black Sea marine ecosystem, specifically its northwestern shelf, has been subject to anthropogenic pressures due to terrestrial organic and inorganic matter inputs carried by regional rivers, mainly Danube, Dnieper, Dniester and Bug as well as many other small rivers, leading to development of eutrophic conditions in the basin (Konovalov and Murray, 2001; Mee, 1992; Tugrul et al., 2014). The study results indicated that "potentially mobile P" pool increased from oxic to anoxic/sulfidic parts of the Black Sea (Figure 4.7) suggested the deoxygenation would further enhance the mobilization of P as recently experienced in the eutrophic and hypoxic/anoxic basins (Sommer et al., 2017; Schroller-Lomnitz et al., 2019; Ballagh et al., 2020; Spiegel et al., 2021; Moncelon et al., 2021) where redox-sensitive mobilization of P from sediments led to further development of eutrophication in these basins.

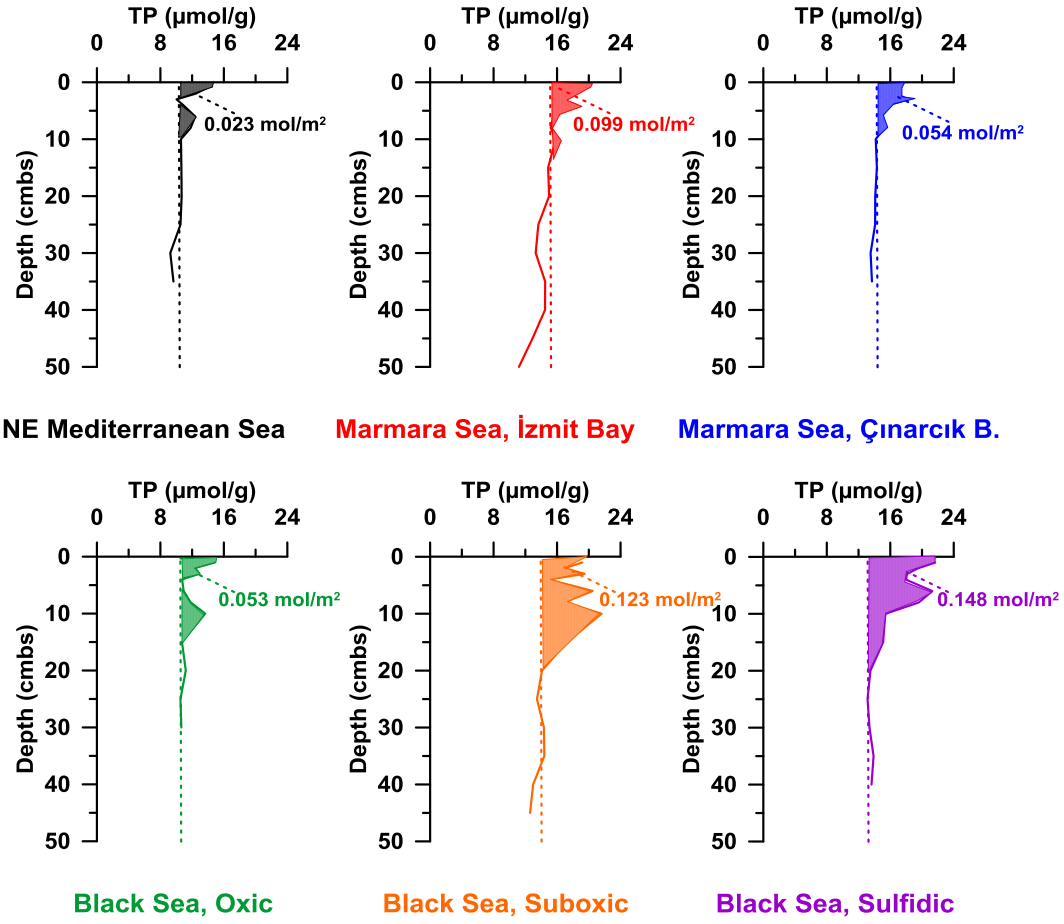

Figure 4.7. Amount of mobile phosphorus in the NE Mediterranean, Marmara and Black Seas. Dashed lines indicated the burial concentration of sedimentary P.

Marmara Sea ecosystem has also been affected by natural (Black Sea inflows) and anthropogenic pressures by direct discharges mainly from the İstanbul city (Tuğrul and Morkoç, 1989; Tugrul and Polat, 1995; Ediger et al., 2016; Yalçın et al., 2017; Tan and Aslan, 2020). Furthermore, recent studies in the Marmara Sea indicated dissolved oxygen deficiency in the deep waters due to increasing organic matter inputs in the upper layer (Ediger et al., 2016; Yalçın et al., 2017) and limited ventilation of deep waters by strong density gradient between water masses (Beşiktepe et al. 1994; Tugrul and Polat, 1995; Tugrul et al., 2002; Ediger et al., 2016). The calculated pool of "potentially mobile P" in the two different regions of the Marmara Sea ranged from 0.054 mol/m^2 in the Çınarcık Basin to 0.099 mol/m^2 in the İzmit Bay much greater than calculated in the oligotrophic NE

Mediterranean Sea. However, in the İzmit Bay, the pool of "potentially mobile P" was very similar to calculated in the suboxic part of the Black Sea indicated that dissolved oxygen deficiency in the deep waters enhanced redox-driven P release in the semi-enclosed İzmit Bay where domestic, agricultural, and industrial pollution have been experienced (Tan and Aslan, 2020).

The primary production in the surface waters of the oligotrophic Eastern Mediterranean is lower compared to measurements in the Black Sea and Marmara Sea based on the studies reported by Van Santvoort et al. (2002), Ergin et al. (1994) and Yılmaz (2002). In the low-nutrient upper layer waters of the Eastern Mediterranean Sea, primary production is mainly limited by phosphorus due to unusually high NO_3/PO_4 ratios in the deep waters as ~28/1 (Krom et al., 1991; Yılmaz and Tugrul, 1998) and in atmospheric and regional rivers (Kocak at al., 2010) as also reported recently by the ^{14}C bioassay experiments conducted in the Turkish coastal waters of the Mediterranean and Aegean Seas (Tufekci et al, 2013). Therefore, redox dependent P fluxes have become significant in the oligotrophic Mediterranean Sea. The sediment "potentially mobile P" calculated in the NE Mediterranean Sea was 0.023 mol/m^2 much lower than calculated in the Marmara and Black Seas due to oligotrophic nature of the Mediterranean Sea, having low primary productivity and sedimentation rates (Figure 4.7). However, increased inputs of nutrients from terrestrial sources (rivers, wastewaters) to the NE Mediterranean coastal areas have enhanced primary production and biodegradable particulate organic matter production (Coban-Yıldız et al., 2000; Yılmaz, 2002; Dogan-Saglamtimur and Tugrul, 2004), leading to eutrophication in the inner bays (Tugrul et al., 2011, 2016, 2018, Kaptan, 2013). Further development of eutrophication in the coastal sites may cause the releases of excess amount of P to the deep waters adversely affecting the ecosystem health and Good Environmental Status of the P-limited NE Mediterranean Sea.

The organic matter enrichments in the Black, Marmara and Northeastern Mediterranean Seas due to the development of eutrophication from terrestrial and natural nutrient and organic matter inputs have led to increase in the accumulation

rates of organic matter buried in sediments. It is known that organic matter biogeochemistry of the sediments has been affected by a series of redox-driven reactions (Jørgensen, 1996) as well as anthropogenic inputs of the particulate organic and inorganic matter that might be transported to offshore regions of the continental seas (Middelburg et al., 1993; Deininger and Frigstad, 2019; Katz et al., 2020). There exist positive correlations between surface sediment geochemical variables (C, N, P) and pool of "potentially mobile P" indicated that excess amounts organic matter accumulation by surface primary production and terrestrial inputs enhanced the mobilization of P (Figure 4.8). Therefore, it is important to know the biogeochemical processes for the long-term removal or releases of P in these three interconnected marine basins for the ecosystem health and eutrophication management efforts.

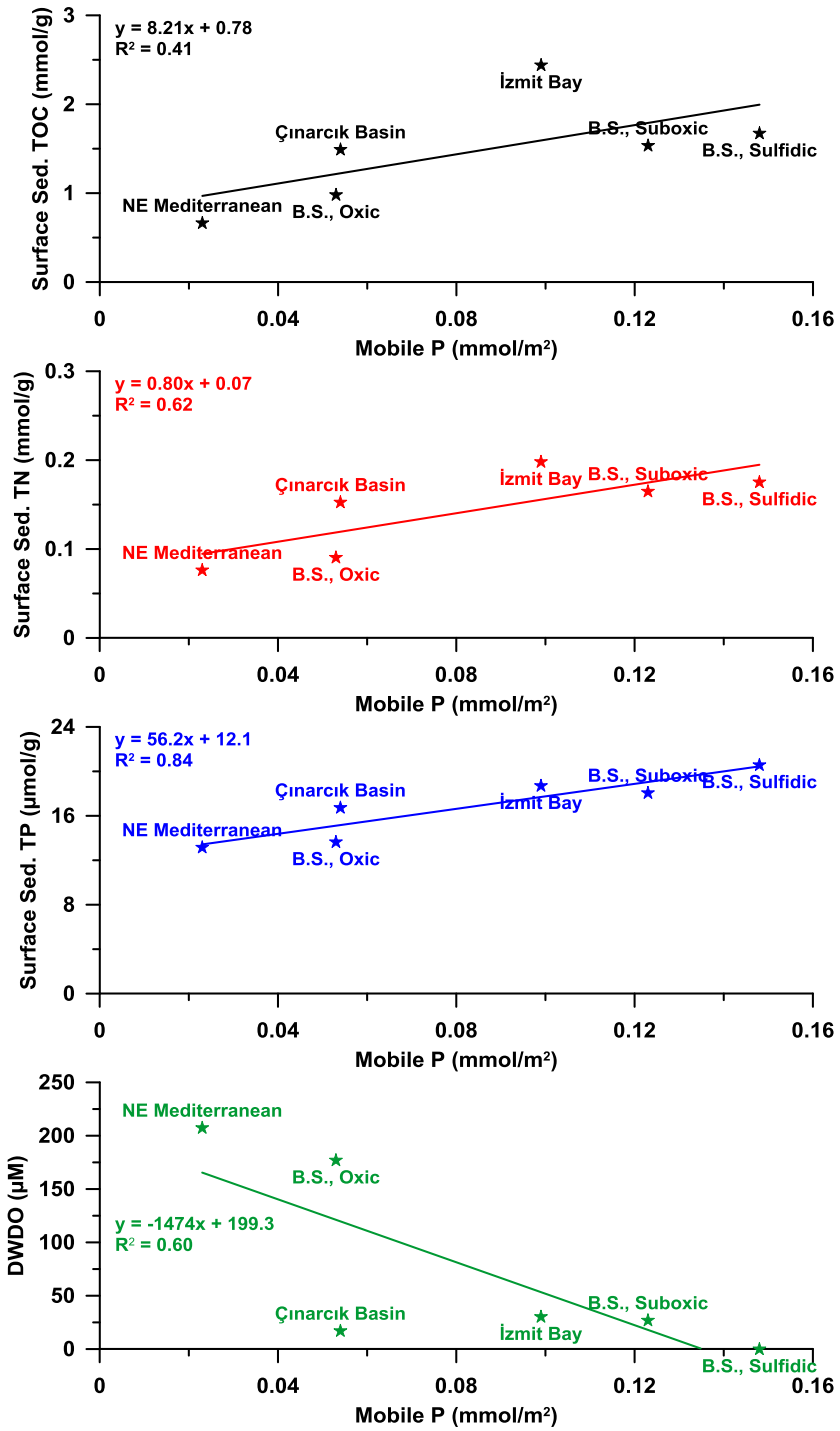

Figure 4.8. Relationship between amount of mobile P and the surface (0-2 cm) sediment TOC, TN, TP and DWDO concentrations in the NE Mediterranean, Marmara and Black Seas.

4.3.4 Conclusions

The results of this study showed that porewater and sediment biogeochemistry of phosphorus displayed great variability in the three interconnected marine basins: Black, Marmara and NE Mediterranean Seas. Maximum porewater PO_4, NH_4 and Si concentrations were measured in the hypoxic Marmara Sea and suboxic/anoxic Black Sea with the maximum surface sediment TOC, TN, Org-P and TP concentrations. Minimum values measured in the NE Mediterranean Sea were due to its oxic and oligotrophic nature with low sedimentation and primary production rates. The surface sediment P pool is mainly dominated by Org-P in the Marmara and Black Seas while the Ca-bound P is the dominant form of TP pool in the NE Mediterranean Sea. The Fe-bound P was found an important P-fraction of TP pool in the semi-enclosed İzmit Bay (Marmara Sea) and suboxic and anoxic/sulfidic parts of the Black Sea as also experienced in recent studies performed in the anoxic basins of the Black and Baltic Seas. The decline in the TP concentrations of all sediment core samples indicated the mobilization of P to the overlying water, which is also in line with the diffusive P fluxes discussed in Chapters 2 and 3 of this dissertation. The pool of "potentially mobile P" varied between 0.023 and 0.148 mol/m^2 in the studied sites with the maximum values recorded in suboxic and anoxic/sulfidic parts of the Black Sea. There exist positive correlations between surface sediment geochemical variables (C, N, P) and pool of "potentially mobile P". Furthermore, "potentially mobile P" pool increased from oxic to anoxic/sulfidic parts of the Black Sea. All these findings suggested the further development of eutrophication and deoxygenation would further enhance the releases of P in these three interconnected marine basins and shift the N/P molar ratios of the deep-water nutrient stocks to even smaller values, with important ramifications for the overlying phytoplankton ecosystem.

Acknowledgements

This study has been supported by DEKOSIM (Centre for Marine Ecosystem and Climate Research, Project Code BAP-08-11-DPT.2012K120880) Project, the

Scientific and Technological Research Council of Turkey (TUBİTAK-2247, 119C027) Project and TUBA-GEBIP Program of the Turkish Academy of Sciences. We would like to thank crew of R/V Bilim-2 and METU-IMS technical personnel for helping multi core operations and analysis of biogeochemical parameters.

CHAPTER 5

SYNTHESIS AND CONCLUSIONS: REDOX DEPENDENT BENTHIC NUTRIENT FLUXES AND THEIR IMPORTANCE FOR THE FUTURE HEALTH OF TURKISH SEAS

The integrated results of the preceding chapters suggest that the deep-sea and sedimentary nutrient recycling is an important component of water column nutrient budgets. This should not be overlooked in the implementation of different national and international policy frameworks focusing on remediation of excess nutrients from the marine or coastal environment. An important policy instrument-compulsory for EU member states but still accepted by Turkey as a major guideline is the Marine Strategy Framework Directive (MSFD) (2008/56/EC, European Commission 2008). MSFD is one of the several marine environment policies to protect more effectively the marine environments across Europe which identifies 11 descriptors to achieve Good Environmental Status (GES) (Table 5.1).

Table 5.1. Marine Strategy Framework Directive (2008/56/EC) descriptors

Descriptors	GES has been achieved
D1	Biodiversity is maintained
D2	Non-indigenous species do not adversely alter the ecosystem
D3	The population of commercial fish species is healthy
D4	Elements of food webs ensure long-term abundance and reproduction
D5	Eutrophication is minimized
D6	The seafloor integrity ensures functioning of the ecosystem
D7	Permanent alteration of hydrographical conditions does not adversely affect the ecosystem
D8	Concentrations of contaminants give no effects
D9	Contaminants in seafood are below safe levels
D10	Marine litter does not cause harm
D11	Introduction of energy (including underwater noise) does not adversely affect the ecosystem

My dissertation particularly contributes to D4, D5 and D6 in Table 5.1. Here, in this final chapter, I give a synthesis of comparative nutrient dynamics in the

Marmara and the Northeastern Mediterranean and emphasize the differences in the two basins that need to be taken into account in the assessment of these descriptors.

Recent studies in the Marmara Sea indicated dissolved oxygen deficiency in the deep waters due to increasing organic matter inputs in the upper layer (Ediger et al., 2016; Yalçın et al., 2017) and limited ventilation of deep waters by strong density gradient between water masses (Beşiktepe et al. 1994; Tugrul and Polat, 1995; Tugrul et al., 2002; Ediger et al., 2016). The change in the nutrient dynamics in the Marmara Sea during the last two decades is, therefore, caused by the rapid deoxygenation and eutrophication in the region and should be under focus for future implementation plan for the ecosystem health of Marmara Sea.

Despite of oligotrophic nature of the NE Mediterranean Sea, its coastal ecosystem is highly fueled by terrestrial nutrient and organic matter inputs from the major rivers and wastewater discharges leading to development of coastal eutrophication in the inner bay waters (Dogan-Saglamtimur and Tugrul 2004; Tugrul et al., 2009; 2011; 2016; 2018). Ongoing eutrophication might induce hypoxia and reduce seafloor in the NE Mediterranean coastal ecosystem resulting in internal nutrients loading due to changing redox state of the seafloor as also experienced recently in the Baltic Sea (Vahtera et al., 2007; Ferreira et al., 2011; Malmaeus et al., 2012; Noffke et al., 2012).

Though biochemistry of water column and biogeochemistry of surface sediments in the Northeastern (NE) Mediterranean and Marmara Sea have been studied extensively, relatively few studies were performed to understand the sediment porewater and solid-phase biogeochemistry in these regions having distinct trophic conditions and deep water redox state. For the ecosystem health of NE Mediterranean and recently deoxygenating Marmara Sea, quantification of redox dependent benthic nutrient fluxes are of critical importance to attain Good Environmental Status (GES).

Organic matter biogeochemistry of the coastal and/or deep sea sediments has been affected by a series of redox reactions (Jørgensen, 1996; Foster and Fulweiler,

2019; Schroller-Lomnitz et al., 2019; Lenstra et al., 2021; Song et al., 2021), environmental (T, S) conditions (Dijkstra et al., 2014) and terrestrial inputs of the particulate inorganic/organic matter (Middelburg et al., 1993; Yemenicioglu and Tunc, 2013; Deininger and Frigstad, 2019; Katz et al., 2020). In this study, the measured TC (TOC+TIC) concentrations ranged from 0.92 mmol/g dw (dry weight) to 7.09 mmol/g dw with the maximum concentrations measured in the NE Mediterranean Sea having carbonate-rich sediments (Figure 5.1). It is well known that from 1 to 40% of primary production is sinking below the euphotic zone and it exponentially attenuates to the base of the mesopelagic zone at around 1000 m. In the water column, organic matter is remineralized, converting organic matter to CO_2. Therefore, only 1% of the surface production is buried in seafloor (Herndl and Reinthaler, 2013). However, this proportion of organic matter sedimented at the seafloor might change due to terrestrial inputs of nutrients and organic matter modifying the organic matter composition and concentrations and grain size distributions of the sediment column (Yemenicioglu and Tunc, 2013; Akcay, 2015). Differences in the sedimentation rates and currents and wave energy also affect distributions of sediment organic matter biogeochemistry (De Falco et al., 2004; Katz et al., 2020). The TOC concentrations throughout the sediment column ranged from 0.24-0.70 mmol/g dw in the NE Mediterranean Sea to 0.47-2.70 mmmol/g dw in the Marmara Sea (Figure 5.1). In the NE Mediterranean Sea, sediment organic matter (C, N) concentrations were lower compared to concentrations measured in the Marmara Sea (Figure 5.1), typical for the oligotrophic offshore and deep sea regions having low primary productivity and sedimentation rates. TOC concentrations from the all core samples decreased with sediment depth throughout the sediment column indicated organic matter degradation processes. Expectedly, the spatial and downcore distributions of TN concentrations were very similar to recorded in TOC concentrations and ranged between 0.02 and 0.23 mmol/g dw in the studied core samples (Figure 5.1). The lower primary production and sedimentation rates in the oligotrophic NE Mediterranean Sea resulted in lower particulate organic matter flux and burial at

the seafloor. Therefore, the TOC and TN concentrations in the NE Mediterranean core samples were 3-4 fold lower than measured in the core samples of Marmara Sea (Figure 5.1).

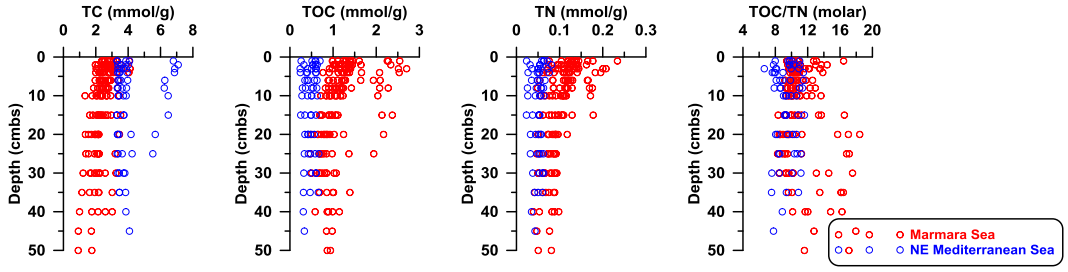

Figure 5.1. Solid-phase depth profiles of total carbon (TC), total organic carbon (TOC) and total nitrogen (TN) concentrations in the NE Mediterranean and Marmara Sea.

From the sediment organic C and N content, molar ratios of C/N were calculated and presented in Figure 5.1. The calculated C/N molar ratios in surface sediments varied between 6.6 and 18.4 and did not significantly change with sediment depth (Figure 5.1). A low C/N molar ratio in marine sediments is an indicative of relatively fresh and undegraded organic matter. Nitrogen and phosphorus are deposited to the seafloor bounding algal cells or organic detritus which undergo decomposition in the water column with faster loss of organic nitrogen and phosphorus, than of carbon, however, resulted in higher C/N and N/P molar ratios relative to Redfield molar ratio C/N/P (Jørgensen, 1996). The study of Boynton et al. (2018) showed that the calculated molar ratios (C/N/P) from the surface sediment data suggested phytoplankton to be the primary source of organic matter based on Redfield ratios of phytoplankton composition (C/N/P=106/16/1) since surface sediment C/N molar ratios mostly ranged from 6.6 to 20 and this distribution suggests a preferential loss of N to denitrification or anammox. In this study, C/N molar ratios calculated from the obtained sediment core samples were generally greater than the classical Redfield Ratio of C/N (C/N=106/16).

The sediment core samples obtained in the NE Mediterranean and Marmara Sea appeared to represent undisturbed accumulations. The measured porewater

nutrients (Si, N, P) concentrations showed spatial variations in the studied sites (Figure 5.2). Porewater nutrient concentrations throughout the obtained sediment core samples ranged between 0.06 and 58.2 µM for PO_4, 0.34 and 91.5 µM for NO_3, 0.17 to 666 µM for NH_4 and 1.22 to 335 µM for Si, respectively (Figure 5.2). Biogeochemical cycling of key nutrients (N, P) is highly linked to dissolved oxygen concentrations and metal (Mn, Fe) cycles due to rapid degradation of labile organic matter by the redox-processes as denitrification, manganese and iron reduction as well as sulfate reduction and methanogenesis in the uppermost centimeters of sediment column resulting in nutrient releases from the sediments (Williams, 1987; Christensen et al., 1988; Jørgensen, 1996; Ignatieva, 1999; Rasheed, 2004; Al-Rousan et al., 2004; Hille et al., 2005; Rasheed et al., 2006; Rydin et al., 2011; Cheng et al., 2014; Mu et al., 2017). Expectedly, maximum porewater PO_4, NH_4 and Si concentrations were measured in the suboxic Marmara Sea where the measured NO_3 concentrations were relatively lower compared to those recorded in the oligotrophic NE Mediterranean Sea having oxic conditions in the deep waters (Figure 5.2). Vertical profiles of porewater NO_3 concentrations in the studied sites suggested that denitrification process took place in the uppermost millimeters of sediment core samples obtained from the suboxic Marmara Sea whilst oxic respiration was the major process for the organic matter remineralization in the oligotrophic NE Mediterranean Sea (Figure 5.2).

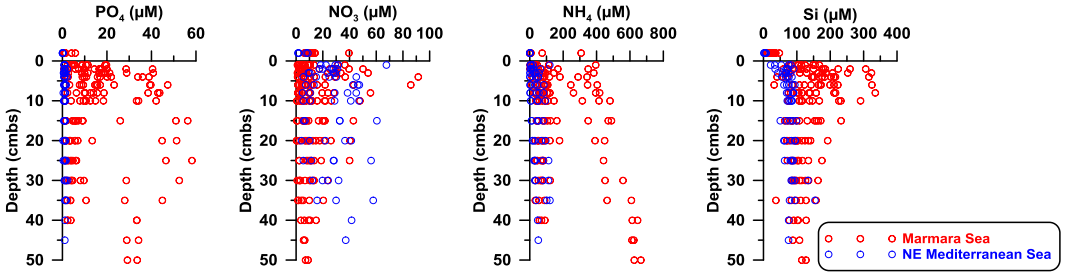

Figure 5.2. Sediment porewater nutrient (PO_4, NO_3, NH_4, Si) profiles in the NE Mediterranean and Marmara Sea.

In order to compare redox dependent benthic nutrient fluxes in the NE Mediterranean and Marmara Sea having distinct biogeochemical properties,

diffusive nutrient fluxes were calculated based on Fick's First Law of Diffusion (Figure 5.3, Table 5.2). A positive flux indicated that sediment acts a source whereas a negative flux indicated that sediment acts as a sink. Calculated porewater diffusive fluxes showed spatial variability in the NE Mediterranean and Marmara Sea with the maximum fluxes of PO_4, NH_4 and Si calculated in the Marmara Sea. In the all studied sites in the NE Mediterranean Sea, sediments act as a source for PO_4, NO_3, NH_4 and Si whilst sediments in the highly eutrophic and suboxic/anoxic sites of the İzmit Bay (Marmara Sea) act as a sink for NO_3 due to rapid utilization of NO_3 ion as a terminal electron acceptor by denitrification process (Table 5.2). The increases in dissolved inorganic nutrients (PO_4, NH_4, Si) and iron concentrations in the eutrophic and suboxic/anoxic/sulfidic regions is highly coupled to redox state in the marine environment since the role of sediments in these regions has important for dissolved iron, inorganic phosphate, ammonium and reactive silicate sources to the bottom waters (Noffke et al., 2012; Mu et al., 2017). The correlation between calculated diffusive nutrient fluxes and the deep waters dissolved oxygen concentrations indicated the redox-dependency on the benthic nutrient dynamics in the NE Mediterranean and Marmara Sea (Figure 5.3, Figure 5.4) as the lower deep water dissolved oxygen concentration resulted in higher porewater diffusive PO_4, NH_4 and Si fluxes which is in agreement with the high rates of organic matter decomposition and release of reactive silicate and phosphate, and nitrate loss at the sediment-water interface. Furthermore, the calculated diffusive nutrient fluxes with the other results performed in oligotrophic (oxic) and highly eutrophic (anoxic/sulfidic) sites showed that the organic matter decomposition with limited trapping of nutrients in the benthic interface might further enhance eutrophication specifically in the Marmara Sea, analogous to benthic 'vicious cycle' in the much shallower Baltic Sea (Table 5.2).

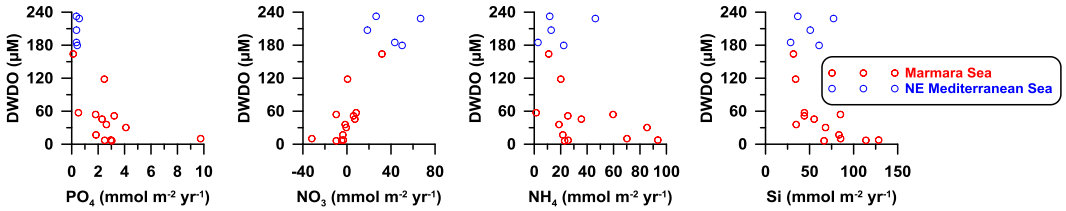

Figure 5.3. Relationship between calculated diffusive nutrient fluxes and deep water dissolved oxygen concentrations in the NE Mediterranean and Marmara Sea.

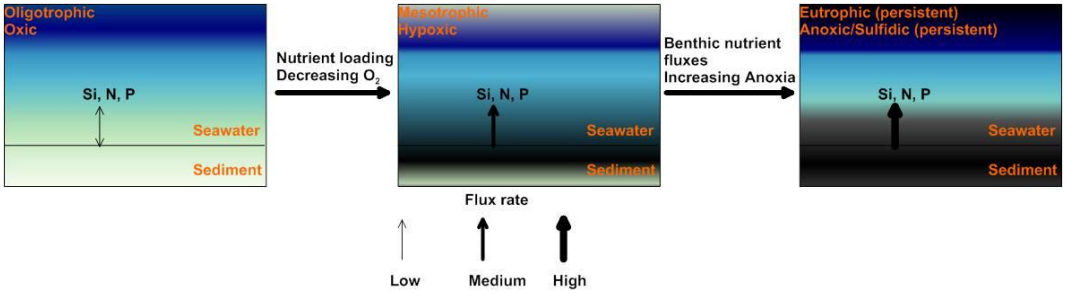

Figure 5.4. Changes in porewater diffusive nutrient fluxes during exposure to eutrophication and deoxygenation.

Table 5.2. Diffusive nutrient fluxes estimated from the porewater profiles of different regions having distinct trophic and redox states

Region	Trophic Status	Deep Water Redox State	PO_4 (mmol m^{-2} yr^{-1})	NO_3 (mmol m^{-2} yr^{-1})	NH_4 (mmol m^{-2} yr^{-1})	Si (mmol m^{-2} yr^{-1})
NE Mediterranean Sea[1]	Oligotrophic	Oxic	0.35-0.57	18.5-66.9	2.81-46.2	28.5-77.2
Marmara Sea[1]	Mesotrophic to Dystrophic	Oxic to Suboxic	0.11-9.76	-31.9-31.8	1.45-93.5	31.7-128.4
Eastern Mediterranean Sea[2]	Oligotrophic	Oxic	0.60	4.14	6.79	34.51
Red Sea[3]	Oligotrophic	Oxic	1.28	6.32	2.08	20.04
Peruvian OMZ[4]	Eutrophic to Dystrophic	Suboxic/Anoxic	2.3-227.6			
Baltic Sea[5]	Eutrophic to Dystrophic	Suboxic/Anoxic/Sulfidic	0.47-67.82		15.64-1441.23	
Çınarcık Basin (Marmara Sea)[6]	Mesotrophic to Eutrophic	Suboxic	0.60		2.04	

[1]This study; [2]Christensen et al., 1988; [3]Rasheed et al., 2006; [4]Noffke et al., 2012; [5]Ignatieva, 1999; [6]Çağatay et al., 2004

The results of this study showed that porewater and sediment biogeochemistry displayed great variability in the NE Mediterranean and Marmara Sea having distinct trophic condition and deep water redox-state. Maximum porewater PO_4,

NH_4 and Si concentrations were measured in the suboxic Marmara Sea whilst minimum values measured in the NE Mediterranean Sea due to its oxic and oligotrophic nature with low sedimentation and primary production rates. Expectedly, maximum fluxes of PO_4, NH_4 and Si were calculated in the Marmara Sea having suboxic conditions. The correlation between calculated diffusive nutrient fluxes and the deep waters dissolved oxygen concentrations indicated the redox-dependency on the benthic nutrient dynamics in the NE Mediterranean and Marmara Sea as the lower deep water dissolved oxygen concentration resulted in higher porewater diffusive PO_4, NH_4 and Si fluxes (Figure 5.4). Therefore, redox dependent benthic nutrient feedbacks in the shelf waters of the NE Mediterranean and Marmara Sea might affect surface water biochemistry by the enhancement of dissolved nutrients transported from deep waters with the major processes in the marine environments such as winter mixing, upwelling, eddies and diffusion.

Based on the 11 descriptors presented by MSFD (Table 5.1), eutrophication should be minimized for the achievement of Good Environmental Status (GES). The study results suggested that the porewater biogeochemistry and the redox dependent benthic nutrient fluxes may eventually change the water column nutrients concentrations and compositions leading to further ecological problems such as enhanced eutrophication, deep water anoxia, changes in phytoplankton abundance and composition, and mucilage formation recently observed in the Marmara Sea. Therefore, the studies based on sediment biogeochemistry are directly linked to Descriptors D1, D4, D5, D6 and D8 presented by MSFD (Table 5.1). For the ecosystem health of NE Mediterranean and recently deoxygenating Marmara Sea, monitoring studies for the redox dependent benthic nutrient dynamics and organic matter geochemistry are of critical importance to attain Good Environmental Status (GES) in these distinct marine basins.

Common management goals of the MSFD or other policies for marine protection for many of the world's coastal-estuarine ecosystems are to improve their good ecological status. Management advices and the ecological targets are often based upon the current compartmentalization of benthic and pelagic habitats. However,

they describe the ecological status of pelagic or benthic habitats, separately and there are few studies combining indicators across habitats and specifically focusing on benthic nutrient fluxes (Dimitriou et al., 2015; Griffiths et al., 2017). Human-induced pressures affect important benthic-pelagic coupling processes altering the flow of ecosystem services in coastal ecosystems. In many coastal ecosystems, eutrophication problems change the physical and biological processes affecting nutrients between benthic and pelagic habitat, food web dynamics, predator-prey feedbacks, and fishing (Griffiths et al., 2017). Therefore, a better understanding of benthic nutrient and organic matter dynamics in specific ecosystems, such as the coastal area of the NE Mediterranean Sea and the hypoxic Marmara Sea, is essential. For the maintenance of ecosystem services in the Turkish Seas, the inorganic (nutrients, metals) and organic matter exchanges between pelagic and benthic habitats should be monitored, modeled and included in the eutrophication management efforts.

REFERENCES

Akcay, I. 2015. Spatial variations of Particulate Organic Matter (POM) composition and concentrations in surface waters and sediments of the Mersin Bay. Dissertation, Institute of Marine Sciences, Middle East Technical University.

Al-Rousan, S., Rasheed, M., Badran, M., 2004. Nutrient diffusive fluxes from sediments in the northern Gulf of Aqaba, Red Sea. Scientia Marina, 68(4), 483-490.

Aydın, I., Aydın, F., Saydut, A., Hamamcı, C., 2009. A sequential extraction to determine the distribution of phosphorus in the seawater and marine surface sediment. Journal of Hazardous Materials 168, 664-669.

Ballagh, F.E.A., Rabouille, C., Andrieux-Loyer, F., Soetaert, K., Elkalay, K., Khalil, K., 2020. Spatio-temporal dynamics of sedimentary phosphorus along two temperate eutrophic estuaries: A data-modelling approach. Continental Shelf Research, 193, 104037.

Barbanti, A., Ceccherelli, V. U., Frascari, F., Reggiani, G., Rosso, G., 1992. Nutrient regeneration processes in bottom sediments in a Po delta lagoon (Italy) and the role of bioturbation in determining the fluxes at the sediment-water interface. Hydrobiologia, 228(1), 1-21.

Basen, M., Krüger, M., Milucka, J., Kuever, J., Kahnt, J., Grundmann, O., Meyerdierks, A., Widdel, F., Shima, S., 2011. Bacterial enzymes for dissimilatory sulfate reduction in a marine microbial mat (Black Sea) mediating anaerobic oxidation of methane. Environmental microbiology, 13(5), 1370-1379.

Berner, R.A., Rao, J.L., 1994. Phosphorus in sediments of the Amazon River and estuary: Implications for the global flux of phosphorus to the sea. Geochimica Cosmochimica Acta, 58, 2333-2340.

Beşiktepe, S., Sur, H.İ., Özsoy, E., Latif, M.A., Oğuz, T., Ünlüata, Ü., 1994. Circulation and hydrography of the Marmara Sea. Prog. Oceanography 34: 285-334.

Bologa, A.S., Frangopol, P.T., Vedernikov, V.I., Stelmakh, L.V., Yunev, O.A., Yilmaz, A., Oguz, T., 1999. Distribution of planktonic primary production in the Black Sea. In Environmental degradation of the Black Sea: challenges and remedies (pp. 131-145). Springer, Dordrecht

Boynton, W.R., Ceballos, M.A.C., Bailey, E.M., Hodgkins, C.L.S., Humphrey, J.L., Testa, J.M., 2018. Oxygen and nutrient exchanges at the sediment-water interface: a global synthesis and critique of estuarine and coastal data. Estuaries and coasts, 41(2), 301-333.

Butcher, S.S., Charlson, R.J., Orians, G.H., Wolfe, G.V., 1992. Global Biogeochemical Cycles. Academic Press, London.

Cheng, X., Zeng, Y., Guo, Z., Zhu, L., 2014. Diffusion of nitrogen and phosphorus across the sediment-water interface and in seawater at aquaculture areas of Daya Bay, China. International journal of environmental research and public health, 11(2), 1557-1572.

Christensen, J.P., Goldsmith, V., Walline, P., Schneller, A., El Sayed, S.Z., 1988. Sedimentary nutrient regeneration on the oligotrophic Eastern Mediterranean continental shelf. Oceanologica Acta, Special issue.

Cline, J.D., 1969. Spectrophotometric determination of hydrogen sulfide in natural waters. Limnology and Oceanography, 14(3), 454-458.

Cline, J.D., Richards, F.A., 1972. Oxygen deficient conditions and nitrate reduction in the eastern tropical North Pacific Ocean. Limnology and Oceanography, 17(6), 885-900.

Coban-Yıldız, Y., Tuğrul, S., Ediger, D., Yılmaz, A., Polat, S.Ç., 2000. A comparative study on the abundance and elemental composition of POM in

three interconnected basins: the Black, the Marmara and the Mediterranean Seas. Mediterranean Marine Science, 1/1, 51-63.

Cui, M., Ma, A., Qi, H., Zhuang, X., Zhuang, G., 2015. Anaerobic oxidation of methane: an “active” microbial process. MicrobiologyOpen, 4(1), 1-11.

Çagatay, M.N., Özcan, M., Güngör, E., 2004. Pore-water and sediment geochemistry in the Marmara Sea (Turkey): early diagenesis and diffusive fluxes. Geochemistry: Exploration, Environment, Analysis, 4(3), 213-225.

Çağatay, M.N., Yildiz, G., Bayon, G., Ruffine, L., Henry, P., 2018. Seafloor authigenic carbonate crusts along the submerged part of the North Anatolian Fault in the Sea of Marmara: Mineralogy, geochemistry, textures and genesis. Deep-Sea Research Part II 153, 92-109.

De Falco, G., Magni, P., Teräsvuori, L.M.H., Matteucci, G., 2004. Sediment grain size and organic carbon distribution in the Cabras lagoon (Sardinia, western Mediterranean). Chemistry and Ecology, 20(sup1), 367-377.

Deininger, A., Frigstad, H., 2019. Reevaluating the role of organic matter sources for coastal eutrophication, oligotrophication and ecosystem health. Frontiers in Marine Science, 6, 210.

D'Hondt, S., Spivack, A.J., Pockalny, R., Ferdelman, T.G., Fischer, J.P., Kallmeyer, J.,Abrams, L.J., Smith, D.C., Graham, D., Hasiuk, F., Schrum, H., Stancin, A.M., 2009. Subseafloor sedimentary life in the South Pacific Gyre. PNAS 106, 11651–11656.

Diaz, R.J., Rosenberg, R., 2008. Spreading dead zones and consequences for marine ecosystems. Science, 321(5891), 926-929.

Dijkstra, N., Kraal, P., Kuypers, M.M., Schnetger, B., Slomp, C.P., 2014. Are iron-phosphate minerals a sink for phosphorus in anoxic Black Sea sediments?. PloS one, 9(7), e101139.

Dijkstra, N., Kraal, P., Séguret, M.J.M., Flores, M.R., Gonzalez, S., Rijkenberg, M.J., Slomp, C.P., 2018. Phosphorus dynamics in and below the redoxcline in the Black Sea and implications for phosphorus burial. Geochimica et Cosmochimica Acta, 222, 685-703.

Dimitriou, P., Papageorgiou, N., Arvanitidis, C., Assimakopoulou, G., Pagou, K.,Papadopoulou, K.N., Pavlidou, A., Pitta, P., Reizopoulou, S., Simboura, N.,Karakassis, I., 2015. One step forward: benthic pelagic coupling and indicators for good environmental status. PLoS One 10 (10), 1–17.

Dogan-Saglamtimur, N., Tugrul, S., 2004. Effect of riverine nutrients on coastal water ecosystems: A case study from the Northeastern Mediterranean Shelf. Fresenius Environmental Bulletin, 13, 1288-1294.

Ediger, D., Beken, Ç., Yüksek, H., Tugrul, S., 2016. Eutrophication in the Sea of Marmara. In: The Sea of Marmara; Marine Biodiversity, Fisheries, Conservation and Governance. (Ozsoy, E., Cagatay, M.N., Balkıs, N., Balkıs, N and Ozturk, B). Turkish Marine Research Foundation (TUDAV), Publication No: 42, Istanbul, Turkey, 723-736.

Eijsink, L.M., Krom, M.D., Herut, B., 2000. Speciation and burial flux of phosphorus in the surface sediments of the eastern Mediterranean. American Journal of Science, 300(6), 483-503.

Erdogan, E., 2014. Distribution of particulate organic matter, its elemental composition (C/N/P) and variation with environmental factors in the shelf waters and sediments in the northeastern Mediterranean (Mersin Bay). Dissertation, Institute of Graduate School of Natural and Applied Sciences, Mersin University.

Ergin, M., Bodur, M.N., Yildiz, M., Ediger, D., Ediger, V., Yemenicioğlu, S., Yücesoy, F., 1994. Sedimentation rates in the Sea of Marmara: a comparison of results based on organic carbon-primary productivity and ^{210}Pb dating. Continental Shelf Research, 14(12), 1371-1387.

Ergin, M., Yörük, R.,1990. Distribution and texture of the bottom sediments in a semi-enclosed coastal inlet, the Izmit Bay from the Eastern Sea of Marmara (Turkey). Estuarine, Coastal and Shelf Science, 30(6), 647-654.

Ermis, E. 2017. Spatial variations of seafloor iron cycle in Cilician basin (Eastern Mediterranean). Dissertation, Institute of Marine Sciences, Middle East Technical University.

Escobar-Briones, E., García-Villalobos, F.J., 2009. Distribution of total organic carbon and total nitrogen in deep-sea sediments from the southwestern Gulf of Mexico. Boletín de la Sociedad Geológica Mexicana, 61(1), 73-86.

European Commission, 2008. Directive 2008/56/EC of the European Parliament and of the Council of 17 June 2008, establishing a framework for community action in the field of marine environmental policy (Marine Strategy Framework Directive).

Evans, G., Erten, H., Alavi, S.N., Von Gunten, H.R., Ergin, M., 1989. Superficial deep-water sediments of the eastern Marmara basin. Geo-Marine Letters, 9(1), 27-36.

Fang, T-H., Chen, J-L., Huh, C-A., 2007 Sedimentary phosphorus species and sedimentation flux in the East China Sea. Continental Shelf Research 27, 1465-1476.

Farrow, C.R., Ackerman, J.D., Smith, R.E., Snider, D., 2019. Riverine transport and nutrient inputs affect phytoplankton communities in a coastal embayment. Freshwater Biology.

Fenchel, T., King, G.M., Blackburn, T.H., 1998. Bacterial Biogeochemistry: the Ecophysiology of Mineral Cycling. Academic Press, San Diego: 307 pp.

Ferreira, J.G., Andersen, J.H., Borja, A., Bricker, S.B., Camp, J., Cardoso da Silva, M., Garcés, E., Heiskanen, A.S., Humborg, C., Ignatiades, L., Lancelot, C., Menesguen, A., Tett, P., Hoepffnerm, N., Claussen, U., 2011. Overview of eutrophication indicators to assess environmental status within the

European Marine Strategy Framework Directive. Estuarine, Coastal and Shelf Science. 93, 117–131.

Foster, S.Q., Fulweiler, R.W., 2019. Estuarine sediments exhibit dynamic and variable biogeochemical responses to hypoxia. Journal of Geophysical Research: Biogeosciences, 124(4), 737-758.

Gao, Z., Zheng, X. L., Li, W., Song, H., 2008. Determination of nutrient fluxes across the sediment-water interface in a nitrate-rich reservoir. In: Bioinformatics and Biomedical Engineering, 2008. ICBBE 2008. The 2nd International Conference on. IEEE, 2008. p. 3319-3322.

Géli, L., Henry, P., Zitter, T., Dupré, S., Tryon, M., Çağatay, M.N., de Lépinay, B.M., Le Pichon, X., Şengör, A.M.C., Görür, N., Natalin, B., Uçarkuş, G., Özeren, S., Volker, D., Gasperini, L., 2008. Gas emissions and active tectonics within the submerged section of the North Anatolian Fault zone in the Sea of Marmara. Earth Planet. Sci. Lett. 274 (1-2), 34–39.

Grasshoff, K., Ehrhardt, M., Kremling, K., 1983. Determination of nutrients. In: Methods of Seawater Analysis (2nd ed.), Verlag Chemie Gmbh, Weiheim, Germany, pp. 125-188.

Griffiths, J. R., Kadin, M., Nascimento, F.J.A., Tamelander, T., Tornroos, A., Bonaglia, S., Bonsdorff, E., Bruchert, V., Gardmark, A., Jarnstrom, M., Kotta, J., Lindegren, M., Nordstrom, M.C., Norkko, A., Olsson, J., Weigel, B., Zydelis, R., Blenckner, T., Niiranen, S., Winder, M., 2017. The importance of benthic−pelagic coupling for marine ecosystem functioning in a changing world. Glob. Change Biol., 23, 2179− 2196.

Halbach, P., Kuşçu, İ., Inthorn, M., Kuhn, T., Pekdeğer, A., Seifert, R., 2002. Methane in sediments of the deep Marmara Sea and its relation to local tectonic structures. In Integration of Earth Science Research on the Turkish and Greek 1999 Earthquakes (pp. 71-85). Springer, Dordrecht.

Hélène, O., Karine, O., Stéphanie, D., Carla, S., Anne-Sophie, A., Clément, G., Ruffine, L., 2020. Geological and biological diversity of seeps in the Sea of

Marmara. Deep Sea Research Part I: Oceanographic Research Papers, 161, 103287.

Herndl, G.J., Reinthaler, T. 2013. Microbial control of the dark end of the biological pump. Nature Geoscience 6, 718–724.

Hille, S., Nausch, G., Leipe, T., 2005. Sedimentary deposition and reflux of phosphorus (P) in the Eastern Gotland Basin and their coupling with P concentrations in the water column. Oceanologia, 47(4).

Ignatieva, N. V., 1999. Nutrient exchange across the sediment-water interface in the eastern Gulf of Finland. Boreal environment research, 4(4), 295-306.

Jeitner, T.M., 2014. Optimized ferrozine-based assay for dissolved iron. Analytical biochemistry, 454, 36-37.

Jilbert, T., Slomp, C.P., 2013. Iron and manganese shuttles control the formation of authigenic phosphorus minerals in the euxinic basins of the Baltic Sea. Geochimica et Cosmochimica Acta, 107, 155-169.

Jørgensen, B.B., 1996. Material flux in the sediment. Eutrophication in coastal marine ecosystems, 115-135.

Kaptan, M.S., 2013. Assessment of the trophic status of the Mersin bay waters, northEastern Mediterranean. Dissertation, Institute of Marine Sciences, Middle East Technical University.

Katz, T., Weinstein, Y., Alkalay, R., Biton, E., Toledo, Y., Lazar, A., Zlatkin, O., Soffer, R., Rahav, E., Sisma-Ventura, G., Bar, T., Ozer, T., Gildor, H., Almogi-Labin, A., Kanari, M., Berman-Frank, I., Herut, B., 2020. The first deep-sea mooring station in the eastern Levantine basin (DeepLev), outline and insights into regional sedimentological processes. Deep Sea Research Part II: Topical Studies in Oceanography, 171, 104663.

Kocak, M., 2015. Solubility of Atmospheric Nutrients over the Eastern Mediterranean: Comparison between Pure-Water and Sea-Water, Implications Regarding Marine Production, Turk. J. Fish. Aquat., Sci, 15, 59-71.

Kocak, M., Kubilay, N., Tugrul, S., Mihalopoulos, N., 2010. Atmospheric nutrient inputs to the northern levantine basin from a long-term observation: sources and comparison with riverine inputs. Biogeosciences, 7, 12, 4037-4050.

Konovalov, S.K., Luther III, G.W., Yücel, M., 2007. Porewater redox species and processes in the Black Sea sediments. Chemical Geology, 245(3-4), 254-274.

Konovalov, S.K., Murray, J.W., 2001. Variations in the chemistry of the Black Sea on a time scale of decades (1960–1995). J. Mar. Syst. 31, 217–243.

Kostka, J.E., Luther III, G.W., 1994. Partitioning and speciation of solid phase iron in saltmarsh sediments. Geochimica et Cosmochimica Acta, 58(7), 1701-1710.

Kress, N., Herut, B., 2001. Spatial and seasonal evolution of dissolved oxygen and nutrients in the Southern Levantine Basin (Eastern Mediterranean Sea). Chemical characterization of the water masses and inferences on the N:P ratios. Deep-Sea Research I, 48, 2347-2372.

Kristensen, E., 2000. Organic matter diagenesis at the oxic/anoxic interface in coastal marine sediments, with emphasis on the role of burrowing animals. In Life at interfaces and under extreme conditions (pp. 1-24). Springer, Dordrecht.

Krom, M.D., Herut, B., Mantoura, R.F.C., 2004. Nutrient budget for the Eastern Mediterranean: Implications for phosphorus limitation. Limnology and Oceanography, 49(5), 1582-1592.

Krom, M.D., Kress, N., Brenner, S., Gordon, L.I., 1991. Phosphorus limitation of primary productivity in the eastern Mediterranean Sea. Limnology and Oceanography, 36(3), 424-432.

Le Pichon, X., Sengör, A.M.C., Demirbag, E., Rangin, C., Imren, C., Armijo, R., Görür, N., Cagatay, N., Mercier de Lepinay, B., Meyer, B., Saatcilar, R., Tok, B., 2001. The active Main Marmara fault. Earth Planet. Sci. Lett. 192, 595–616.

Lenstra, W.K., Hermans, M., Séguret, M.J., Witbaard, R., Severmann, S., Behrends, T., Slomp, C.P., 2021. Coastal hypoxia and eutrophication as key controls on benthic release and water column dynamics of iron and manganese. Limnology and Oceanography, 66(3), 807-826.

Li, Y.-H., Gregory, S., 1974. Diffusion of ions in sea water and in deep-sea sediments. Geochim. Cosmochim. Acta 38 (5), 703–714.

Malmaeus, M., Rydin, E., Jonsson, P., Lindgren, D., Karlsson, M., 2012. Estimating the amount of mobile phosphorus in Baltic coastal soft sediments of central Sweden. Boreal environment research, 17(6), 425-436.

Mee, L., 1992. The Black Sea in crisis: A need for concerted international action, Ambio 21(4), 278-286.

Menzel, D.W., Corwin, N. 1965. The measurement of total phosphorus in seawater based on the liberation of organically bound fractions by persulfate oxidation. Limnology and Oceanography, 10, 280-282.

Middelburg, J.J., Vlug, T., Jaco, F., Van der Nat, W.A., 1993. Organic matter mineralization in marine systems. Global and Planetary Change, 8(1-2), 47-58.

Milucka, J., Ferdelman, T.G., Polerecky, L., Franzke, D., Wegener, G., Schmid, M., Lieberwirth, I., Wagner, M., Widdel, F., Kuypers, M.M.M., 2012. Zero-valent sulphur is a key intermediate in marine methane oxidation. Nature, 491(7425), 541-546.

Moncelon, R., Gouazé, M., Pineau, P., Beneteau, E., Bréret, M., Philippine, O., Robin, F.X., Dupuy, C., Metzger, E., 2021. Coupling between sediment biogeochemistry and phytoplankton development in a temperate freshwater marsh (Charente-Maritime, France): Evidence of temporal pattern. Water Research, 189, 116567.

Mortimer, C.H., 1942. The exchange of dissolved substances between mud and water in lakes. The Journal of Ecology, 147-201.

Mu, D., Yuan, D., Feng, H., Xing, F., Teo, F.Y., Li, S., 2017. Nutrient fluxes across sediment-water interface in Bohai Bay Coastal Zone, China. Marine pollution bulletin, 114(2), 705-714.

Murray, J.M., Codispoti, L.A., Freiderich, G.E., 1995. Oxidation–reduction environments: the suboxic zone in the Black Sea. In: Huang, C.P., O'Melia, C.R., Morgan, J.J. (Eds.), Aquatic Chemistry, ACS Advances in Chemistry Series, 244, pp. 157–176.

Noffke A., Hensen C., Sommer S., Scholz F., Bohlen L., Mosch T., Graco M., Wallmann K., 2012. Benthic iron and phosphorus fluxes across the Peruvian oxygen minimum zone. Limnol. Oceanogr. 57, 851–867.

Nteziryayo, L.R., Danielsson, Å., 2018. Sediment DSi and DIP fluxes under changing oxygen availability in bottom waters. Boreal Environment Research, 23, 159-174.

Oguz, T., 2005. Black Sea ecosystem response to climatic teleconnections. Oceanography, 18(2), 122-133.

Paulmier, A., Ruiz-Pino, D., 2009. Oxygen minimum zones (OMZs) in the modern ocean. Progress in Oceanography, 80(3), 113-128.

Paytan, A., McLaughlin, K., 2007. The oceanic phosphorus cycle. Chemical reviews, 107(2), 563-576.

Polat, C., Tuğrul, S., Çoban, Y., Basturk, O., Salihoglu, I., 1998. Elemental composition of seston and nutrient dynamics in the Sea of Marmara. Hydrobiologia 363:157–167. http://dx.doi.org/10.1023/A:1003117504005.

Polat, Ç., Tugrul, S., 1995. Nutrient and Organic Carbon Exchanges between the Black and Marmara Seas through the Bosporus Strait, Cont. Shelf Res. 15(9), 1115-1132.

Psenner R., Bostrom, B., Dinka, M., Pettersson, K., Pucsko, R., Sager, M., 1988. Fractionation of phosphorus in suspended matter and sediments. Arch. Hydrobiol. Beih. Ergebn. Limnol. 30, 98–109.

Raiswell, R., Canfield, D.E., Berner, R. A., 1994. A comparison of iron extraction methods for the determination of degree of pyritisation and the recognition of iron-limited pyrite formation. Chemical Geology, 111(1-4), 101-110.

Rasheed, M., 2004. Nutrient Fluxes from sediments of the northern Gulf of Aqaba under various anthropogenic activities. Lebanese science journal/Journal scientifique libanais, 5(1), 3-16.

Rasheed, M., Al-Rousan, S., Manasrah, R., Al-Horani, F., 2006. Nutrient fluxes from deep sediment support nutrient budget in the oligotrophic waters of the Gulf of Aqaba. Journal of oceanography, 62(1), 83-89.

Rebreanu, L., Vanderborght, J.P., Chou, L., 2008. The diffusion coefficient of dissolved silica revisited. Marine chemistry, 112(3), 230-233.

Reeburgh, W.S., 1976. Methane consumption in Cariaco Trench waters and sediments. Earth and Planetary Science Letters, 28(3), 337-344.

Reeburgh, W.S., 1980. Anaerobic methane oxidation: rate depth distributions in Skan Bay sediments. Earth and Planetary Science Letters, 47(3), 345-352.

Rodellas, V., Garcia-Orellana, J., Masqué, P., Feldman, M., Weinstein, Y., 2015. Submarine groundwater discharge as a major source of nutrients to the Mediterranean Sea. Proceedings of the National Academy of Sciences, 112(13), 3926-3930.

Ross, D., Degens, E., 1974. Recent sediments of Black Sea, in: Te Black Sea-Geology, Chemistry, and Biology. pp. 183–199.

Ruffine, L., Ondreas, H., Blanc-Valleron, M.M., Teichert, B.M.A., Scalabrin, C., Rinnert, E.,Birot, D., Croguennec, C., Ponzevera, E., Pierre, C., Donval, J.P., Alix, A.S., Germain,Y., Bignon, L., Etoubleau, J., Caprais, J.C., Knoery, J., Lesongeur, F., Thomas, B.,Roubi, A., Legoix, L., Burnard, P., Chevalier, N., Lu, H., Dupré, S., Fontanier, C.,Dissard, D., Olgun, N., Yang, H., Strauss, H., Özaksoyj, V., Perchoc, J., Podeur, C.,Tarditi, C., Özbekij, E., Guyader, V., Marty, B., Madre, D., Grall, C., Embriaco, D.,Polonia, A., Gasperini, L., Cagatay, M.N., Pitel-Roudaut, M., Henry, P., Géli, L., 2018. Multidisciplinary investigation on cold seeps with vigorous gas emissions in the Sea of Marmara (MarsiteCruise): Strategy for site detection and sampling and first scientific outcome. Deep Sea Research Part II: Topical Studies in Oceanography, 153, 36-47.

Ruttenberg, K.C., 2003. Te global phosphorus cycle, in: Treatise on Geochemistry 8. pp. 585–643.

Ruttenberg, K.C., Berner, R.A., 1993. Authigenic apatite formation and burial in sediments from non-upwelling, continental margin environments. Geochimica et cosmochimica acta, 57(5), 991-1007.

Rydin, E., 2000. Potentially mobile phosphorus in Lake Erken sediment. Water Research, 34(7), 2037-2042.

Rydin, E., Malmaeus, J.M., Karlsson, O.M., Jonsson, P., 2011. Phosphorus release from coastal Baltic Sea sediments as estimated from sediment profiles. Estuarine, Coastal and Shelf Science, 92(1), 111-117.

Sarı, E., Çağatay, N., 2010. Sediment core studies on the North Anatolian Fault Zone in the Eastern Sea of Marmara: Evidence of Sea Level Changes and Fault Activity. Bulletin of the Mineral Research Exploration 140: 1-18.

Schroller-Lomnitz, U., Hensen, C., Dale, A.W., Scholz, F., Clemens, D., Sommer, S., Noffke, A., Wallmann, K., 2019. Dissolved benthic phosphate, iron and carbon fluxes in the Mauritanian upwelling system and implications for ongoing deoxygenation. Deep Sea Res. Part I 143, 70–84.

Simboura, N., Panayotidis, P., Papathanassiou, E., 2005. A synthesis of the biological quality elements for the implementation of the European Water Framework Directive in the Mediterranean ecoregion: the case of Saronikos Gulf. Ecological indicators, 5(3), 253-266.

Slomp, C.P., Epping, E.H., Helder, W., Raaphorst, W.V., 1996. A key role for iron-bound phosphorus in authigenic apatite formation in North Atlantic continental platform sediments. Journal of marine Research, 54(6), 1179-1205.

Sommer, S., Clemens, D., Yücel, M., Pfannkuche, O., Hall, P.O.J., Almroth-Rosell, E., Schulz-Vogt, H.N., Dale, A.W., 2017. Major bottom water ventilation events do not significantly reduce basin-wide benthic N and P release in the Eastern Gotland Basin (Baltic Sea). Frontiers in Marine Science, 4(18).

Song, G.D., Liu, S.M., Zhang, J., Zhu, Z.Y., Zhang, G.L., Marchant, H.K., Kuypers, M.M.M., Lavik, G., 2021. Response of benthic nitrogen cycling to estuarine hypoxia. Limnology and Oceanography, 66(3), 652-666.

Spiegel, T., Vosteen, P., Wallmann, K., Paul, S.A., Gledhill, M., Scholz, F., 2021. Updated estimates of sedimentary potassium sequestration and phosphorus release on the Amazon shelf. Chemical Geology, 560, 120017.

Stookey, L.L., 1970. Ferrozine-A new spectrophotometric reagent for iron. Analytical chemistry, 42(7), 779-781.

Strickland, J.D.H., Parsons, T.R., 1972. A Practical Handbook of Seawater Analysis, 2nd edition. Bulletin of the Fisheries Research Board of Canada, No. 167, 310 pp.

Sundby, B., Gobeil, C., Silverberg, N., Alfonso, M., 1992. The phosphorus cycle in coastal marine sediments. Limnology and oceanography, 37(6), 1129-1145.

Tan, İ., Aslan, E., 2020. Metal pollution status and ecological risk assessment in marine sediments of the inner Izmit Bay. Regional Studies in Marine Science, 33, 100850.

Tanhua, T., Hainbucher, D., Schroeder, K., Cardin, V., Álvarez, M., Civitarese, G., 2013. The Mediterranean Sea system: a review and an introduction to the special issue. Ocean Science, 9(5), 789-803.

Toderascu, R., Rusu, E., 2013. Evaluation of the circulation patterns in the Black Sea using remotely sensed and in situ measurements. International Journal of Geosciences, 4(7), 1009-1017.

Tryon M.D., Henry P., Cagatay, M.N., Zitter, T.A.C., Geli, L., Gasperini, L., Burnard, P., Bourlange, S., Grall, C., 2010. Pore fluid chemistry of the North Anatolian Fault Zone in the Sea of Marmara: a diversity of sources and processes. Geochem Geophys Geosys, 11, 1–22.

Tufekci, V., Kuzyaka, E., Tufekci, H., Avaz, G., Gunay, A.S., Tugrul, S., 2013. Determination of limited nutrients in the Turkish coastal waters of the Mediterranean and Aegean Seas. J. Black Sea/Mediterranean Environment Vol. 19, No. 3: 299-311.

Tugrul, S., Kuçuksezgin, F., Yemenicioglu, S. Uysal, Z., 2009: Long Term Biomonitoring, Trend and Compliance Monitoring Program in Coastal Areas from Aegean, Northeastern Mediterranean and Eutrophication Monitoring in Mersin Bay (MEDPOL Phase IV). Ministry of Environment and Forestry, Ankara.

Tugrul, S., Ozhan, K., Akcay, I., 2018. Assessment of trophic status of the northeastern Mediterranean coastal waters: eutrophication classification tools revisited. Environ Sci Pollut Res, https://doi.org/10.1007/s11356-018-2529-6.

Tugrul, S., Polat, Ç., 1995. Quantitative comparison of the influxes of nutrients and organic carbon into the Sea of Marmara both from anthropogenic sources and from the Black Sea. Water Science and Technology 32(2), 115-121.

Tugrul, S., Uysal, Z., Erdogan, E., Yucel, N., 2011. Changes of eutrofication indicator parameters (TP, DIN, Chl-a and TRIX) in the cilician basin (Northeast Mediterranean). Ekoloji, 20(80), 33-41.

Tugrul, S., Yucel, N., Akcay, I., 2016. Chemical oceanography of north eastern Mediterranean. In: The Turkish part of the Mediterranean Sea; Marine Biodiversity, Fisheries, Conservation and Governance. (Turan, C., Salihoglu, B., Ozbek, E.O. and Ozturk, B). Turkish Marine Research Foundation (TUDAV), Publication No: 43, Istanbul, Turkey, 15-29.

Tuğrul, S., Beşiktepe T., Salihoğlu, I., 2002. Nutrient exchange fluxes between the Aegean and Black Seas through the Marmara Sea. Mediterranean Marine Science, 3, 33-42.

Tuğrul, S., Morkoç, E., 1989. Oceanographic Characteristics of İzmit Bay. NATO TU-WATERS Project, Technical Report. TÜBİTAK, MRC Publ, Kocaeli, Turkey.

Tuğrul, S., Murray, J.W., Friederich, G.E., Salihoğlu, I., 2014. Spatial and temporal variability in the chemical properties of the oxic and suboxic layers of the Black Sea. J. Mar. Syst. 135:29–43. http://dx.doi.org/10.1016/j.jmarsys.2013.09.008.

Ullman, W. J., Aller, R.C., 1982. Diffusion coefficients in nearshore marine sediments. Limnology and Oceanography, 27(3), 552-556.

UNEP, 1989. State of the Mediterranean Marine Environment. MAP Technical Series No. 28, UNEP, Athens.

UNEP/MAP, 2005: Sampling and analysis techniques for the eutrophication monitorıng strategy of MED POL, MAP Technical Reports Series No. 163, Athens.

UNEP/MAP, 2006. Methods for sediment sampling and analysis, Review Meeting of MED POL - Phase III Monitoring Activities, Athens.

Ünlüata, Ü., Oğuz, T., Latif, M. A., Özsoy, E., 1990. On the Physical Oceanography of the Turkish Straits, in: The Physical Oceanography of Sea Straits, L. J. Pratt (editor), NATO/ASI Series, Kluwer, Dordrecht, 25-60.

Vahtera, E., Conley, D.J., Gustafsson, B.G., Kuosa, H., Pitkänen, H., Savchuk, O.P., Tamminen, T., Viitasalo, M., Voss, M., Wasmund, N., Wulff, F., 2007. Internal ecosystem feedbacks enhance nitrogen-fixing cyanobacteria blooms and complicate management in the Baltic Sea. Ambio 36: 186–194.

Van Helmond, N.A., Robertson, E.K., Conley, D.J., Hermans, M., Humborg, C., Kubeneck, L.J., Lenstra, W.K., Slomp, C.P., 2020. Removal of phosphorus and nitrogen in sediments of the eutrophic Stockholm archipelago, Baltic Sea. Biogeosciences 17, 2745–2766.

Van Santvoort, P.J.M., De Lange, G.J., Thomson, J., Colley, S., Meysman, F.J.R., Slomp, C.P., 2002. Oxidation and origin of organic matter in surficial Eastern Mediterranean hemipelagic sediments. Aquatic Geochemistry, 8(3), 153-175.

Vedernikov, V.I., Demidov, A.B., 1993. Primary production and chlorophyll in the deep regions of the Black Sea. Oceanology, 33(2), 229-235.

Williams, G.R., 1987. The coupling of biogeochemical cycles of nutrients. Biogeochemistry, 4(1), 61-75.

Yalçın, B., Artüz, M.L., Pavlidou, A., Çubuk, S., Dassenakis, M., 2017. Nutrient dynamics and eutrophication in the Sea of Marmara: Data from recent oceanographic research. Science of the Total Environment, 601, 405-424.

Yang, H., Lu, H., Ruffine, L., 2018. Geochemical characteristics of iron in sediments from the Sea of Marmara. Deep Sea Research Part II: Topical Studies in Oceanography, 153, 121-130.

Yemenicioglu, S., Tunc, S.C., 2013. Geology and Geochemistry of Recent Sediments from the Mediterranean Sea: Sediment Texture of Northeastern Mediterranean Basin. Open Journal of Geology, 3, 371-378.

Yılmaz, A., 2002. Biogeochemistry of the seas surrounding Turkey: cycling and distributions. Turkish Journal of Engineering and Environmental Sciences, 26(2), 219-236.

Yılmaz, A., Tugrul, S., 1998. The effect of cold- and warm- core eddies on the distribution and stoichiometry of dissolved nutrients in the northeastern Mediterranean. Journal of Marine Systems, 16, 253-268.

Yücel, M., Konovalov, S.K., Moore, T.S., Janzen, C.P., Luther III, G.W., 2010. Sulfur speciation in the upper Black Sea sediments. Chemical Geology, 269(3-4), 364-375.

APPENDICES

A. Measurements of porewater nutrients and sediment geochemical parameters in the NE Mediterranean Sea

Station	Latitude	Longitude	Bottom Depth (m)	Depth (cmbs)	PO_4 (µM)	NO_3 (µM)	NH_4 (µM)	Si (µM)	TC (mmol/g)	TOC (mmol/g)	TN (mmol/g)	TOC/TN (Molar)	r-Fe (µmol/g)
1	36.548	34.264	52	-1	0.13	1.63	1.03	3.03					
				1	1.00	67.62	119.70	75.20	3.33	0.59	0.06	10.03	38.67
				2	0.87	19.85	63.42	72.93	3.37	0.60	0.05	11.03	44.21
				3	0.68	9.12	55.05	57.10	3.37	0.61	0.06	10.91	39.24
				4	0.78	5.32	52.05	66.50	3.35	0.60	0.05	11.47	44.37
				6	1.68	7.32	84.05	87.20	3.36	0.63	0.05	11.49	33.91
				8	1.28	4.82	81.95	90.40	3.34	0.62	0.06	10.99	35.29
				10	0.68	5.32	93.15	82.30	3.38	0.63	0.06	9.94	33.05
				15	1.28	5.62	81.95	88.00	3.31	0.60	0.05	11.60	40.27
				20	1.38	4.12	95.45	95.40	3.34	0.56	0.06	10.11	33.42
				25	0.98	5.42	112.55	84.20	3.32	0.58	0.05	11.17	32.34
				30	0.85	19.77	111.95	133.10	3.36	0.60	0.05	11.16	31.10
				35	1.73	29.92	120.55	154.30	3.47	0.66	0.06	10.86	39.72
2	36.440	34.346	208	-1	0.07	1.40	0.45	2.96					
				1	1.00	18.42	7.85	33.90	3.31	0.70	0.07	9.77	43.23
				2	1.00	17.42	10.35	68.90	3.56	0.63	0.08	7.77	47.84
				3	0.50	10.12	25.75	68.40	3.46	0.60	0.07	8.14	46.90
				4	0.70	15.02	34.75	76.40	3.44	0.61	0.08	7.99	39.71
				6	0.60	13.32	30.15	69.60	3.45	0.57	0.07	8.56	43.69
				8	0.40	10.42	40.55	69.50	3.38	0.54	0.06	8.59	38.79
				10	0.60	10.72	49.45	77.00	3.40	0.50	0.06	9.01	39.52
				15	0.60	6.62	53.15	50.40	3.29	0.49	0.05	9.13	36.92
				20	0.30	10.22	69.75	84.00	3.35	0.48	0.06	8.25	37.75
				25	0.40	11.52	77.65	88.20	3.38	0.48	0.06	8.39	32.65
				30	2.30	12.12	78.95	86.70	3.45	0.48	0.06	7.57	31.04
				35	1.40	15.72	101.65	93.90	3.46	0.47	0.05	9.36	32.60

Station	Latitude	Longitude	Bottom Depth (m)	Depth (cmbs)	PO_4 (µM)	NO_3 (µM)	NH_4 (µM)	Si (µM)	TC (mmol/g)	TOC (mmol/g)	TN (mmol/g)	TOC/TN (Molar)	r-Fe (µmol/g)
3	36.354	34.381	323	-1	0.09	8.82	1.73	6.37					
				1	0.80	29.32	20.45	82.10	3.86	0.51	0.06	7.99	29.74
				2	0.91	26.88	7.91	90.48	3.85	0.53	0.05	9.71	26.31
				3	0.60	23.42	1.45	67.60	3.70	0.41	0.05	8.06	24.98
				4	1.00	24.82	0.95	85.20	3.49	0.38	0.05	7.86	20.60
				6	1.10	42.52	2.05	93.90	3.55	0.43	0.05	8.91	19.44
				8	1.10	38.52	1.95	89.30	3.63	0.51	0.06	8.67	17.97
				10	1.30	40.92	6.55	85.80	3.71	0.50	0.05	9.38	13.55
				15	1.00	32.72	11.35	98.90	3.74	0.48	0.05	9.38	15.48
				20	1.30	41.32	15.75	93.60	3.43	0.42	0.05	8.04	22.39
				25	1.60	28.32	24.95	80.60	3.63	0.67	0.06	10.69	24.50
				30	1.60	31.82	29.95	93.80	3.71	0.61	0.06	10.07	25.89
4	36.138	33.923	85	-1	0.06	2.12	0.63	1.22					
				1	1.00	31.56	3.45	53.40	6.79	0.26	0.02	11.01	27.63
				2	2.20	27.96	21.25	73.10	7.09	0.32	0.03	10.24	29.02
				3	1.40	27.87	35.25	65.20	6.88	0.24	0.04	6.64	19.68
				4	2.10	45.05	48.95	73.20	6.86	0.24	0.03	8.94	21.85
				6	1.40	46.21	46.45	75.90	6.27	0.35	0.04	9.86	21.79
				8	1.20	45.03	54.85	88.50	6.23	0.29	0.03	11.36	23.82
				10	1.00	47.13	46.45	84.10	6.47	0.28	0.03	10.60	18.03
				15	1.00	60.48	45.45	78.90	6.48	0.25	0.02	10.80	17.68
				20	0.90	36.59	29.15	61.20	5.68	0.35	0.03	10.62	14.86
				25	1.00	27.97	31.55	63.40	5.52	0.33	0.03	10.35	12.74
5	35.852	33.017	1165	-1	0.22	7.50	1.96	7.87					
				1	0.78	22.34	3.75	21.50	4.09	0.60	0.06	9.56	41.60
				2	0.98	30.94	2.55	35.00	4.02	0.53	0.05	9.76	36.20
				3	0.98	29.34	2.45	43.10	3.89	0.50	0.05	9.96	32.14
				4	0.98	30.14	1.85	54.80	3.94	0.40	0.05	7.63	32.86
				6	0.98	47.34	2.85	61.40	3.97	0.40	0.05	8.11	28.15
				8	1.08	28.94	3.25	74.10	3.90	0.36	0.05	7.87	19.78
				10	1.08	28.84	5.65	71.30	3.88	0.41	0.04	9.28	22.10
				15	0.98	32.64	9.95	67.90	3.72	0.35	0.04	9.25	27.22
				20	0.98	21.94	18.35	63.80	4.18	0.42	0.04	9.49	24.46
				25	1.18	56.14	30.85	88.50	4.24	0.43	0.05	8.56	29.16
				30	1.08	23.94	35.45	83.10	3.79	0.32	0.04	8.51	26.67
				35	1.08	57.74	38.65	78.10	3.84	0.31	0.04	7.53	28.93
				40	1.18	41.54	47.35	75.50	3.86	0.31	0.03	8.86	29.59
				45	1.08	37.14	50.95	75.10	4.08	0.33	0.04	7.77	31.82

B. Results of Seawater physico-chemical and biochemical parameters obtained in Marmara Sea in winter and summer periods of 2019

Station	Date	Depth (m)	Latitude	Longitude	Temperature (˚C)	Salinity (psu)	Denisty (sig-t)	TP (µM)	PO_4 (µM)	NO_3+NO_2 (µM)	NO_2 (µM)	NH_4 (µM)	Si (µM)	DO (µM)	Chl-*a* (µg/L)	SDD (m)
IZ-17	1/5/2019	0	40.729	29.352	9.79	27.89	21.44	0.81	0.20	4.69	0.44	0.66	12.36	286.9	3.77	
		10			14.36	34.87	26.01	0.80	0.74	7.44	0.13	0.15	14.14	120.5	0.54	
		25			16.18	38.71	28.56	0.92	0.80	7.96	0.04	0.23	17.26	89.3	0.06	
		50			15.87	38.83	28.73	1.04	0.92	8.78	0.02	0.11	21.09	69.4	0.03	
		75			15.61	38.81	28.78	1.09	0.81	8.30	0.22	0.32	17.45	65.2	0.03	
		100			15.57	38.81	28.79	1.12	0.96	8.91	0.03	0.13	22.62	62.2	0.03	
		150			15.04	38.77	28.88	1.21	1.11	9.84	0.05	0.91	29.61	34.3		
		207			14.67	38.73	28.93	1.26	1.18	9.13	0.03	0.63	36.55	20.9		
IZ-7	1/5/2019	0	40.761	29.460	10.08	28.22	21.65	0.82	0.36	4.74	0.39	0.63	11.08	262.6	3.08	
EK-19	1/5/2019	0	40.771	29.620	10.63	28.63	21.88	0.88	0.69	7.56	0.34	0.83	16.19	216.2	2.55	
IZ-2	1/5/2019	0	40.730	29.610	10.88	28.65	21.86	0.88	0.51	6.89	0.48	0.89	12.33	209.8	1.21	
		10			14.90	35.52	26.40	0.89	0.65	7.43	0.32	0.77	12.78	143.7	0.96	
		25			15.97	38.56	28.49	0.99	0.90	8.73	0.11	0.22	19.71	76.3	0.13	
		50			15.82	38.73	28.66	1.23	1.08	8.43	0.03	0.16	23.95	47.4	0.05	
		100			15.69	38.75	28.71	1.36	1.14	8.36	0.06	0.21	26.41	35.6	0.10	
		157			15.63	38.76	28.74	1.34	1.13	8.34	0.06	1.18	26.75	30.5		
IZ-25	1/5/2019	0	40.730	29.778	10.84	28.49	21.74	0.85	0.72	9.97	0.52	8.84	13.12	195.3	0.26	
IZ-30	1/6/2019	0	40.732	29.889	10.98	28.13	21.44	0.68	0.60	8.12	0.70	2.54	15.25	201.0	1.22	
		10			14.59	34.50	25.67	0.93	0.90	8.70	0.41	0.77	19.01	75.0	0.13	
		29			15.88	38.63	28.57	0.99	0.96	8.44	0.58	0.78	20.35	54.2	0.09	
IZ-5C	1/6/2019	0	40.740	29.552	10.83	28.83	22.01	0.63	0.47	6.17	0.36	1.10	12.03	210.7	2.21	
		10			13.54	33.24	24.92	0.82	0.73	7.88	0.15	0.59	15.83	104.9	0.18	
		25			16.24	38.61	28.47	0.85	0.78	7.81	0.05	0.44	17.19	95.6	0.08	
		60			15.69	38.75	28.71	1.14	1.04	8.28	0.05	0.30	24.74	48.2	0.07	
45-C	1/6/2019	0	40.780	28.861	10.12	25.88	19.82	0.38	0.24	2.90	0.33	0.44	7.19	283.0	1.90	5
		12			9.14	26.93	20.79	0.55	0.26	3.26	0.23	0.25	6.41	237.0	2.10	
		20			15.42	36.66	27.16	1.10	0.62	7.33	0.13	0.30	14.43	124.9	0.41	

Station	Date	Depth (m)	Latitude	Longitude	Temperature (˚C)	Salinity (psu)	Denisty (sig-t)	TP (µM)	PO_4 (µM)	NO_3+NO_2 (µM)	NO_2 (µM)	NH_4 (µM)	Si (µM)	DO (µM)	Chl-*a* (µg/L)	SDD (m)
		50			15.79	38.82	28.74	1.21	0.89	8.58	0.03	0.14	20.49	74.8	0.07	
		100			15.24	38.79	28.85	1.30	1.02	9.66	0.02	0.25	24.76	46.1	0.03	
		200			14.77	38.74	28.92	1.22	1.11	10.02	0.02	0.18	31.52	27.3		
		300			14.59	38.72	28.95	1.32	1.17	8.67	0.02	0.27	38.49	9.8		
		900			14.56	38.71	28.96	1.25	1.14	6.86	0.03	0.44	43.90	8.9		
		1202			14.60	38.70	28.96	1.39	1.10	4.52	0.16	0.76	43.00	6.4		
K47K35	1/6/2019	0	40.771	28.617	9.21	26.55	20.48	0.58	0.24	2.25	0.13	0.49	6.54	268.1	1.39	8
		10			9.16	26.62	20.54	0.38	0.31	2.97	0.07	0.50	7.40	223.1	0.85	
		20			9.38	27.81	21.44	0.65	0.55	5.62	0.09	0.71	11.52	147.7	0.51	
		35			16.19	38.79	28.62	0.76	0.68	7.23	0.02	0.20	16.34	92.0	0.08	
		50			15.92	38.82	28.71	0.93	0.87	8.40	0.03	0.27	19.47	76.1	0.08	
		100			15.51	38.81	28.80	1.06	0.97	9.46	0.02	0.25	24.31	51.0	0.04	
		200			14.91	38.76	28.90	1.27	1.07	9.63	0.03	0.23	30.88	25.0		
		300			14.62	38.72	28.94	1.22	1.07	8.03	0.06	0.38	35.32	8.1		
		400			14.57	38.72	28.95	1.28	1.17	8.05	0.05	0.36	41.34	9.3		
		579			14.54	38.71	28.96	1.35	0.84	4.76	0.04	0.18	26.45	9.4		
MD-18	1/6/2019	0	40.700	28.342	9.62	26.31	20.23	0.59	0.14	2.11	0.29	1.34	7.22	294.0	2.12	7
		10			9.87	26.57	20.40	0.59	0.10	1.29	0.08	0.24	2.33	247.5	0.94	
		25			10.36	28.82	22.07	0.41	0.31	3.63	0.11	0.73	5.79	145.8	0.41	
		45			16.41	38.90	28.65	0.62	0.45	4.53	0.12	0.46	8.99	106.2	0.04	
		100			15.37	38.81	28.83	0.97	0.89	9.36	0.05	0.65	23.34	55.8	0.02	
		145			15.24	38.80	28.85	1.09	0.69	6.49	0.04	0.19	17.21	51.7		
EK-9	1/6/2019	0	40.650	28.340	9.59	26.46	20.35	0.82	0.13	1.71	0.23	0.15	4.44	297.1	1.61	7
		10			9.93	27.02	20.74	0.60	0.18	2.87	0.23	1.46	5.83	249.9	1.26	
		20			11.82	30.03	22.77	0.78	0.37	5.24	0.18	0.67	9.66	162.7	0.40	
		30			16.57	38.67	28.44	0.48	0.41	5.38	0.05	0.52	10.25	131.0	0.17	
		50			16.40	38.92	28.67	0.70	0.51	6.40	0.04	0.52	13.29	122.0	0.09	
		75			15.54	38.83	28.81	0.92	0.83	8.61	0.06	0.46	22.11	71.0	0.04	
		102			15.34	38.81	28.84	1.10	0.92	9.39	0.06	0.53	24.61	54.3	0.03	
EK-10	1/6/2019	0	40.583	28.340	9.73	27.56	21.19	0.47	0.20	1.76	0.16	0.17	6.88	291.7	1.18	7
		10			9.93	28.05	21.54	0.53	0.32	2.58	0.11	0.34	5.18	239.8	1.01	
		20			13.42	33.63	25.24	0.57	0.50	5.71	0.10	0.28	9.77	153.2	0.20	
		30			16.57	38.81	28.54	0.68	0.51	5.43	0.06	0.48	14.20	137.1	0.11	
		56			15.80	38.84	28.76	0.78	0.66	6.49	0.06	0.56	15.69	118.4	0.04	
EK-11	1/6/2019	0	40.505	28.341	9.66	28.26	21.75	0.28	0.23	0.51	0.13	1.18	3.23	300.0	1.65	
		10			9.66	28.26	21.75	0.55	0.22	0.75	0.11	0.76	2.98	291.7	1.76	
		20			13.77	33.78	25.29	0.64	0.45	5.02	0.10	0.60	7.77	174.8	0.43	
		30			16.61	38.86	28.58	0.77	0.54	5.81	0.05	0.80	13.63	147.4	0.06	
		47			15.91	38.84	28.73	0.84	0.65	6.71	0.05	0.22	17.99	124.1	0.03	
EK-12	1/6/2019	0	40.437	28.342	9.64	28.60	22.02	0.32	0.24	1.03	0.11	0.54	3.54	294.1	1.01	

Station	Date	Depth (m)	Latitude	Longitude	Temperature (˚C)	Salinity (psu)	Denisty (sig-t)	TP (µM)	PO_4 (µM)	NO_3+NO_2 (µM)	NO_2 (µM)	NH_4 (µM)	Si (µM)	DO (µM)	Chl-*a* (µg/L)	SDD (m)
		10			10.14	29.04	22.28	0.30	0.27	1.30	0.17	0.86	3.97	284.3	1.29	
		20			10.42	29.39	22.51	0.48	0.33	3.52	0.12	0.21	6.55	209.4	0.45	
		30			15.66	37.20	27.52	0.54	0.49	5.73	0.16	0.44	9.84	169.6	0.19	
		45			16.22	38.68	28.53	0.53	0.40	4.31	0.09	0.47	8.65	164.2	0.14	
L00K59.5	2/6/2019	0	41.003	28.991	8.68	20.59	15.90	0.16	0.15	2.30	0.26	1.48	5.83	290.1	1.89	
		10			10.18	26.88	20.59	0.18	0.16	3.04	0.29	1.33	6.04	257.3	2.00	
		15			9.98	29.35	22.55	0.63	0.22	1.90	0.18	0.51	4.53	231.6	1.60	
		25			15.02	36.90	27.44	0.96	0.73	8.58	0.21	0.10	16.04	94.7	0.30	
		53			15.71	38.81	28.75	1.02	0.95	9.59	0.09	0.15	22.95	70.3	0.11	
K59K59	2/6/2019	0	40.983	28.984	9.21	22.71	17.49	0.33	0.19	3.41	0.27	1.17	6.65	260.8	0.31	
		10			10.13	27.06	20.74	0.61	0.21	2.30	0.22	1.26	4.94	244.0		
		15			10.22	29.97	23.00	0.73	0.39	6.41	0.42	0.69	8.35	162.3		
		25			15.61	37.82	28.01	1.05	0.75	9.98	0.21	0.15	16.36	99.4		
		46			15.89	38.78	28.69	0.97	0.79	7.59	0.11	0.14	17.69	77.7		
K57L00	2/6/2019	0	40.947	28.999	9.36	23.39	17.99	0.26	0.13	2.36	0.21	1.24	6.01	292.7	0.71	
EK-1	2/6/2019	0	40.903	28.966	9.14	24.77	19.10	0.37	0.02	1.12	0.14	0.51	4.04	304.1	0.56	
		10			8.87	26.72	20.66	0.42	0.02	0.45	0.04	0.37	1.01	306.0	1.05	
		17			9.18	28.76	22.21	0.80	0.34	5.12	0.17	0.53	8.79	195.4	0.07	
		25			15.51	37.73	27.96	1.01	0.75	8.80	0.07	0.23	17.61	93.4	0.78	
		51			15.82	38.80	28.72	0.86	0.67	6.80	0.05	0.13	15.33	84.0	0.06	
45-C	2/6/2019	0	40.787	28.884	8.96	27.56	21.31	0.48	0.02	0.24	0.04	0.17	2.56	311.3	0.64	11
		10			8.95	27.57	21.32	0.50	0.07	0.51	0.05	0.33	2.00	296.9	0.87	
		15			9.00	28.46	22.00	0.59	0.33	3.65	0.11	0.90	8.15	211.9	0.82	
		20			14.30	35.92	26.83	0.65	0.58	7.71	0.10	0.21	11.74	141.1	0.31	
		50			15.80	38.82	28.74	0.97	0.90	9.33	0.03	0.34	22.16	63.7	0.03	
		100			15.21	38.79	28.85	1.14	0.86	7.54	0.04	0.21	20.58	37.5		
		200			14.71	38.73	28.93	1.27	1.12	9.93	0.03	0.36	41.52	13.7		
		300			14.58	38.72	28.95	1.21	0.99	6.93	0.02	0.20	34.11	8.5		
		500			14.54	38.71	28.96	1.40	1.07	7.64	0.02	0.29	41.87	9.9		
		750			14.55	38.71	28.96	1.19	1.05	6.92	0.02	0.24	39.87	10.6		
		900			14.56	38.71	28.96	1.14	1.05	6.24	0.02	0.24	39.73	8.5		
		1212			14.60	38.70	28.96	1.24	1.00	4.04	0.10	0.63	39.53	5.5		
EK-6	2/7/2019	0	40.958	27.521	8.86	27.70	21.43	0.44	0.02	0.12	0.05	1.94	0.85	316.9	0.65	
		23			8.94	27.83	21.52	0.49	0.03	0.11	0.03	0.24	0.89	315.1	0.98	
EK-7	2/7/2019	0	40.943	27.521	8.82	27.75	21.48	0.58	0.02	0.28	0.07	2.10	1.04	315.7	1.47	
		30			11.78	32.35	24.57	0.77	0.54	7.87	0.12	0.34	13.67	120.4	0.23	
		42			16.10	38.78	28.63	0.84	0.54	7.18	0.07	0.21	13.55	106.2	0.29	
EK-8	2/7/2019	0	40.906	27.526	8.77	27.90	21.60	0.44	0.02	0.09	0.03	0.19	1.23	318.8	1.83	7
		10			8.78	27.90	21.59	0.56	0.03	0.11	0.05	0.88	0.85	316.0	1.46	

Station	Date	Depth (m)	Latitude	Longitude	Temperature (˚C)	Salinity (psu)	Denisty (sig-t)	TP (µM)	PO_4 (µM)	NO_3+NO_2 (µM)	NO_2 (µM)	NH_4 (µM)	Si (µM)	DO (µM)	Chl-*a* (µg/L)	SDD (m)
		25			9.07	28.78	22.24	0.71	0.29	5.01	0.08	0.20	8.66	162.1	0.51	
		32			15.38	37.66	27.94	0.90	0.53	6.95	0.04	0.13	12.79	123.7	0.09	
		69			15.49	38.81	28.80	1.15	0.87	9.73	0.05	0.12	22.37	64.3	0.03	
EK-5	2/7/2019	0	40.962	28.216	8.86	27.88	21.57	0.56	0.15	4.61	0.19	3.70	1.55	312.4	1.50	10
		25			15.82	38.02	28.12	0.83	0.47	5.63	0.04	0.41	9.60	136.3	0.15	
		35			16.47	38.76	28.53	1.04	0.72	8.07	0.03	0.52	16.28	95.6	0.11	
		50			15.91	38.81	28.71	1.15	0.92	9.40	0.02	0.12	22.98	61.9	0.04	
		79			15.36	38.80	28.82	1.31	0.96	9.64	0.03	0.23	24.31	51.8	0.03	
EK-4	2/7/2019	0	41.009	28.211	8.77	27.86	21.56	0.59	0.11	0.25	0.02	0.73	1.53	312.3	1.78	9
		20			11.28	31.50	24.00	0.98	0.66	7.26	0.08	0.58	13.54	108.9	0.37	
		35			15.98	38.79	28.67	1.18	0.90	9.54	0.04	0.41	22.90	59.4	0.07	
		53			15.53	38.81	28.79	1.22	0.96	10.12	0.06	0.14	24.86	50.7	0.04	
EK-3	2/7/2019	0	41.064	28.215	8.69	27.75	21.49	0.39	0.10	0.17	0.03	0.78	1.42	311.1	1.01	10
		18			8.72	27.83	21.55	0.34	0.12	0.08	0.02	0.48	1.41	309.3	1.27	
K56K45	2/7/2019	0	40.935	28.752	8.80	24.81	19.18	0.39	0.11	0.89	0.13	0.21	3.36	309.5	1.10	10
		15			8.91	25.61	19.79	0.44	0.22	2.70	0.15	1.17	4.80	255.8	0.92	
		20			14.68	36.54	27.23	0.76	0.56	7.14	0.08	0.65	11.95	104.9	0.15	
		50			15.85	38.83	28.73	0.90	0.60	7.68	0.11	0.71	12.90	69.5	0.05	
		77			15.33	38.79	28.83	1.15	0.93	10.42	0.04	0.11	26.58	48.6	0.04	
K58K45	2/7/2019	0	40.963	28.751	8.78	24.78	19.16	0.49	0.08	0.78	0.10	1.44	2.90	308.7	1.90	7
		17			13.12	33.31	25.06	1.99	1.39	7.05	1.45	13.23	18.64	35.6	0.26	
		31			16.07	38.64	28.53	1.74	1.31	6.99	1.62	10.10	18.29	41.1	0.17	
L01.3K59.5	2/9/2019	0	41.030	29.011	7.32	18.50	14.42	0.31	0.06	0.65	0.07	0.61	3.71	334.3	0.81	
		20			9.83	24.49	18.79		0.58	6.63	0.10	1.09	13.89	151.6	0.24	
		38			15.97	38.55	28.49		0.76	8.71	0.06	0.45	17.81	90.4	0.22	
L02.4L01.5	2/9/2019	0	41.040	29.026	7.31	18.46	14.39	0.34	0.10	0.76	0.06	0.38	3.57	323.9	0.84	
		35			15.40	37.50	27.81	0.65	0.48	5.01	0.09	0.93	12.27	179.0		
L04.5L03	2/9/2019	0	41.057	29.046	7.32	18.49	14.41	1.11	0.24	2.70	0.10	0.96	7.66	275.2	0.51	
		48			15.68	38.41	28.45	1.23	0.89	8.63	0.13	2.86	19.82	86.4		
L05L03.7	2/9/2019	0	41.083	29.061	7.19	18.19	14.19	0.28	0.07	0.44	0.10	0.22	3.35	335.1	0.61	
		60			15.74	38.23	28.30	1.18	0.90	8.76	0.11	2.37	19.98	80.6		
L06L03.6	2/9/2019	0	41.100	29.061	7.15	18.11	14.13	0.25	0.09	0.44	0.08	0.75	3.68	339.7	0.49	
		35			9.16	22.98	17.70	0.87	0.67	6.32	0.12	2.25	14.86	155.9	0.35	
		57			15.64	37.95	28.11	1.17	0.92	8.41	0.12	3.19	18.30	85.0	0.11	
L06.5L04	2/9/2019	0	41.108	29.065	7.16	18.11	14.13	0.27	0.14	0.39	0.08	0.69	3.36	340.9	0.62	
		52			15.66	38.06	28.19	1.20	0.96	9.01	0.17	2.32	19.89	84.4		
L07.4L05	2/9/2019	0	41.124	29.082	7.16	18.09	14.12	0.26	0.10	0.48	0.12	0.77	3.25	340.8	0.97	
		57			15.53	37.75	27.97	0.87	0.72	5.47	0.16	3.88	13.08	95.6		

Station	Date	Depth (m)	Latitude	Longitude	Temperature (˚C)	Salinity (psu)	Denisty (sig-t)	TP (µM)	PO_4 (µM)	NO_3+NO_2 (µM)	NO_2 (µM)	NH_4 (µM)	Si (µM)	DO (µM)	Chl-*a* (µg/L)	SDD (m)
L08.3L04	2/9/2019	0	41.137	29.068	7.10	18.04	14.09	0.37	0.18	0.95	0.12	0.18	5.49	324.4	0.42	
		55			15.57	37.83	28.03	1.10	0.90	8.37	0.18	2.54	18.40	92.4		
L09.5L03	2/9/2019	0	41.159	29.051	7.14	18.03	14.07	0.31	0.12	0.71	0.18	1.50	3.69	340.5	0.67	
		43			13.96	34.37	25.71	0.95	0.73	6.40	0.22	2.90	15.74	139.3		
L10.6L04.8	2/9/2019	0	41.173	29.080	7.08	18.02	14.07	0.26	0.10	0.34	0.15	0.82	3.08	342.1	0.52	
		62			15.48	37.66	27.92	1.03	0.81	8.11	0.20	1.95	18.47	83.1		
L12L06.5	2/9/2019	0	41.194	29.108	7.03	17.96	14.02	0.36	0.10	0.34	0.09	0.32	2.87	340.7	0.91	
		45			11.02	27.44	20.89	0.76	0.54	5.24	0.17	0.87	13.29	175.6	0.45	
		55			15.27	37.20	27.61	1.28	0.84	7.18	0.24	1.43	17.53	117.5	0.26	
L13.4L0.8	2/9/2019	0	41.224	29.134	6.93	17.97	14.04	0.27	0.13	0.19	0.07	0.54	2.61	344.4	0.45	
		50			13.28	32.66	24.53	1.10	0.72	8.40	0.36	3.01	16.64	92.0	0.16	
		66			15.26	37.17	27.59	1.38	1.27	9.44	0.36	4.00	17.97	78.2	0.26	
L01.5K59.5	7/27/2019	0	41.025	28.992	21.70	18.70	11.96	0.77	0.09	0.29	0.05	0.26	3.91	242.7	0.39	
L02.4L01.5	7/27/2019	0	41.041	29.027	22.90	17.84	11.00	0.57	0.05	0.10	0.02	0.27	2.24	241.5	0.19	
L04.5L03	7/27/2019	0	41.061	29.048	24.09	17.59	10.49	0.73	0.04	0.09	0.02	0.28	3.50	239.4	0.18	
L05L03.7	7/27/2019	0	41.083	29.062	24.04	17.59	10.51	0.80	0.04	0.15	0.02	0.28	1.97	244.9	0.13	
L06L03.6	7/27/2019	0	41.102	29.063	24.72	17.49	10.24	0.38	0.03	0.09	0.02	0.27	2.01	239.8	0.23	
L06.5L04	7/27/2019	0	41.111	29.070	24.31	17.54	10.39	0.38	0.02	0.12	0.05	0.34	3.60	236.0	0.12	
		10			23.75	17.73	10.69	0.79	0.06	0.59	0.06	0.46	4.78	243.9	0.26	
		20			15.23	18.87	13.53	1.27	0.30	3.09	0.19	2.21	8.97	211.2	0.40	
		34			11.96	23.30	17.53	1.53	0.68	4.97	0.26	3.03	13.27	133.8	0.19	
		49			14.80	36.53	27.20	1.87	0.96	6.92	0.30	5.10	16.57	84.6	0.26	
L07.4L05	7/27/2019	0	41.122	29.083	24.36	17.53	10.37	0.90	0.07	0.18	0.04	0.36	2.49	243.5	0.33	8.5
L08.3L04	7/27/2019	0	41.138	29.071	24.60	17.50	10.28	1.04	0.07	0.09	0.02	0.28	2.04	239.2	0.27	
L09.5L03.5	7/27/2019	0	41.161	29.058	24.87	17.44	10.17	0.81	0.05	0.10	0.03	0.34	2.20	237.7	0.15	10.5
L10.6L04.8	7/27/2019	0	41.173	29.079	25.12	17.36	10.04	0.80	0.04	0.13	0.04	0.29	2.05	236.8	0.07	10.5
L12L06.5	7/27/2019	0	41.198	29.109	25.20	17.34	10.00	0.44	0.03	0.09	0.03	0.33	2.04	235.1	0.05	
		10			24.90	17.80	10.43	0.43	0.03	0.06	0.04	0.30	2.94	236.0	0.06	
		25			16.67	18.17	12.71	0.74	0.11	0.94	0.12	0.58	4.44	278.5	0.15	
		35			9.85	19.70	15.05	0.90	0.30	2.81	0.26	1.57	9.19	216.2	0.16	
		45			12.55	26.93	20.23	1.20	0.86	7.19	0.38	3.89	17.38	92.5	0.43	
		70			14.85	36.67	27.29	1.84	1.04	9.15	0.41	4.69	20.13	49.6	0.18	
L13.4L08	7/27/2019	0	41.223	29.133	25.21	17.29	9.96	0.41	0.09	0.05	0.03	0.33	1.91	236.3	0.15	11.5
L14.9L09.3	7/27/2019	0	41.247	29.155	25.29	17.43	10.04	0.42	0.11	0.09	0.03	0.33	3.28	236.4	0.07	14
K57L00	7/27/2019	0	40.952	29.001	20.42	21.97	14.75	1.14	0.27	0.70	0.09	0.32	4.43	219.1	0.25	7.5
K54K58	7/27/2019	0	40.899	28.969	19.06	22.22	15.27	0.69	0.14	0.30	0.06	0.40	3.92	243.1	0.16	8.5
		8			18.62	23.42	16.28	0.77	0.35	0.82	0.06	0.33	6.14	151.2	0.35	

Station	Date	Depth (m)	Latitude	Longitude	Temperature (˚C)	Salinity (psu)	Denisty (sig-t)	TP (µM)	PO_4 (µM)	NO_3+NO_2 (µM)	NO_2 (µM)	NH_4 (µM)	Si (µM)	DO (µM)	Chl-*a* (µg/L)	SDD (m)
		25			13.50	34.46	25.87	1.12	0.96	9.15	0.22	0.29	19.57	61.1	0.12	
		54			15.54	38.75	28.74	1.20	1.10	10.40	0.13	0.29	23.48	43.4	0.03	
K58K45	7/27/2019	0	40.965	28.751	24.89	22.91	14.27	0.34	0.08	0.06	0.03	0.57	1.88	227.0	0.18	10.5
		10			24.06	23.14	14.67	0.76	0.24	0.20	0.08	2.32	5.22	197.1	0.29	
		27			15.17	36.60	27.17	2.14	1.64	2.05	0.65	30.90	14.91	51.0	0.61	
K56K45	7/27/2019	0	40.933	28.750	24.77	22.96	14.34	0.24	0.09	0.06	0.03	0.22	0.64	231.5	0.08	12
		10			24.14	23.23	14.72		0.12	0.32	0.06	0.28	3.49	210.9	0.35	
		15			15.09	27.38	20.09	0.68	0.30	1.82	0.06	0.26	7.93	166.7	0.46	
		23			13.34	33.46	25.13	0.81	0.78	7.30	0.06	0.26	16.79	71.2	0.21	
		30			14.94	37.87	28.20	1.03	0.93	10.15	0.07	0.11	18.52	63.7	0.12	
		82			15.29	38.77	28.82	1.77	1.12	10.26	0.12	0.19	26.87	29.3		
K54K45	7/27/2019	0	40.903	28.753	24.88	22.92	14.28	0.82	0.13	0.15	0.04	0.28	3.13	229.3	0.13	12
45-C	7/27/2019	0	40.779	28.856	22.44	21.59	13.95	0.36	0.05	0.05	0.02	0.31	2.20	241.2	0.27	10
		10			21.32	23.58	15.74	0.77	0.07	0.05	0.02	0.19	1.82	246.9	0.68	
		18			12.69	30.59	23.04	0.82	0.34	0.24	0.04	0.24	8.56	141.2	0.20	
		25			14.43	36.97	27.62	1.50	0.79	7.55	0.05	0.19	17.39	67.7	0.92	
		40			15.48	38.74	28.75	1.29	1.02	10.69	0.05	0.15	24.71	34.3	0.04	
		75			15.16	38.77	28.85	1.22	1.00	10.27	0.04	0.16	27.81	34.9	0.01	
		150			14.82	38.74	28.90	1.32	1.15	10.20	0.03	0.15	31.68	16.9		
		300			14.51	38.70	28.94	1.26	1.16	8.00	0.03	0.14	39.92	5.5		
		500			14.46	38.70	28.95	1.20	1.05	7.44	0.03	0.16	42.26	5.9		
		750			14.43	38.69	28.95	1.46	1.10	7.37	0.03	0.28	44.34	7.2		
		900			14.42	38.69	28.95	1.77	1.13	6.81	0.03	0.22	44.00	5.1		
		1207			14.43	35.92	26.81	1.79	1.27	4.54	0.17	0.28	47.92	3.8		
K52L02	7/27/2019	0	40.866	29.034	22.97	24.20	15.78	0.61	0.11	0.09	0.04	0.38	2.24	238.2	0.17	
K49.5L04	7/27/2019	0	40.826	29.066	23.56	23.96	15.43	1.07	0.12	0.54	0.06	0.33	2.84	235.1	0.30	
K51L14	7/27/2019	0	40.861	29.221	23.00	24.93	16.32	0.51	0.06	0.07	0.05	0.53	0.80	248.3	0.86	
		10			17.44	26.78	19.11	0.56	0.18	1.05	0.13	0.43	5.23	211.9	0.36	
		43			15.50	38.63	28.66	1.66	0.96	9.67	0.69	3.53	20.09	50.9	0.08	
K50L12	7/27/2019	0	40.834	29.198	23.21	24.48	15.92	0.89	0.07	0.12	0.02	0.20	0.73	250.1	0.34	
		10			17.45	26.59	18.97	1.04	0.18	0.66	0.06	0.24	5.27	211.2	0.65	
		20			12.62	29.50	22.21	1.18	0.66	6.05	0.23	0.26	16.01	88.8	0.58	
		40			15.39	38.51	28.59	1.85	1.04	10.26	0.05	0.15	24.45	37.5	0.03	
		82			15.32	38.77	28.81	1.36	1.12	10.02	0.09	0.22	28.24	23.8	0.01	
K48.5L10	7/27/2019	0	40.809	29.169	22.89	24.00	15.64	0.32	0.05	0.29	0.06	0.35	1.87	241.4	0.35	
K47L08	7/27/2019	0	40.784	29.136	22.95	23.82	15.49	0.34	0.03	0.07	0.05	0.50	1.18	249.0	0.11	
		10			16.87	26.56	19.08	0.95	0.10	0.20	0.02	0.35	3.33	230.1	0.26	
		18			12.55	29.98	22.60	1.04	0.42	2.10	0.07	0.25	11.51	115.6	0.76	
		28			14.79	37.69	28.09	1.58	0.69	6.52	0.14	0.30	16.34	77.4	0.35	

Station	Date	Depth (m)	Latitude	Longitude	Temperature (˚C)	Salinity (psu)	Denisty (sig-t)	TP (µM)	PO_4 (µM)	NO_3+NO_2 (µM)	NO_2 (µM)	NH_4 (µM)	Si (µM)	DO (µM)	Chl-*a* (µg/L)	SDD (m)
		40			15.49	38.67	28.69	1.86	0.89	9.83	0.14	0.94	23.09	46.6	0.03	
		100			15.22	38.77	28.83	1.32	0.98	10.12	0.02	0.18	28.89	34.8		
		200			14.72	38.72	28.91	1.09	1.04	9.54	0.02	0.20	35.11	10.3		
		250			14.61	38.71	28.92	1.28	1.04	7.69	0.05	0.20	41.64	7.2		
		414			14.47	38.70	28.94	1.36	1.09	7.62	0.04	0.21	43.10			
K46L13	7/27/2019	0	40.767	29.217	22.07	24.50	16.25	0.60	0.04	0.17	0.03	0.33	3.79	254.1	0.41	
K44L21	7/28/2019	0	40.733	29.350	23.14	25.76	16.90	0.28	0.05	0.21	0.04	0.38	1.13	246.9	0.33	
K44L26	7/28/2019	0	40.733	29.433	22.49	25.67	17.01	0.38	0.06	0.06	0.02	0.35	1.02	248.2	0.56	
K45L31	7/28/2019	0	40.751	29.519	23.11	25.89	17.01	0.43	0.02	0.05	0.02	0.29	1.13	248.3	0.84	
		10			18.82	26.20	18.35	0.37	0.08	0.09	0.03	0.35	3.31	223.6	0.88	
		18			13.54	30.28	22.64	0.75	0.65	5.56	0.12	0.31	18.44	71.0	0.50	
		30			15.29	38.37	28.50	1.14	1.00	9.80	0.11	0.21	24.11	33.8	0.11	
		60			15.44	38.64	28.68	1.54	1.09	9.98	0.24	0.26	28.73	26.5	0.04	
K44L47	7/28/2019	0	40.735	29.769	22.65	26.37	17.50	0.33	0.27	1.10	0.10	0.40	7.08	188.3	0.59	6.5
K44L53.5	7/28/2019	0	40.733	29.889	22.32	26.40	17.61	0.55	0.17	0.08	0.02	0.64	2.30	240.5	1.81	4.5
		10			17.74	27.18	19.36	0.45	0.16	0.12	0.03	0.61	5.72	147.0	0.59	
		16			14.49	28.60	21.15	0.81	0.25	0.13	0.07	0.40	9.54	121.9	0.59	
		21			13.35	32.10	24.08		1.35	2.55	0.42	2.31	27.87	26.3	0.23	
		31			15.36	38.43	28.54	1.93	1.73	0.48	0.19	5.34	32.35	4.6	0.07	
K44L39	7/28/2019	0	40.733	29.650	22.94	26.22	17.31	0.41	0.20	0.44	0.09	0.38	0.92	228.8	0.77	6
		10			18.73	26.98	18.97	0.50	0.33	0.43	0.11	0.46	6.21	150.7	1.01	
		17			13.64	29.56	22.06	0.78	0.70	1.00	0.11	0.43	12.34	62.5	0.23	
		25			14.25	35.98	26.89	1.28	1.22	4.19	0.09	0.17	22.06	26.9	0.03	
		80			15.53	38.72	28.72	1.41	1.19	9.63	0.08	0.23	24.24	18.3		
		129			15.43	38.73	28.75	1.49	1.26	9.55	0.12	0.51	24.51	6.4		
K41.5L18	7/28/2019	0	40.692	29.299	23.37	24.17	15.64	0.46	0.18	8.68	0.07	0.40	2.76	248.2	0.15	12.5
K40L15	7/28/2019	0	40.669	29.249	22.45	24.15	15.88	0.38	0.17	0.49	0.06	0.27	0.98	250.4	0.14	10
		10			18.60	25.84	18.13	0.64	0.27	0.47	0.08	0.31	5.37	197.9	0.46	
		22			13.89	34.52	25.84	1.06	0.97	1.11	0.15	0.35	17.50	53.1	0.11	
		31			15.07	38.08	28.34	1.16	1.05	8.62	0.17	0.20	19.99	57.1	0.08	
		60			15.42	38.73	28.75	1.23	0.93	9.56	0.09	0.27	18.34	48.3		
K43L05	7/28/2019	0	40.716	29.083	22.13	22.53	14.74	0.46	0.16	7.65	0.04	0.39	2.38	244.4	0.06	12.5
		10			17.89	26.49	18.79	0.57	0.24	0.39	0.04	0.22	3.14	218.2	0.42	
		20			12.95	32.72	24.64	0.68	0.60	0.50	0.05	0.14	13.08	95.1	1.06	
		26			14.14	36.48	27.30	0.86	0.69	2.96	0.05	0.26	13.55	86.7	0.35	
K40K46	7/28/2019	0	40.666	28.766	22.54	22.15	14.35	0.26	0.20	3.93	0.05	0.32	2.82	227.1	0.13	12
K33K44	7/28/2019	0	40.551	28.733	22.92	22.42	14.44	0.35	0.23	0.99	0.05	0.24	2.97	227.7	0.24	12.5
K26.5L05	7/28/2019	0	40.441	29.084	24.81	24.48	15.47	0.48	0.08	1.33	0.04	0.20	0.25	243.0	0.12	8

Station	Date	Depth (m)	Latitude	Longitude	Temperature (˚C)	Salinity (psu)	Denisty (sig-t)	TP (µM)	PO_4 (µM)	NO_3+NO_2 (µM)	NO_2 (µM)	NH_4 (µM)	Si (µM)	DO (µM)	Chl-*a* (µg/L)	SDD (m)
		10			19.21	25.70	17.88	0.70	0.17	0.45	0.04	0.21	2.00	247.4	0.17	
		20			12.41	30.63	23.13	0.72	0.53	0.46	0.07	0.13	11.27	85.9	0.22	
		30			14.92	38.03	28.33	1.51	1.02	2.15	0.06	0.10	19.67	55.9	0.05	
		61			15.39	38.74	28.77	1.61	1.32	9.65	1.29	0.38	29.17	9.4	0.02	
K25K56	7/28/2019	0	40.418	28.936	24.29	24.29	15.48	0.95	0.15	8.31	0.06	0.33	2.12	242.2	0.09	
		10			21.82	24.98	16.67	0.62	0.14	0.41	0.03	0.21	2.08	248.6	0.09	
		20			12.38	29.48	22.24	1.15	0.48	0.43	0.04	0.21	10.86	104.1	0.60	
		25			14.00	36.41	27.28	1.23	0.88	1.83	0.06	0.10	18.04	62.9	0.12	
		40			15.40	38.64	28.69	1.57	1.14	8.67	0.09	0.37	24.34	20.9	0.03	
		109			15.21	38.75	28.82	2.46	2.16	8.98	0.03	4.32	40.50			
K27K48	7/28/2019	0	40.450	28.800	23.92	23.41	14.92	0.72	0.19	0.38	0.04	0.30	2.10	236.3	0.11	
K25.5K31	7/28/2019	0	40.429	28.513	24.81	22.93	14.31	0.49	0.09	0.48	0.04	0.29	0.68	233.9	0.09	
		10			22.31	23.03	15.07	0.50	0.09	0.48	0.03	0.25	1.05	254.6	0.11	
		20			12.91	29.38	22.06	0.85	0.65	0.45	0.22	0.35	14.10	112.1	0.21	
		32			15.75	38.46	28.47	1.58	0.82	4.01	0.37	0.25	15.68	91.4	0.33	
K26K20	7/28/2019	0	40.435	28.336	23.06	22.51	14.47	0.35	0.10	6.38	0.03	0.28	1.86	237.7	0.13	
		10			21.76	24.48	16.31	0.44	0.12	0.42	0.03	0.27	1.20	250.3	0.15	
		20			12.84	29.74	22.35	0.49	0.32	0.47	0.07	0.30	7.27	154.4	0.29	
		48			16.00	30.01	21.91	0.77	0.68	1.86	0.13	0.12	15.62	97.4	0.32	
K34K20	7/28/2019	0	40.565	28.331	25.01	23.10	14.37	0.41	0.10	6.96	0.04	0.24	1.51	231.6	0.01	
K42K20	7/29/2019	0	40.698	28.330	24.87	22.96	14.31	0.50	0.04	0.44	0.03	0.25	0.25	236.9	0.16	
		17			19.54	25.31	17.50	0.52	0.13	0.49	0.03	0.30	2.20	247.3	0.37	
		25			12.90	31.50	23.70	1.05	0.32	0.52	0.04	0.27	8.19	150.3	0.61	
		30			14.36	36.92	27.59	1.57	0.80	0.79	0.06	0.14	16.70	70.6	0.54	
		40			15.65	38.74	28.71	1.48	0.84	9.09	0.05	0.08	18.29	57.3	0.04	
		90			15.13	38.77	28.85	1.58	0.99	8.99	0.03	0.11	25.35	40.1		
		136			14.89	38.75	28.89	1.29	0.93	9.54	0.03	0.21	27.39	38.0		
K42K30	7/29/2019	0	40.699	28.500	24.53	22.77	14.26	0.35	0.08	9.28	0.02	0.27	1.99	241.8	0.34	
K47K35	7/29/2019	0	40.767	28.567	24.39	22.82	14.34	0.18	0.03	0.32	0.02	0.26	0.56	236.7	0.34	13.5
K54K23	7/29/2019	0	40.900	28.386	23.72	22.82	14.53	0.31	0.02	0.44	0.02	0.25	0.47	234.2	0.16	15
		10			23.70	22.82	14.53	0.32	0.03	0.48	0.02	0.33	0.48	239.3	0.25	
		20			13.78	27.94	20.78	0.68	0.28	0.53	0.03	0.17	7.43	151.0	0.39	
		27			15.12	38.07	28.32	0.94	0.66	0.55	0.04	0.09	15.88	89.6	0.35	
		50			15.67	38.77	28.73	1.04	0.82	5.31	0.03	0.13	15.32	50.9	0.02	
		100			15.22	38.77	28.83	1.14	0.95	7.59	0.02	0.13	22.29	39.7		
		250			14.62	38.72	28.92	1.25	1.01	9.51	0.02	0.11	27.68	14.4		
		430			14.46	38.70	28.95	1.35	1.12	7.40	0.05	0.12	38.92	7.7		
K53K17	7/29/2019	0	40.886	28.285	24.28	22.89	14.42	0.59	0.13	7.54	0.03	0.22	4.31	228.1	0.41	14.5
K57.5K13	7/29/2019	0	40.956	28.218	24.62	22.98	14.39	0.54	0.07	0.07	0.04	0.29	0.61	228.8	0.10	13.5

Station	Date	Depth (m)	Latitude	Longitude	Temperature (˚C)	Salinity (psu)	Denisty (sig-t)	TP (µM)	PO_4 (µM)	NO_3+NO_2 (µM)	NO_2 (µM)	NH_4 (µM)	Si (µM)	DO (µM)	Chl-*a* (µg/L)	SDD (m)
		10			24.27	23.00	14.51	1.09	0.15	0.05	0.03	0.34	1.13	238.6	0.23	
		23			12.98	31.91	24.00	0.95	0.45	1.80	0.08	0.21	9.36	129.6	2.67	
		30			15.36	38.11	28.29	1.39	0.71	6.22	0.15	0.10	13.44	102.8	1.41	
		50			15.69	38.79	28.74	1.49	1.00	9.84	0.10	0.06	20.87	56.6	0.03	
		125			15.06	38.76	28.86	1.61	1.05	9.69	0.09	0.15	25.38	43.2		
L00.5K13	7/29/2019	0	41.005	28.218	24.35	22.95	14.45	0.75	0.12	0.22	0.05	0.20	1.49	226.6	0.31	16
L04K13	7/29/2019	0	41.059	28.218	25.13	23.14	14.37	0.58	0.06	0.09	0.05	0.31	0.76	226.3	0.34	17.5
		17			14.32	29.47	21.85	0.94	0.52	4.37	0.29	0.17	11.78	109.2	1.16	
		25			14.35	36.34	27.15	1.74	0.88	8.08	0.45	0.25	15.72	65.1	3.24	
		30			15.46	38.40	28.49	1.05	0.98	9.44	0.38	0.20	18.02	57.7	1.61	
K56K03	7/29/2019	0	40.933	28.051	25.22	23.00	14.24	0.31	0.09	0.14	0.07	0.38	1.21	232.5	0.19	14.5
K49K03	7/29/2019	0	40.816	28.052	25.23	23.12	14.32	0.72	0.05	0.06	0.02	0.32	0.84	235.2	0.09	16.5
		10			24.09	23.19	14.70	0.62	0.08	0.06	0.03	0.40	1.56	244.3	0.12	
		23			12.66	31.10	23.44	0.80	0.23	0.39	0.06	0.26	5.43	163.6	0.72	
		29			15.46	38.40	28.49	1.40	0.84	9.72	0.12	0.15	16.51	75.1	0.18	
		40			15.86	38.78	28.69	1.75	0.76	7.08	0.07	0.20	13.34	65.1	0.07	
		100			15.42	38.79	28.80	1.94	0.89	9.53	0.07	0.28	19.99	55.2		
		200			14.98	38.76	28.88	2.05	0.93	9.58	0.06	0.19	24.34	52.2		
		300			14.61	38.72	28.93	3.05	1.09	9.57	0.06	0.10	34.47	16.2		
		500			14.47	38.70	28.95	2.22	0.98	6.26	0.06	0.23	28.68	15.8		
		800			14.46	38.70	28.95	1.37	1.03	8.61	0.06	0.03	35.94	24.5		
		1000			14.49	38.72	28.96	3.02	0.83	6.82	0.06	0.30	28.10	37.4		
		1242			14.52	38.73	28.96	1.77	0.86	6.69	0.10	0.24	27.71	45.7		
K42K03	7/29/2019	0	40.701	28.051	26.17	23.18	14.09	0.77	0.04	0.22	0.05	0.51	0.20	231.6	0.07	13.5
K33K03	7/29/2019	0	40.553	28.050	25.38	23.18	14.33	0.61	0.02	0.08	0.05	0.40	0.70	238.4	0.15	12
		10			23.45	23.58	15.18	1.39	0.07	0.21	0.07	0.33	2.09	222.7	0.25	
		21			12.70	31.44	23.70	1.15	0.30	1.00	0.06	0.17	7.94	149.4	0.30	
		28			16.69	38.58	28.34	1.30	0.33	3.34	0.15	0.11	8.40	162.8	0.13	
		48			16.67	39.07	28.72	1.39	0.33	3.58	0.11	0.22	8.09	155.9	0.09	
K25K02	7/29/2019	0	40.417	28.033	25.99	23.84	14.64	2.66	1.75	0.14	0.03	0.37	0.51	235.4	0.18	9
K23J57	7/29/2019	0	40.384	27.952	25.54	23.90	14.82	3.45	3.27	0.08	0.04	0.36	0.37	240.2	0.49	8
		12			23.72	24.67	15.92	2.00	1.56	0.87	0.08	0.23	4.59	205.7	0.74	
		24			13.24	32.49	24.40	1.42	0.69	4.26	0.27	0.27	13.99	99.5	0.34	
		39			15.55	38.52	28.57	2.07	1.44	8.51	0.50	0.24	27.64	49.6	0.12	
K34J47	7/29/2019	0	40.567	27.785	25.12	23.02	14.28	0.54	0.02	0.11	0.04	0.28	0.34	232.1	0.10	
		10			23.89	23.77	15.19	0.88	0.09	0.10	0.05	0.27	2.67	223.4	0.14	
		22			12.67	31.36	23.64	0.92	0.24	1.70	0.16	0.21	6.31	163.3	0.13	
		35			16.71	38.82	28.52	1.03	0.23	2.30	0.12	0.22	6.14	175.0	0.08	
		65			16.70	39.17	28.80	1.13	0.14	2.33	0.23	0.19	5.70	189.5		

Station	Date	Depth (m)	Latitude	Longitude	Temperature (˚C)	Salinity (psu)	Denisty (sig-t)	TP (µM)	PO_4 (µM)	NO_3+NO_2 (µM)	NO_2 (µM)	NH_4 (µM)	Si (µM)	DO (µM)	Chl-*a* (µg/L)	SDD (m)
K41.5J45	7/29/2019	0	40.692	27.755	24.97	22.98	14.29	0.23	0.02	0.13	0.02	0.32	0.74	229.5	0.09	
K52J47	7/29/2019	0	40.900	27.795	25.22	22.93	14.19	0.21	0.03	0.11	0.02	0.39	0.56	230.9	0.10	
K57J47	7/29/2019	0	40.948	27.783	24.78	22.62	14.08	0.20	0.04	0.13	0.03	0.36	0.59	231.9	0.07	
		14			22.85	23.18	15.04	0.23	0.08	0.07	0.02	0.21	2.14	245.3	0.52	
		35			16.65	38.99	28.66	0.57	0.50	5.64	0.13	0.11	11.12	140.3	0.07	
		70			15.35	38.80	28.82	0.95	0.88	9.67	0.09	0.16	20.06	66.2		
K55J36	7/30/2019	0	40.917	27.603	25.64	23.41	14.42	0.20	0.08	0.13	0.03	0.35	0.50	227.8	0.11	
K49J36	7/30/2019	0	40.829	27.600	24.18	23.98	15.27	0.41	0.10	0.08	0.04	0.40	0.63	232.7	0.10	
		10			23.82	23.84	15.27	0.32	0.09	0.09	0.04	0.28	1.13	241.5	0.17	
		23			13.79	33.41	25.00	0.46	0.34	0.82	0.05	0.24	8.21	136.2	0.27	
		30			14.87	37.71	28.09	0.84	0.76	7.95	0.09	0.13	14.79	93.0	0.15	
		50			15.48	38.76	28.76	0.99	0.92	10.02	0.07	0.12	20.21	64.6	0.02	
		80			15.38	38.83	28.84	1.03	0.69	5.69	0.05	0.31	13.04	77.9		
		200			14.74	38.75	28.92	1.08	0.92	7.69	0.05		23.37	43.6		
		300			14.56	38.71	28.94	1.13	1.06	8.55	0.04		32.10	22.8		
		450			14.49	38.70	28.95	1.07	1.01	7.75	0.04		32.80	16.5		
		750			14.56	38.74	28.96	0.87	0.81	6.74	0.04		25.44	53.8		
		900			14.55	38.74	28.96	1.14	0.90	7.40	0.04		26.80	58.1		
		1118			14.56	38.76	28.97	1.10	0.92	7.64	0.06		29.22	61.1		
K43J28	7/30/2019	0	40.742	27.461	25.26	23.12	14.32	0.25	0.07	0.08	0.05	0.19	0.88	219.6	0.10	14
K39J24	7/30/2019	0	40.628	27.407	25.21	23.58	14.68	0.29	0.09	0.09	0.04	0.22	0.51	227.0	0.18	14
		10			25.08	23.65	14.76	0.38	0.09	0.10	0.05	0.23	0.60	229.2	0.21	
		20			15.16	32.14	23.73	0.54	0.22	0.08	0.03	0.11	4.83	179.3	0.29	
		29			16.82	38.87	28.53	0.61	0.30	2.54	0.18	0.11	6.74	181.4	0.24	
		50			16.04	38.95	28.78	0.91	0.66	6.87	0.10	0.15	14.88	109.6	0.06	
		114			15.37	38.86	28.86	0.97	0.84	8.28	0.09	0.14	20.57	79.9		
K22J49	7/30/2019	0	40.364	27.813	25.21	24.94	15.70	0.48	0.18	0.38	0.07	0.18	2.60	209.8	0.38	13
		10			24.33	25.26	16.19	0.54	0.25	0.75	0.10	0.20	5.59	187.8	0.42	
		23			15.46	35.66	26.38	1.02	0.83	4.74	0.24	0.12	18.41	88.9	0.22	
		34			16.00	38.71	28.60	1.35	1.06	6.57	0.22	0.12	22.35	68.8	0.21	
K20.5J37.5	7/30/2019	0	40.344	27.624	25.63	24.63	15.34	0.51	0.11	0.10	0.06	0.13	0.64	228.9	0.37	11
		10			25.12	24.88	15.68	0.54	0.12	0.12	0.06	0.31	1.41	216.7	0.22	
		21			15.91	36.80	27.16	0.68	0.27	0.40	0.12	0.13	6.75	166.1	0.83	
		25.5			16.57	38.63	28.41	0.95	0.57	3.19	0.65	0.28	14.55	113.2	0.20	
K23.5J38	7/30/2019	0	40.389	27.631	25.88	24.33	15.04	0.46	0.08	0.22	0.06	0.19	0.37	225.0	0.16	15
		10			24.92	24.83	15.70	0.54	0.09	0.16	0.06	0.15	1.73	220.0	0.26	
		22			15.90	36.22	26.71	0.59	0.46	2.17	0.14	0.17	11.63	124.7	0.20	
		39			16.53	39.00	28.70	0.70	0.53	4.82	0.13	0.13	12.45	135.0	0.19	
K27J26	7/30/2019	0	40.450	27.435	25.94	23.61	14.48	0.32	0.09	0.24	0.03	0.25	0.42	229.9	0.37	13

Station	Date	Depth (m)	Latitude	Longitude	Temperature (˚C)	Salinity (psu)	Denisty (sig-t)	TP (µM)	PO_4 (µM)	NO_3+NO_2 (µM)	NO_2 (µM)	NH_4 (µM)	Si (µM)	DO (µM)	Chl-*a* (µg/L)	SDD (m)
K31J22	7/30/2019	0	40.514	27.369	25.95	23.89	14.69	0.41	0.04	0.21	0.05	0.13	0.45	227.5	0.04	11.5
		10			25.23	24.52	15.37	0.48	0.07	0.18	0.02	0.20	0.64	224.2	0.42	
		18			18.58	29.05	20.58	0.50	0.09	0.34	0.09	0.10	2.36	216.5	0.19	
		23			17.13	38.16	27.91	0.93	0.15	0.25	0.04	0.06	2.99	196.3	0.20	
		35			16.87	39.11	28.71	0.48	0.05	0.64	0.23	0.09	1.78	228.7	0.16	
		57.5			16.72	39.22	28.82	0.24	0.06	0.75	0.30	0.09	1.96	230.7		
K34J17	7/30/2019	0	40.565	27.283	26.09	23.66	14.48	0.17	0.04	0.24	0.02	0.02	0.46	228.1	0.07	15.5
K30J08	7/30/2019	0	40.501	27.133	26.05	23.55	14.41	0.23	0.03	0.24	0.02	0.21	0.47	227.5	0.13	13
		10			24.85	23.61	14.80	0.30	0.04	0.25	0.03	0.12	0.55	228.0	0.09	
		20			19.72	31.63	22.27	0.34	0.08	0.85	0.07	0.06	2.71	210.9	0.26	
		30			16.83	39.11	28.72	0.39	0.18	2.20	0.14	0.10	5.21	190.4	0.17	
		40			16.73	39.22	28.83	0.12	0.05	0.49	0.18	0.05	1.39	239.2	0.10	
		61			16.76	39.25	28.84	0.44	0.05	0.57	0.17	0.09	1.86	235.4		
K26I59	7/30/2019	0	40.433	26.984	25.57	24.25	15.07	0.33	0.04	0.27	0.03	0.04	0.58	229.5	0.09	11
K26I54	7/30/2019	0	40.433	26.900	26.14	24.31	14.95	0.27	0.03	0.27	0.03	0.24	0.32	231.3	0.25	13
K26I50	7/30/2019	0	40.432	26.836	25.95	24.01	14.78	0.36	0.03	0.27	0.03	0.22	0.85	231.6	0.14	13
K46I47	7/30/2019	0	40.430	26.790	26.16	24.27	14.92	0.14	0.03	0.30	0.03	0.17	0.33	230.1	0.12	13
		10			25.36	24.33	15.19	0.23	0.07	0.29	0.03	0.13	0.68	228.9	0.19	
		20			20.41	31.94	22.32	0.59	0.05	0.44	0.09	0.10	1.76	234.0	0.29	
		40			16.81	39.24	28.82	0.50	0.03	0.49	0.12	0.05	1.84	235.4	0.13	
		77			16.78	39.25	28.84	0.54	0.04	0.54	0.13	0.05	1.87	237.1		
K24I42	7/30/2019	0	40.402	26.698	25.41	23.87	14.84	0.26	0.04	0.33	0.04	0.24	0.47	234.7	0.13	
K21.6I39	7/30/2019	0	40.355	26.650	25.26	23.84	14.86	0.25	0.06	0.39	0.07	0.09	1.26	238.3	0.47	
K17.2I33.5	7/30/2019	0	40.295	26.568	25.58	23.94	14.84	0.32	0.07	0.33	0.04	0.18	0.45	232.2	0.16	
		10			25.21	24.34	15.24	0.56	0.05	0.36	0.04	0.21	0.44	234.0	0.14	
		20			18.56	36.49	26.27	0.32	0.04	0.38	0.06	0.08	1.48	238.7	0.21	
		30			16.91	39.23	28.79	0.24	0.04	0.43	0.08	0.05	1.69	238.4	0.07	
		69			16.85	39.26	28.82	0.30	0.04	0.48	0.08	0.16	1.72	240.5		
K06.5I21.5	7/30/2019	0	40.118	26.360	23.42	28.09	18.59	0.24	0.04	0.44	0.06	0.28	0.68	238.1	0.09	
K03.5I18	7/30/2019	0	40.060	26.289	23.35	28.19	18.68	0.30	0.02	0.39	0.05	0.22	0.77	242.7	0.12	
K02I13	7/30/2019	0	40.031	26.219	23.53	27.77	18.31	0.23	0.02	0.41	0.06	0.25	0.46	237.7	0.12	
		10			19.94	35.69	25.30	0.32	0.02	0.42	0.06	0.16	0.96	250.3	0.12	
		20			17.54	39.23	28.63	0.40	0.02	0.41	0.06	0.18	1.26	245.3	0.04	
		40			16.87	39.32	28.86	0.30	0.02	0.46	0.08	0.17	1.14	239.2	0.09	
		60			16.73	39.32	28.90	0.24	0.02	0.62	0.15	0.31	1.43	229.8	0.12	
		91			16.42	39.29	28.95	0.34	0.03	0.90	0.27	0.25	1.67	224.0	0.27	
K00I09	7/30/2019	0	40.003	26.155	23.97	27.02	17.62	0.17	0.02	0.43	0.07	0.22	0.87	244.3	0.05	
K00I00	7/30/2019	0	39.999	26.003	24.34	29.40	19.31	0.14	0.02	0.44	0.07	0.24	0.63	218.3	0.08	

C. Measurements of porewater nutrients and sediment geochemical parameters in the Marmara Sea

Date	Station	Depth (cmbs)	PO_4 (µM)	NO_3 (µM)	NH_4 (µM)	Si (µM)	TC (mmol/g)	TOC (mmol/g)	TN (mmol/g)	TOC/TN (Molar)	d-Fe (µM)	Cl (mM)	SO_4 (mM)	Br (mM)	Li (µM)	Na (mM)	K (mM)	Mg (mM)	Ca (mM)	H_2S (µM)
1/6/2019	IZ-30	-1	5.80	39.56	307.5	15.8														
		1	19.80	10.56	395.0	113.2	2.55	2.26	0.18	12.73		611	26.8	0.75	20.17	521.53	11.74	65.52	8.52	6
		2	40.50	7.06	349.8	185.3	1.97	1.65	0.13	12.98		747	30.5	0.89	23.05	613.59	13.68	77.19	9.75	1907
		3	40.80	11.86	383.5	188.5	3.59	2.70	0.20	13.50		675	28.2	0.86	20.17	574.49	13.11	71.93	8.63	2162
		4	36.00	9.96	342.9	175.2	3.28	2.53	0.18	13.87		534	24.9	0.67	15.85	434.51	10.52	57.59	7.06	1502
		6	47.30	11.96	404.1	199.3	2.91	2.09	0.17	12.60		640	26.5	0.76	15.85	457.13	11.27	63.17	6.85	3204
		8	43.70	4.16	418.5	157.8	2.80	2.28	0.18	12.94		575	23.6	0.73	14.41	457.38	10.36	62.15	6.26	2704
		10	42.10	5.76	480.7	167.3	1.34	0.91	0.07	13.65		653	24.6	0.80	14.41	533.74	12.38	67.69	6.65	2624
		15	51.00	5.46	489.2	153.3	2.73	2.13	0.13	16.53		646	24.5	0.79	12.97	511.41	11.66	68.65	5.79	1709
		20	51.30	8.86		124.4	1.36	1.24	0.07	17.03		572	23.8	0.73	10.09	451.74	11.06	61.33	6.07	
		25	58.20	11.36		104.2	1.39	1.37	0.08	17.14		687	15.6	0.95	11.53	545.71	12.46	66.01	7.34	
		30	52.50	6.66		114.1	1.22	1.07	0.06	17.54		618	11.0	0.79	10.09	464.96	10.63	65.00	3.25	
		35	44.90	5.26		111.6	1.14	0.99	0.06	16.41		610	9.3	0.93	10.09	499.22	13.60	62.97	4.24	
		40	33.40	10.46	645.9	102.0	1.00	0.86	0.05	16.24		543	7.3	0.71	10.09	441.67	11.15	57.73	3.68	
		45	34.20	5.56	623.4	88.0	0.92	0.85	0.05	17.95		573	1.0	0.74	10.09	470.29	11.12	50.95	3.67	
		50	33.60	8.96	665.5	114.9	0.92	0.86	0.05	17.10		330	0.8	0.50	8.64	361.99	9.16	46.17	3.60	
7/24/2019	1	-1	1.01	14.21	1.0	27.1														
		1	10.62	36.52	26.9	102.7	2.37	1.11	0.12	9.4	6.78	653	32.2	0.78	31.70	610.13	14.64	72.30	13.71	
		2	17.70	39.64	50.9	149.9	2.40	1.12	0.12	9.5	7.85	640	31.5	0.75	27.37	558.32	13.52	65.68	12.73	
		3	17.46	33.48	94.3	187.8	2.36	1.13	0.11	10.2	3.28	619	29.6	0.70	25.93	495.88	13.68	62.40	12.07	
		4	16.94	29.16	117.7	202.0	2.26	1.12	0.11	10.4	0.58	629	30.2	0.72	24.49	541.29	13.90	65.23	12.43	
		6	15.78	21.68	107.6	142.6	2.25	1.00	0.11	9.2		607	29.8	0.73	25.93	529.02	13.82	63.23	12.00	
		8	13.86	19.52	116.3	105.7	2.12	0.99	0.10	9.9	0.19	642	30.2	0.76	24.49	540.83	14.37	64.92	12.37	
		10	10.62	21.92	108.2	107.3	2.08	0.92	0.09	10.1		647	31.1	0.76	27.37	552.22	14.70	67.48	12.87	
		15	5.94	20.88	123.8	85.8	1.82	0.74	0.08	9.1	0.48	571	28.0	0.65	23.05	479.71	13.93	59.11	11.39	
		20	3.06	21.00	120.7	70.9	1.73	0.64	0.07	8.6		564	27.7	0.68	24.49	483.23	14.04	59.48	11.16	
		25					1.70	0.61	0.07	9.3	0.19	496	25.2	0.66	20.17	439.20	13.06	53.75	10.11	
		30	4.62	13.44	122.0	108.5	1.82	0.70	0.07	9.5		629	30.8	0.75	27.37	559.92	15.11	65.73	12.47	
7/24/2019	2	-1	0.99	11.55	0.4	26.7														
		1	5.58	9.42	18.5	124.9	3.08	1.30	0.13	10.3	26.59									
		2	17.46	6.58	49.9	223.8	2.79	1.01	0.10	10.3	31.77									
		3	16.50	7.04	71.5	252.5	2.54	0.98	0.08	11.7	10.20									

Date	Station	Depth (cmbs)	PO_4 (µM)	NO_3 (µM)	NH_4 (µM)	Si (µM)	TC (mmol/g)	TOC (mmol/g)	TN (mmol/g)	TOC/TN (Molar)	d-Fe (µM)	Cl (mM)	SO_4 (mM)	Br (mM)	Li (µM)	Na (mM)	K (mM)	Mg (mM)	Ca (mM)	H_2S (µM)
		4	20.10	6.72	88.8	215.6	2.46	0.76	0.07	10.8	2.68									
		6	15.18	6.34	96.2	172.6	2.59	0.91	0.08	10.8										
		8	9.90	2.72	77.3	116.2	2.72	0.90	0.09	10.5	1.34									
		10	9.42	4.24	59.3	116.3	2.68	0.85	0.08	11.1										
		15	5.94	4.72	39.7	107.6	2.45	0.69	0.06	11.2	1.67									
		20	3.54	0.80	32.5	98.3	2.15	0.50	0.05	9.8										
		25	4.02	2.34	31.4	134.5	2.21	0.47	0.05	8.9										
		30	4.02	2.60	32.6	125.9	2.23	0.50	0.05	10.2										
1/5/2019	IZ-2	-1	4.10	13.75	74.2	9.0														
		1	8.97	8.96	113.5	84.7	4.07	2.54	0.23	10.87										
		2	16.50	17.46	168.2	113.3	3.56	2.34	0.16	14.40										2
		3	21.20	23.76	83.9	129.3	4.12	2.51	0.21	12.11										6
		4	38.90	3.86	289.4	165.2	4.05	2.08	0.20	10.64										2
		6	39.70	4.86	346.2	164.6	3.37	1.93	0.16	11.77										16
		8	38.50	4.66	394.9	157.9	3.34	2.08	0.17	12.29										16
		10	34.20	15.76	414.8	146.7	3.45	2.04	0.17	11.87										16
		15	56.30	6.06	469.8	171.6	3.54	2.37	0.18	13.34										25
		20	44.80	7.46	448.5	141.1	2.18	2.17	0.12	18.43										
		25	46.50	13.46	81.2	105.2	2.13	1.94	0.07	25.99										
		30	28.70	23.66	558.4	96.3	1.65	1.02	0.08	13.07										2
		35	28.00	20.36	608.6	97.4	1.62	1.01	0.07	13.50										
		40	33.40	6.16	613.7	127.8	1.75	0.99	0.08	12.02										
		45	28.90	6.46	612.1	108.0	1.73	0.98	0.08	12.78										
		50	29.20	7.06	625.9	127.3	1.75	0.94	0.08	11.60										
7/24/2019	3	-1	0.81	9.10	0.2	36.7														
		1	4.74	6.58	44.2	167.4	2.52	1.38	0.13	10.7	9.58									
		2	9.90	6.08	108.4	259.3	2.51	1.29	0.13	10.3	2.27									
		3	19.38	6.56	144.5	323.5	2.39	1.31	0.12	11.0	0.34									
		4	21.90	6.82	180.7	315.7	2.29	1.21	0.11	10.9	3.93									
		6	39.30	4.04	245.8	324.8	2.38	1.10	0.12	9.2	0.82									
		8	42.90	2.00	261.7	334.9	2.45	1.20	0.12	10.1	2.27									
		10	33.30	0.68	314.8	290.8	2.32	1.17	0.11	10.2	7.85									
		15	25.98	0.52	349.8	232.4	2.19	1.06	0.11	10.0										
		20	13.38	2.68	390.8	192.4	1.96	0.83	0.10	8.6										
		25	6.30	2.38	441.7	175.2	1.92	0.74	0.09	8.3	0.39									
		30	9.66	2.48	451.0	163.4	1.93	0.80	0.09	8.5										
		35	10.62	1.28	463.2	157.4	1.93	1.39	0.09	16.1										
7/24/2019	4	-1	0.95	11.28	4.3	47.6														

Date	Station	Depth (cmbs)	PO_4 (µM)	NO_3 (µM)	NH_4 (µM)	Si (µM)	TC (mmol/g)	TOC (mmol/g)	TN (mmol/g)	TOC/TN (Molar)	d-Fe (µM)	Cl (mM)	SO_4 (mM)	Br (mM)	Li (µM)	Na (mM)	K (mM)	Mg (mM)	Ca (mM)	H_2S (µM)
		1	4.02	3.70	34.3	154.6	2.40	1.30	0.12	10.9	9.34									
		2	5.82	2.36	71.2	174.6	1.99	1.06	0.10	10.2	22.03									
		3	8.70	1.84	73.3	176.0	2.02	1.17	0.10	12.2	16.15									
		4	8.94	1.62	78.5	183.1	2.20	1.12	0.11	10.1	9.97									
		6	8.58	1.30	105.0	211.3	2.21	1.10	0.11	9.7	3.87									
		8	10.26	1.24	120.5	216.0	2.23	1.05	0.11	9.3										
		10	12.54	0.69	144.8	225.8	2.03	0.96	0.10	9.3	0.39									
		15	8.94	1.06	162.0	158.3	2.06	0.92	0.11	8.4										
		20	6.90	0.34	178.2	134.6	1.93	0.85	0.09	9.4	0.44									
		25					1.88	0.86	0.09	9.5										
		30					1.91	0.85	0.09	9.7	0.59									
		35					1.94	0.80	0.09	8.8										
		40					1.98	0.83	0.09	9.3										
7/25/2019	5	-1	1.07	12.22	1.2	25.5														
		1	11.46	1.82	10.9	105.0	2.73	0.98	0.10	9.4										
		2	19.98	6.18	28.9	128.9	2.52	1.05	0.09	11.1										
		3	19.26	7.82	33.6	165.0	2.42	0.91	0.09	10.0										
		4	15.78	13.54	46.6	147.1	2.40	0.91	0.09	10.4										
		6	16.98	11.02	56.2	122.5	2.28	0.89	0.08	10.6										
		8	12.54	10.70	66.5	136.6	2.33	0.82	0.09	9.5										
		10	10.38	2.84	75.1	113.6	2.25	0.83	0.08	10.0										
		15	4.98	16.82	77.3	83.2	2.15	0.70	0.08	9.2										
		20	5.70	14.78	78.5	77.6	2.07	0.65	0.07	8.9										
		25	5.94	8.78	75.6	116.6	2.07	0.69	0.07	9.1										
		30	8.10	0.86	75.1	135.1	2.04	0.68	0.07	10.2										
		35					1.80	0.62	0.06	10.5										
		40					1.79	0.63	0.06	10.2										
7/25/2019	6	-1	1.27	10.71	0.2	33.4														
		1	19.14	2.54	5.0	148.7	3.26	1.61	0.17	9.7	9.92									
		2	28.62	7.70	35.5	180.2	3.05	1.37	0.14	9.8	20.26									
		3	28.86	5.78	58.3	188.4	3.00	1.30	0.13	9.6	15.56									
		4	33.90	5.72	76.3	211.0	2.89	1.34	0.12	10.8	13.23									
		6	23.22	9.04	86.2	170.2	2.83	1.27	0.13	10.0	6.98									
		8	18.66	9.66	85.0	139.6	2.60	1.08	0.11	9.5	10.29									
		10	14.82	9.98	92.8	137.9	2.68	1.07	0.11	9.7	0.51									
		15	7.02	19.82	88.7	86.6	2.35	0.89	0.09	9.9	0.34									

Date	Station	Depth (cmbs)	PO_4 (µM)	NO_3 (µM)	NH_4 (µM)	Si (µM)	TC (mmol/g)	TOC (mmol/g)	TN (mmol/g)	TOC/TN (Molar)	d-Fe (µM)	Cl (mM)	SO_4 (mM)	Br (mM)	Li (µM)	Na (mM)	K (mM)	Mg (mM)	Ca (mM)	H_2S (µM)
		20	3.66	12.64	90.5	90.6	2.16	0.73	0.09	8.5	0.34									
		25	3.66	10.10	82.1	71.6	2.18	0.72	0.09	8.4	0.54									
		30	4.02	10.32	65.0	90.6	2.26	0.69	0.08	8.5	0.29									
		35	2.26	1.88	32.9	37.2	2.19	0.69	0.07	10.1										
7/25/2019	7	-1	1.33	8.12	1.4	31.5														
		1	5.46	1.00	9.5	113.6	2.83	1.46	0.14	10.8	0.29									
		2	9.66	1.94	40.7	306.2	2.94	1.44	0.14	10.2	14.79									
		3	8.70	1.00	44.3	206.8	2.88	1.37	0.14	9.8										
		4	9.78	1.10	64.9	144.6	2.78	1.25	0.12	10.2	1.11									
		6	14.58	2.48	93.7	222.8	2.77	1.25	0.12	10.3	1.93									
		8	15.66	4.68	103.9	211.3	2.71	1.19	0.12	10.2	1.40									
		10	18.42	7.50	92.2	232.0	2.65	1.23	0.12	10.7										
		15	9.18	9.38	105.6	164.0	2.61	1.11	0.11	10.4	1.50									
		20	3.30	9.50	83.0	114.8	2.15	0.80	0.08	9.6										
		25	1.62	10.82	73.9	93.0	2.16	0.68	0.07	9.5										
		30	1.86	10.52	65.6	85.0	2.58	0.85	0.09	9.4										
		35					2.59	1.15	0.10	11.7										
		40	2.34	9.26	70.1	77.4	2.69	1.36	0.10	13.5										
7/25/2019	8	-1	1.23	11.34	0.4	36.1														
		1	2.34	13.52	1.9	103.4	2.56	1.23	0.12	10.2	1.49	640	31.3	0.76	27.37	563.17	13.98	67.12	13.58	
		2	2.62	25.12	1.5	105.2	2.56	1.22	0.12	10.0	2.65	639	31.8	0.78	25.93	524.15	13.24	65.44	12.57	
		3	2.62	30.28	18.8	164.3	2.57	1.28	0.12	10.7	3.86	641	31.7	0.73	25.93	485.97	14.24	62.49	11.96	
		4	2.34	36.76	15.7	151.3	2.42	1.22	0.12	10.5	4.04	635	30.8	0.71	25.93	556.56	15.22	67.09	12.90	
		6	1.38	43.12	12.0	107.8	2.45	1.21	0.12	10.2	4.69	627	30.5	0.69	27.37	553.96	14.04	65.65	12.54	
		8	1.38	28.28	25.1	115.1	2.42	1.15	0.11	10.0	3.25	639	30.3	0.69	27.37	545.02	14.12	65.53	12.64	
		10	1.26	21.32	41.5	107.8	2.39	1.04	0.11	9.6	2.56	637	30.9	0.76	27.37	544.15	14.59	66.48	12.75	
		15	1.14	7.28	47.8	131.2	2.16	0.96	0.10	9.9	2.74	659	31.2	0.76	27.37	556.39	14.32	66.44	12.65	
		20	1.68	6.60	74.8	102.0	1.99	0.93	0.09	10.3		591	29.2	0.71	27.37	525.52	15.12	62.03	12.69	
		25					1.99	0.70	0.08	8.3										
		30					2.07	0.69	0.09	8.0										
		35					2.02	0.70	0.08	9.0										
		40					2.02	0.61	0.07	8.4										
1/6/2019	EK-12	-1	0.47	6.06	1.1	13.2														
		1	0.89	30.98	22.6	78.4	2.42	2.28	0.14	16.44										
		2	0.69	50.08	21.4	59.6	2.14	1.39	0.13	10.87										
		3	1.49	53.88	68.4	73.8	2.06	1.36	0.12	11.09										
		4	1.69	91.48	37.2	59.0	1.99	1.32	0.12	10.99										
		6	3.19	85.88	8.6	32.0	1.96	1.29	0.11	11.34										

Date	Station	Depth (cmbs)	PO_4 (µM)	NO_3 (µM)	NH_4 (µM)	Si (µM)	TC (mmol/g)	TOC (mmol/g)	TN (mmol/g)	TOC/TN (Molar)	d-Fe (µM)	Cl (mM)	SO_4 (mM)	Br (mM)	Li (µM)	Na (mM)	K (mM)	Mg (mM)	Ca (mM)	H_2S (µM)
		8	2.29	55.68	34.4	81.8	1.87	1.24	0.11	11.01										
		10	3.89	47.78	40.4	75.4	1.78	1.18	0.11	11.00										
		15	5.69	42.88	48.0	99.2	1.63	1.07	0.10	10.89										
		20	5.69	40.38	46.4	103.2	1.55	1.03	0.09	11.28										
		25	4.69	40.08	44.4	83.6	1.56	0.98	0.09	11.23										
1/6/2019	EK-10	-1	0.71	6.84	2.6	16.4	1.55	0.97	0.09	11.18										
		1	5.09	9.98	20.1	77.1	2.90	1.41	0.14	9.79										
		2	14.39	4.88	38.0	110.8	2.88	1.45	0.14	10.18										16
		3	11.39	6.08	44.6	109.0	2.85	1.41	0.14	9.74										11
		4	10.79	10.68	47.9	70.7	2.82	1.38	0.14	9.80										
		6	9.39	15.78	42.7	87.7	2.75	1.27	0.13	9.74										
		8	9.89	9.48	55.5	101.5	2.62	1.21	0.13	9.38										
		10	7.89	11.98	47.9	74.7	2.42	1.08	0.11	10.04										
		15	4.49	7.78	44.2	63.9	2.28	0.98	0.11	9.31										
		20	1.69	26.08	52.4	96.2	2.19	0.88	0.09	9.60										
		25	2.69	18.78	44.0	86.4	2.16	0.85	0.09	9.23										
		30	2.99	13.08	51.5	98.4	2.17	0.85	0.09	9.67										
		35	3.59	9.88	54.9	83.6	2.17	0.85	0.09	9.62										
		40	3.79	14.98	57.1	103.7	2.14	0.89	0.09	10.14										
1/6/2019	MD-18	-1	0.82	10.53	7.1	22.3														
		1	8.79	4.88	12.1	83.0	3.33	0.99	0.08	13.08		639	30.3	0.78	25.93	547.44	11.14	68.56	11.22	
		2	7.29	29.58	25.7	87.0	3.23	1.02	0.07	13.70		591	30.0	0.78	24.49	473.34	12.86	63.66	12.29	
		3	9.99	7.68	31.1	81.5	3.14	0.98	0.07	13.56		605	29.5	0.76	23.05	492.17	11.24	66.02	10.47	
		4	2.49	21.88	14.1	40.6	3.08	1.66	0.06	27.02		602	29.4	0.75	25.93	544.17	12.84	66.23	11.03	
		6	7.69	6.38	35.5	85.6	2.93	1.64	0.05	30.42		640	31.4	0.78	24.49	509.87	11.22	66.93	12.56	
		8	6.29	23.88	39.6	75.0	2.79	1.42	0.05	28.99		326	17.5	0.49	15.85	312.57	9.52	43.86	8.36	
		10	0.89	26.38	36.6	73.2	2.92	0.71	0.06	12.52		542	27.2	0.71	21.61	427.10	11.14	59.93	10.78	
		15	1.69	21.58	45.7	72.9	2.96	0.71	0.05	13.69		481	27.1	0.61	21.61	446.24	11.43	57.70	10.36	322
		20	1.09	17.68	51.5	69.9	3.46	0.78	0.05	15.70		609	30.2	0.76	24.49	536.70	12.71	66.85	15.77	322
		25	2.39	7.78	65.7	100.7	3.20	0.79	0.05	16.81		683	32.6	0.84	27.37	592.95	13.40	74.28	11.85	322
		30	1.69	3.18	75.7	90.5	3.25	0.74	0.05	14.60		575	29.3	0.76	23.05	495.92	12.07	65.21	10.91	6
		35	3.69	3.88	88.8	127.5	3.02	0.68	0.04	16.15		588	29.7	0.81	23.05	500.36	12.51	65.74	11.20	2
		40	2.29	3.58	90.6	90.5	3.02	0.58	0.04	14.84		605	29.4	0.76	24.49	507.95	12.02	67.05	11.69	

D. Measurements of porewater nutrients and sediment geochemical parameters in the Black, Marmara and NE Mediterranean Seas

Date	Station	Latitude	Longitude	Bottom Depth (m)	Depth (cmbs)	PO_4 (µM)	NO_3 (µM)	NH_4 (µM)	Si (µM)	TC	TOC	TN	r-Fe	NH4Cl-rP	BD-rP	NaOH-rP	NaOH-nrP	HCl-rP	Residual-P	Total-P
														Loosely bound-P	Fe-P	Al-P	Org-P	Ca-P	Res-P	TP
										(mmol/g)	(mmol/g)	(mmol/g)	(µmol/g)	(µmol/g)	(µmol/g)	(µmol/g)	(µmol/g)	(µmol/g)	(µmol/g)	(µmol/g)
3/20/2018	2	36.440	34.346	208	-1	0.07	1.40	0.5	3.0											
					1	1.00	18.42	7.9	33.9	3.31	0.70	0.07	50.32	0.06	0.37	0.27	5.30	4.61	3.26	13.9
					2	1.00	17.42	10.4	68.9	3.56	0.63	0.08	45.16	0.04	0.35	0.09	3.57	5.07	3.33	12.4
					3	0.50	10.12	25.8	68.4	3.46	0.60	0.07	26.60	0.04	0.32	0.14	3.57	4.02	1.95	10.0
					4	0.70	15.02	34.8	76.4	3.44	0.61	0.08	31.32	0.04	0.33	0.17	4.02	4.41	1.90	10.9
					6	0.60	13.32	30.2	69.6	3.45	0.57	0.07	37.10	0.03	0.31	0.11	3.73	4.79	3.40	12.4
					8	0.40	10.42	40.6	69.5	3.38	0.54	0.06	43.71	0.04	0.33	0.11	3.26	4.86	3.23	11.8
					10	0.60	10.72	49.5	77.0	3.40	0.50	0.06	37.10	0.05	0.29	0.32	4.16	3.90	1.88	10.6
					15	0.60	6.62	53.2	50.4	3.29	0.49	0.05	33.32	0.03	0.29	0.15	3.96	4.38	1.84	10.6
					20	0.30	10.22	69.8	84.0	3.35	0.48	0.06	27.97	0.05	0.28	0.28	3.72	4.18	2.18	10.7
					25	0.40	11.52	77.7	88.2	3.38	0.48	0.06	31.06	0.05	0.29	0.10	3.17	4.72	2.21	10.5
					30	1.30	12.12	79.0	86.7	3.45	0.48	0.06	35.79	0.04	0.22	0.16	3.01	3.12	2.71	9.3
					35	1.40	15.72	101.7	93.9	3.46	0.47	0.05	36.46	0.03	0.20	0.03	2.85	4.88	1.66	9.6
1/5/2019	IZ-2	40.730	29.610	157	-1	4.1	13.75	74.2	9.0											
					1	8.97	8.96	113.5	84.7	4.07	2.54	0.23	57.38	0.27	4.71	0.54	8.19	5.30	0.13	19.1
					2	16.5	17.46	168.2	113.3	3.56	2.34	0.16	56.65	0.18	3.07	0.47	7.03	5.07	2.46	18.3
					3	21.2	23.76	83.9	129.3	4.12	2.51	0.21	43.33	0.23	3.94	0.36	7.01	5.01	0.06	16.6
					4	38.9	3.86	289.4	165.2	4.05	2.08	0.20	47.12	0.24	4.18	0.38	7.14	5.42	1.12	18.5
					6	39.7	4.86	346.2	164.6	3.37	1.93	0.16	47.11	0.15	2.63	0.62	7.02	5.08	0.02	15.5
					8	38.5	4.66	394.9	157.9	3.34	2.08	0.17	39.22	0.19	3.16	0.66	7.06	4.00	0.12	15.2
					10	34.2	7.76	414.8	146.7	3.45	2.04	0.17	41.94	0.09	3.13	0.49	7.17	4.68	0.27	15.8
					15	56.3	6.06	469.8	171.6	3.54	2.37	0.18	42.96	0.10	2.39	0.59	6.48	5.01	0.29	14.9
					20	44.8	7.46	448.5	141.1	2.18	2.17	0.12	43.84	0.07	2.26	0.60	6.40	3.36	2.31	15.0
					25	46.5	7.46	481.2	105.2	2.13	1.94	0.07	35.48	0.14	1.86	0.93	6.17	1.50	3.04	13.6
					30	28.7	6.66	558.4	96.3	1.65	1.02	0.08	35.54	0.13	2.09	0.67	7.08	1.89	1.45	13.3
					35	28	6.36	608.6	97.4	1.62	1.01	0.07	39.08	0.11	2.35	0.74	6.91	1.02	3.36	14.5
					40	33.4	6.16	613.7	127.8	1.75	0.99	0.08	39.38	0.12	1.45	0.66	6.67	2.34	3.24	14.5
					45	28.9	6.46	612.1	108.0	1.73	0.98	0.08	36.97	0.14	1.79	0.35	4.54	2.07	4.01	12.9

Date	Station	Latitude	Longitude	Bottom Depth (m)	Depth (cmbs)	PO_4 (µM)	NO_3 (µM)	NH_4 (µM)	Si (µM)	TC	TOC	TN	r-Fe	NH4Cl-rP	BD-rP	NaOH-rP	NaOH-nrP	HCl-rP	Residual-P	Total-P
					50	29.2	6.06	625.9	127.3	1.75	0.94	0.08	41.19	0.18	1.17	0.49	4.55	2.22	2.56	11.2
7/25/2019	6	40.594	28.835	190	-1	1.27	10.71	0.2	33.4											
					1	19.14	2.54	5.0	148.7	3.26	1.61	0.17	39.59	0.44	3.02	0.99	9.09	3.20	0.06	16.8
					2	28.62	7.7	35.5	180.2	3.05	1.37	0.14	43.07	0.22	1.51	0.66	8.02	3.43	2.83	16.7
					3	28.86	5.78	58.3	188.4	3.00	1.30	0.13	39.00	0.15	0.97	0.37	8.71	5.59	2.51	18.3
					4	33.9	5.72	76.3	211.0	2.89	1.34	0.12	47.02	0.20	1.30	0.55	8.11	4.13	1.57	15.9
					6	23.22	9.04	86.2	170.2	2.83	1.27	0.13	41.98	0.18	1.12	0.65	8.17	3.81	0.88	14.8
					8	18.66	9.66	85.0	139.6	2.60	1.08	0.11	42.77	0.19	1.24	0.43	7.14	4.62	1.62	15.2
					10	14.82	9.98	92.8	137.9	2.68	1.07	0.11	36.72	0.17	1.10	0.44	5.89	4.25	2.33	14.2
					15	7.02	19.82	88.7	86.6	2.35	0.89	0.09	40.35	0.12	0.73	0.32	6.89	5.42	0.83	14.3
					20	3.66	12.64	90.5	90.6	2.16	0.73	0.09	36.97	0.10	0.65	0.24	4.66	4.95	3.50	14.1
					25	3.66	10.1	82.1	71.6	2.18	0.72	0.09	38.94	0.13	0.79	0.23	4.36	4.96	3.63	14.1
					30	4.02	10.32	65.0	90.6	2.26	0.69	0.08	34.95	0.12	0.84	0.24	4.33	4.68	3.31	13.5
					35	3.26	1.88	62.9	37.2	2.19	0.69	0.07	35.41	0.09	0.66	0.12	3.33	4.98	4.50	13.7
7/22/2019	11	41.664	28.935	480	-1	5.31		33.5	105.9											
					1	77.70	1.78	994.2	291.8	3.86	2.27	0.24	59.78	0.15	1.45	0.42	6.77	6.07	5.14	20.0
					2	82.14	1.42	1097.6	280.9	2.90	1.72	0.18	72.51	0.13	1.25	0.55	6.56	5.21	3.06	16.8
					3	77.58	0.22	1125.7	289.8	3.34	2.00	0.21	45.81	0.06	2.64	0.58	6.13	5.91	3.75	19.1
					4	77.94	0.58	1241.3	327.2	3.10	1.81	0.18	49.00	0.04	2.27	0.39	6.02	5.25	1.73	15.7
					6	62.94	0.92	1004.0	340.2	3.44	2.14	0.22	64.98	0.02	0.99	0.54	4.92	5.91	4.28	16.6
					8	58.58	0.47	1059.1	390.3	2.91	1.94	0.18	49.57	0.06	0.65	0.22	5.85	6.09	4.19	17.1
					10	76.02	0.00	1024.3	476.8	2.66	1.44	0.15	59.52	0.03	0.24	0.47	6.38	4.32	4.03	15.5
					15	54.42	0.00	916.4	426.8	2.86	1.51	0.16	59.52	0.03	0.99	0.47	5.93	5.08	2.33	14.8
					20	53.34	0.00	1231.8	407.3	2.83	1.45	0.16	44.30	0.03	0.55	0.40	6.61	4.77	3.61	16.0
					25	61.66	0.00	1134.8	409.2	3.16	1.47	0.15	31.52	0.08	0.55	0.43	6.51	4.72	4.10	16.4
					30	42.30	0.00	1651.5	407.4	2.80	1.28	0.15	41.18	0.07	0.54	0.25	4.98	5.02	5.63	16.5
7/23/2019	16	41.307	29.958	85	-1	0.43	5.36	9.0	24.0											
					1	3.06	7.16	10.7	147.1	3.02	0.90	0.09	48.7	0.181	2.339	1.629	5.327	5.091	0.345	14.91
					2	1.62	2.72	25.1	184.8	2.51	1.06	0.09	16.1	0.095	0.776	0.880	5.641	4.578	0.411	12.38
					3	1.26	3.28	39.8	165.1	2.24	1.17	0.10	22.9	0.055	0.603	0.602	4.917	4.193	2.567	12.94
					4	1.14	2.68	38.9	175.2	2.38	1.08	0.11	24.2	0.097	0.640	0.837	4.214	4.275	0.680	10.74
					6	0.78	1.52	40.6	172.8	2.06	0.65	0.07	18.9	0.071	0.484	0.523	4.107	3.875	1.868	10.93
					8	1.38	2.56	55.2	177.1	2.28	0.50	0.05	14.5	0.086	0.578	0.451	2.727	3.740	4.209	11.79
					10	0.90	2.72	54.8	162.6	2.34	0.46	0.05	14.4	0.036	0.474	0.235	2.165	3.008	7.737	13.65
					15	1.26	0.20	61.3	158.6	2.38	0.53	0.06	18.9	0.068	0.553	0.299	2.828	3.456	3.516	10.72
					20	3.18	1.44	80.5	130.7	2.33	0.64	0.07	11.8	0.100	0.542	0.397	3.129	4.329	2.705	11.20
					25	6.54	0.44	79.4	135.0	2.53	0.71	0.07	5.5	0.103	0.484	0.352	3.060	3.940	2.591	10.53

Date	Station	Latitude	Longitude	Bottom Depth (m)	Depth (cmbs)	PO_4 (µM)	NO_3 (µM)	NH_4 (µM)	Si (µM)	TC	TOC	TN	r-Fe	NH4Cl-rP	BD-rP	NaOH-rP	NaOH-nrP	HCl-rP	Residual-P	Total-P
					30	7.38	0.12	105.0	148.2	2.64	0.96	0.10	3.0	0.140	0.594	0.237	2.273	3.824	3.575	10.64
7/23/2019	17	41.373	29.968	152	-1	6.02	2.20	128.3	118.5											
					1	48.90	1.64	179.5	463.9	2.91	1.60	0.15	56.4	0.438	4.936	0.831	5.557	3.569	3.863	19.19
					2	107.58	2.20	260.6	550.4	3.19	1.47	0.18	55.0	0.563	3.776	0.550	6.393	4.424	1.229	16.93
					3	157.50	2.84	340.0	607.1	3.14	1.90	0.16	51.9	0.350	2.876	0.677	5.748	4.897	4.934	19.48
					4	158.34	2.36	441.0	717.5	2.39	1.10	0.11	33.7	0.161	2.002	0.325	5.727	3.675	3.068	14.96
					6	137.82	2.24	473.3	613.6	2.58	1.15	0.11	30.8	0.452	3.563	0.755	5.481	5.874	4.366	20.49
					8	150.54	2.68	552.5	638.2	3.13	1.54	0.14	47.7	0.154	2.099	0.770	5.574	4.133	4.252	16.98
					10	169.62	2.68	644.4	589.3	2.82	1.57	0.16	35.7	0.233	2.479	0.559	5.836	4.807	7.703	21.62
					15	189.14	1.08	759.7	609.0	2.84	1.56	0.16	41.1	0.247	3.143	0.449	5.975	4.825	2.592	17.23
					20	137.70	0.78	895.1	550.2	2.67	1.39	0.14	48.8	0.215	2.231	0.383	4.925	5.719	0.629	14.10
					25	164.46	0.64	1040.5	624.7	2.97	1.51	0.15	56.3	0.269	2.270	0.695	4.486	4.572	1.175	13.47
					30	158.46	0.05	1090.4	538.4	2.78	1.45	0.14	56.4	0.290	2.140	0.202	4.977	4.500	2.233	14.34
					35	172.38	0.00	1084.1	557.5	2.32	1.06	0.12	42.0	0.158	2.639	0.536	4.616	4.510	1.938	14.40
					40	181.38	0.00	1158.2	507.0	2.66	1.30	0.13	50.9	0.121	1.967	0.536	4.380	4.229	1.750	12.98
					45	132.90	0.00	1232.9	501.7	2.47	1.26	0.15	42.1	0.168	2.664	0.579	4.083	4.261	0.848	12.60
7/23/2019	18	41.378	29.952	330	-1	5.99	0.05	31.6	117.9											
					1	33.66	0.05	151.9	363.6	3.26	1.86	0.19	63.1	0.044	3.616	0.175	8.686	3.048	6.093	21.66
					2	45.78	0.04	233.8	406.8	2.81	1.48	0.16	61.9	0.048	4.238	0.446	7.107	3.791	3.870	19.50
					3	60.90	0.00	264.6	486.6	2.53	1.33	0.13	52.0	0.061	4.167	0.408	6.083	3.520	3.873	18.11
					4	62.34	0.00	286.8	492.5	2.45	1.26	0.13	45.6	0.073	3.694	0.450	4.389	4.083	5.298	17.99
					6	72.78	0.00	354.5	542.2	2.82	1.53	0.16	56.2	0.080	3.976	0.353	5.497	4.563	6.832	21.30
					8	81.06	0.00	398.8	561.5	2.71	1.41	0.14	55.0	0.144	4.086	0.595	6.033	5.539	3.200	19.60
					10	76.62	0.00	444.2	553.4	2.65	1.39	0.14	40.0	0.055	3.598	0.193	5.295	2.786	3.451	15.38
					15	79.50	0.00	526.0	613.1	2.98	1.67	0.16	29.0	0.126	4.318	0.810	5.470	2.170	2.202	15.10
					20	78.06	0.00	587.0	572.3	2.60	1.45	0.14	33.0	0.073	4.026	0.397	5.843	2.519	0.635	13.49
					25	87.30	0.00	588.5	611.8	2.68	1.51	0.13	35.5	0.097	2.026	0.331	6.736	1.448	2.496	13.13
					30	75.62	0.00	550.2	477.7	2.37	0.95	0.10	11.7	0.463	2.190	0.493	6.588	1.581	2.069	13.38
					35	68.58	0.00	666.8	501.7	2.17	0.95	0.09	6.2	0.362	2.473	0.771	5.817	1.568	2.903	13.89
					40	56.10	0.00	639.8	535.6	2.18	0.99	0.09	8.8	0.172	2.458	0.498	5.842	1.764	2.901	13.64

CURRICULUM VITAE

İSMAİL AKÇAY

Personal Information

Email: ismail@ims.metu.edu.tr
Web: https://www.researchgate.net/profile/Ismail-Akcay-3

Education Information

Doctor of Philosophy, Middle East Technical University, Institute of Marine Sciences, Oceanography, Turkey 2015 - 2022

Master of Science, Middle East Technical University, Institute of Marine Sciences, Oceanography, Turkey 2013 - 2015

Undergraduate, Middle East Technical University, Faculty of Education, Chemistry Education, Turkey 2007 - 2013

Dissertations

Coastal Eutrophication and Hypoxia under Focus: Redox Dependent Benthic Nutrient Fluxes across Sea Boundaries in the Northeastern Mediterranean and Marmara Sea, Middle East Technical University, Institute of Marine Sciences, **Doctor of Philosophy**, 2022

Spatial Variations of Particulate Organic Matter (POM) Composition and Concentrations in Surface Waters and Sediments of the Mersin Bay, Middle East Technical University, Institute of Marine Sciences, **Master of Science**, 2015

Research Areas

Oceanography, Chemical Oceanography, Biogeochemistry, Eutrophication, Nutrient Chemistry

Academic Titles / Tasks

Lecturer, Mersin University, Faculty of Fisheries, 2021 - Continues

Research Assistant, Middle East Technical University, Institute of Marine Sciences, Oceanography, 2015 - 2021

Articles Published in Journals That Entered SCI, SSCI and AHCI Indexes

1. Assessment of trophic status of the northeastern Mediterranean coastal waters: eutrophication classification tools revisited

Tuğrul S., Özhan K., **Akçay İ.**

Envıronmental Science And Pollution Research, vol.26, pp.14742-14754, 2019 (Journal Indexed in SCI)

Articles Published in Other Journals

1. Benthic Nutrient Fluxes across a Productive Shelf Adjacent to an Oligotrophic Basin: Case of the Northeastern Mediterranean Sea

Akçay İ., Tuğrul S., Yücel M.

https://eartharxiv.org/repository/view/2234/ (https://doi.org/10.31223/X5390F), pp.1-27, 2021 (Non-Refereed Journal)

Books & Book Chapters

1. Türkiye Derin Denizlerinde Anaerobik ve Kemosentetik Ekosistemler

Yücel, M., **Akçay, İ.**, Sevgen, S.,Alımlı, N., Ermiş, E., Tanık, G., Esti, M.

in Türkiye'nin Ekstrem Deniz Ortamları, Hüseyin Öztürk, Güler Alkan, Editör, TÜDAV, İstanbul, pp.1-27, 2021

2. Marmara Denizi'nin Geçirdiği Biyojeokimyasal Değişimler Bağlamında 2021 Müsilaj Patlaması, Güncel Baskılar ve Çözüm Önerileri

Yücel M., Özkan K., Fach B. A. , Örek H., Mantıkçı M., Tezcan D., **Akçay I.**, Özhan K., Arkin Ş. S. , Tuğrul S., et al.

in: Marmara Denizi'nin Ekolojisi: Deniz Salyası Oluşumu, Etkileşimleri ve Çözüm Önerileri, Muzaffer Şeker, İzzet Öztürk, Editor, Tüba Basın Yayın, Ankara, pp.249-268, 2021

3. Denizlerde Bütünleşik Kirlilik İzleme İşi 2014-2016 Akdeniz Özet Raporu

Tuğrul S., Kideyş A. E. , Gücü A. C. , Ok M., Güven O., **Akçay İ.**, Gökdağ K., Polat Beken Ç., Tan İ., Atabay H., et al.

Çevre ve Şehircilik Bakanlığı, ÇED İzin ve Denetim Genel Müdürlüğü, Ankara, 2017

4. Chemical Oceanography of Northeastern Mediterranean

Tuğrul S., Yücel N., **Akçay İ.**

in: The Turkish Part of the Mediterranean Sea; Marine Biodiversity, Fisheries, Conservation and Governance, Turan C,Salihoglu B.,Ozbek O,Öztürk B., Editor, Turkish Marine Research Foundation (TUDAV), İstanbul, pp.15-29, 2016

5. Land Base Pollution of the Turkish Mediterranean Sea

Özhan K., **Akçay İ.**, Tuğrul S.

in: The Turkish Part of the Mediterranean Sea Marine Biodiversity, Fisheries, Conservation and Governance, Turan C, Salihoglu B., Ozbek O, Öztürk B., Editor, TUDAV, 2016

Refereed Congress / Symposium Publications in Proceedings

1. Comparison of Porewater Diffusive Nutrient Fluxes with External Inputs in the Northeastern Mediterranean Sea.

Akçay, İ., Tuğrul, S., Yücel, M.

GOLDSCHMIDT (Virtual), Lyon, France, 4 - 9 July 2021

2. Deoxygenation and coastal eutrophication drive distinct benthic nutrient dynamics in the hypoxic Marmara Sea and oxic northeastern Mediterranean Sea

Akçay İ., Yücel M.

GOLDSCHMIDT, Barcelona, Spain, 18 - 23 August 2019, pp.40

3. Biochemical Quality Elements for the Assessment of Eutrophication in Mersin Iskenderun Bays (Northeastern Mediterranean)

Akçay İ., Tuğrul S., Uysal Z.

International Marine Freshwater Sciences Symposium, Antalya, Turkey, 18 - 21 October 2018

4. Riverine nutrient inputs to the Mersin Bay, northeastern Mediterranean

Akçay İ., Tuğrul S.

International Marine Freshwater Sciences Symposium (MARFRESH2018), Turkey, 18 - 21 October 2018

5. Besin Tuzu Değerlerine Bağlı Doğu Akdeniz Suları Trofik Durum Değerlendirme Yöntemi

Akçay İ., Tuğrul S.

III. Ulusal Deniz Bilimleri Konferansı, İzmir, Turkey, 9 - 12 May 2018, pp.288

6. Kuzeydoğu Akdeniz'de çözünmüş besin elementlerinin dağılımı

Tuğrul S., **Akçay İ.**, Örek H., Salihoğlu B., Deliceırmak Ç., Salihoğlu İ.

III. Ulusal Deniz Bilimleri Konferansı, İzmir, Turkey, 9 - 12 May 2018, pp.292

7. Contrasting the permanently anoxic Black Sea with the rapidly deoxygenating Marmara Sea: Distinct redox processes of sulfur, nitrogen and oxygen in the two interconnected enclosed basins

Yücel M., Salihoğlu B., Örek H., Fach B., Arkın S., Özkan K., **Akçay İ.**, Güraslan C., Tezcan D., Gazihan A., Et Al.

Ocean Sciences Meeting 2018, 12 February 2018

8. Variations in the eutrophicaton-related biochemical properties of the Iskenderun and Mersin Bay surface waters

Akçay İ., Tuğrul S.

International Iskenderun Bay Symposium, Turkey, 11 - 13 October 2017, pp.51

9. Geochemical properties of the Iskenderun and Mersin Bay urface sediments

Akçay İ., Tuğrul S.

International Iskenderun Bay Symposium, Hatay, Turkey, 11 - 13 October 2017, pp.52

10. Eutrophication assessment, classification and management in the Northeastern Mediterranean Sea

Tuğrul S., Özhan K., **Akçay İ.**

Sixth International Conference on Environmental Management, Engineering, Planning and Economics (CEMEPE) and SECOTOX Conference, Selanik, Greece, 25 - 30 June 2017, pp.684-693

11. Spatial variations in geochemical properties of surface sediments along the Northeastern Mediterranean coastal regions

Akçay İ., Tuğrul S., Özhan K.

Sixth International Conference on Environmental Management, Engineering, Planning and Economics (CEMEPE) and SECOTOX Conference, Selanik, Greece, 25 - 30 June 2017, pp.587-594

12. Mersin ve İskenderun Körfezi TRIX değerleri ve biyokimyasal parametrelerle değişimi

Tuğrul S., **Akçay İ.**, Özhan K.

I. Ulusal Denizlerde İzleme ve Değerlendirme Sempozyumu, Ankara, Turkey, 21 - 23 December 2016, pp.41-42

13. Kuzeydoğu Akdeniz'de trofik durum değerlendirmesi

Tuğrul S., Özhan K., **Akçay İ.**

I. Ulusal Denizlerde İzleme ve Değerlendirme Sempozyumu, Ankara, Turkey, 21 - 23 December 2016, pp.33-34

14. Kuzeydoğu Akdeniz yüzey sedimanlarında jeokimyasal özelliklerin değişimi

Tuğrul S., Tezcan D., **Akçay İ.**, Başduvar Ş.

I. Ulusal Denizlerde İzleme ve Değerlendirme Sempozyumu, Ankara, Turkey, 21 - 23 December 2016, pp.278

15. Kuzeydoğu Akdeniz yüzey sedimanlarinda metal ve hidrokarbon konsantrasyonlarinin değişimi

Özhan K., Tuğrul S., Başduvar Ş., **Akçay İ.**

I. Ulusal Denizlerde İzleme ve Değerlendirme Sempozyumu, Ankara, Turkey, 21 - 23 December 2016, pp.82-83

16. Comparison of Geochemical Properties of Surface Sediments in Mersin and İskenderun Bay NE Mediterranean

Akçay İ., Tuğrul S., Tezcan D., Ebula A.

41st CIESM Congress, 12 - 16 September 2016, vol.41, pp.204

17. Effects of Terrestrial Inputs on Particulate Organic Matter (POM) Composition (C/N/P Ratio) in Surface Waters and Sediments of the Mersin Bay

Akçay İ., Tuğrul S.

CIESM Congress, 12 - 16 September 2016, vol.41, pp.164

18. Mersin ve İskenderun Körfezlerinin Trofik Durum Değerlendirmesi

Özhan K., **Akçay İ.**, Tuğrul S.

Türkiye Deniz Bilimleri Konferansı 2016, Ankara, Turkey, 31 May - 03 June 2016, pp.323-324

19. Mersin Körfezi Yüzey Sedimanlarinda Jeokimyasal Özelliklerin Bölgesel Değişimi

Akçay İ., Tuğrul S., Başduvar Ş., Özhan K.

TürkiyeDeniz Bilimleri Konferansı, Ankara, Turkey, 31 May - 03 June 2016, pp.381-382

20. Mersin Körfezi'nde Dip Tarama-Dökü Faaliyetinin Sucul Ortama Kısa Süreli Etkilerinin Belirlenmesi

Tuğrul S., **Akçay İ.**, Örek H., Sadighrad, E.

Türkiye Deniz Bilimleri Konferansı, Ankara, Turkey, 31 May - 03 June 2016, pp.267

21. Akdeniz Kıyısal Bölge Sularında Dökü Alanları Belirleme Kriterleri İskenderun ve Mersin Körfezi Uygulamaları

Yücel N., Tuğrul S., **Akçay İ.**, Başduvar Ş., Sadighrad E., Tezcan D., Örek H.

Türkiye Deniz Bilimleri Konferansı, Turkey, 31 May - 03 June 2016

22. Mersin Körfezi Yüzey Sedimanlarında Jeokimyasal Özelliklerin Bölgesel Değişimi

Tuğrul S., **Akçay İ.**, Şehmus B., Özhan K.

Türkiye Deniz Bilimleri Konferansı, Ankara, Turkey, 31 May - 03 June 2016, pp.381

23. Mersin ve İskenderun Körfezlerinin Trofik Durum Değerlendirmesi

Özhan K., **Akçay İ.**, Tuğrul S.

Türkiye Deniz Bilimleri Konferansı, Ankara, Turkey, 31 May - 03 June 2016, pp.323

24. Mersin Körfezi Kıyı Sularında Nehir Etkisi

Yücel N., **Akçay İ.**, Sakallı A., Uysal Z., Tuğrul S.

Türkiye Deniz Bilimleri Konferansı, Ankara, Turkey, 31 May - 03 June 2016, pp.126

25. Mersin Körfezi Deniz Tabanının Habitat Modellemesi

Ebula E., Tezcan D., Tuğrul S., Yalçın U., **Akçay İ.**, Başduvar Ş., Yemenicioğlu S., Tunç Ş. Ç.

II. Kıyı ve Deniz Jeolojisi Sempozyumu ve IODP-ECORD Toplantısı, İstanbul, Turkey, 15 - 16 October 2015

26. Deniz Dip Tarama Uygulamaları ve Tarama Malzemesinin Çevresel Yönetimi (DİPTAR) Projesi ilk sonuçları

Tuğrul S., Tolun L., Yücel N., **Akçay İ.**, Tezcan D., Yalçın U., Abla A.

18. Ulusal Su Ürünleri Sempozyumu, İzmir, Turkey, 1 - 03 October 2015

Projects

1. Altiner S., Tanik G., Yücel M., Alimli N., **Akçay İ.**, Project Supported by Higher Education Institutions, Çınarcık Çukurluğu'nda (Marmara Denizi) foraminifer topluluklarının dağılımı, zaman içinde değişimi ve etkileyen faktörler, 2021 - Continues

2. Yücel, M., Tuğrul, S., Yılmaz A., Salihoğlu B., Fach-Salihoğlu, B., Tezcan, D., **Akçay, İ.** Project supported by TÜBİTAK, Deepsea metal and nutrient cycling in the Marmara and the Black Sea: Improving the detection of redox processes and nanoparticle formation, 2020-Continues

3. Tuğrul S., Uysal Z., Kıdeyş A. E. , Salihoğlu B., Özhan K., Tezcan D., Örek H., Myrsohnychenko., **Akçay İ.**, Project Supported by Other Official Institutions, Denizlerde Bütünleşik Kirlilik İzleme Projesi-2018 Kış ve 2019 Yaz Dönemi İzleme, 2018 - 2020

4. Salihoğlu B., Özhan K., **Akçay İ.**, Karahan A., Uysal Z., Akoğlu E., Tuğrul S., Gücü A. C. , Kideyş A. E. , Yücel M., Et Al., Project Supported by Higher Education Institutions, Erdemli Zaman Serisi Deniz Araştırmaları 2018, 2018 - 2019

5. Tuğrul S., Yücel N., **Akçay İ.**, Tezcan D., Project Supported by Other Private Institutions, Sanko Petrokimya Mamülleri San. ve Tic. A.Ş. Liman Tesislerinde Yapılacak Dip Taraması ve Dökü Alanı Çevresel Yönetim Planı, 2018 - 2018

6. Tuğrul S., Uysal Z., Kıdeyş A. E. , Salihoğlu B., Özhan K., Tezcan D., Örek H., Myrsohnychenko V., **Akçay İ.**, Project Supported by Other Official Institutions, Denizlerde Bütünleşik Kirlilik İzleme Projesi-2017 Yaz-2018 Kış Dönemi Programı, 2017 - 2018

7. Salihoğlu B., Tuğrul S., Fach Salihoğlu B. A., Yücel M., Özhan K., Özkan K., Akoğlu E., Tezcan D., **Akçay İ.**, CB Strateji ve Bütçe Başkanlığı (Kalkınma Bakanlığı) Projesi, Marmara Denizi Bütünleşik Model Sistemi: Faz 1, 2017 - 2018

8. Tuğrul S., **Akçay İ.**, Tezcan, D. Project Supported by Other Private Institutions, Sönmez Çimento Yapi ve Madencilik San. Tic. A.Ş. Liman Tesisi Dolfen İlavesi ve Dip Taraması Projesi, 2017 - 2017

9. Tuğrul S., **Akçay İ.**, Tezcan D. Project Supported by Other Private Institutions, Mersin Uluslararasi Liman İşletmeciliği A.Ş. Tarama-Boşaltma Faaliyeti Sonrasında Dökü Alanı İzleme, 2016 - 2017

10. Tuğrul S., Uysal Z., Kıdeyş A. E. , Gücü A. C. , Salihoğlu B., Özhan K., Örek H., Tezcan D., Ok., M., Güven., O., **Akçay, İ.**, et al., Project Supported by Other Official Institutions, Denizlerde Bütünleşik Kirlilik İzleme Projesi-2016 Akdeniz Bütünleşik Kirlilik İzleme , 2016 - 2017

11. Tuğrul S., Kıdeyş A. E. , Özhan K., **Akçay İ.**, Salihoğlu B., Gücü A. C. , Örek H., Başduvar Ş., Myroshnychenko V., Project Supported by Other Official Institutions, Mersin Körfezi Oşinografik/Kirlilik İzleme Projesi, 2015 - 2017

12. Tuğrul S., Kideyş A. E., **Akçay İ.**, Uysal Z., Salihoğlu B., Tezcan D., Gücü A. C. , Tubitak Project, Deniz Dip Tarama Uygulamaları ve Tarama Malzemesinin Çevresel Yönetimi, 2013 - 2017

13. Tuğrul S., Uysal Z., Kıdeyş A. E. , Salihoğlu B., Özhan K., Örek H., **Akçay İ.**, Project Supported by Other Official Institutions, Akdeniz Bütünleşik Kirlilik İzleme 2016 Kış Dönemi Projesi, 2016 - 2016

14. Tuğrul S., **Akçay İ.**, Project Supported by Other Private Institutions, Mersin Uluslararasi Liman İşletmeciliği A Ş Mersin Limanı Dip Taraması Limana Yanaşma Bölgesinde Tarama Alanı Köşe Koordinatlari Değişimi Uygunluğu Hakkında Değerlendirme Raporu, 2015 - 2016

15. Tuğrul S., Salihoğlu B., Kıdeyş A. E. , Uysal Z., Gücü A. C. , Tezcan D., Örek H., Sakınan S., Özhan K., Güven O., **Akçay, İ.**, et al., Project Supported by Other Official Institutions, Denizlerde Bütünleşik Kirlilik İzleme Projesi-2015 Akdeniz Bütünleşik Kirlilik İzleme, 2015 - 2016

16. Tuğrul S., Salihoğlu B., **Akçay İ.**, Project Supported by Other Private Institutions, Mersin Uluslararası Liman İşletmeciliği A Ş Mersin Limanı Dip Tarama ve Denize Boşaltımı, 2015 - 2016

17. Tuğrul S., Salihoğlu B., Kıdeyş A. E. , Uysal Z., Gücü A. C. , Tezcan D., Örek H., Sakınan S., Özhan K., Güven O., **Akçay, İ.**, et al., Project Supported by Other Official Institutions, Denizlerde Bütünleşik Kirlilik İzleme Projesi -2014 Akdeniz Bütünleşik Kirlilik İzleme, 2014 - 2015

Citations

Total Citations (WOS): 7

Total Citations (Google Scholar): 32